

Developed at the request of:



# Climate: Observations, projections and impacts

Research conducted by:



Turkey



We have reached a critical year in our response to climate change. The decisions that we made in Cancún put the UNFCCC process back on track, saw us agree to limit temperature rise to 2 °C and set us in the right direction for reaching a climate change deal to achieve this. However, we still have considerable work to do and I believe that key economies and major emitters have a leadership role in ensuring a successful outcome in Durban and beyond.

To help us articulate a meaningful response to climate change, I believe that it is important to have a robust scientific assessment of the likely impacts on individual countries across the globe. This report demonstrates that the risks of a changing climate are wide-ranging and that no country will be left untouched by climate change.

I thank the UK's Met Office Hadley Centre for their hard work in putting together such a comprehensive piece of work. I also thank the scientists and officials from the countries included in this project for their interest and valuable advice in putting it together. I hope this report will inform this key debate on one of the greatest threats to humanity.

**The Rt Hon. Chris Huhne MP, Secretary of State for Energy and Climate Change**



There is already strong scientific evidence that the climate has changed and will continue to change in future in response to human activities. Across the world, this is already being felt as changes to the local weather that people experience every day.

Our ability to provide useful information to help everyone understand how their environment has changed, and plan for future, is improving all the time. But there is still a long way to go. These reports – led by the Met Office Hadley Centre in collaboration with many institutes and scientists around the world – aim to provide useful, up to date and impartial information, based on the best climate science now available. This new scientific material will also contribute to the next assessment from the Intergovernmental Panel on Climate Change.

However, we must also remember that while we can provide a lot of useful information, a great many uncertainties remain. That's why I have put in place a long-term strategy at the Met Office to work ever more closely with scientists across the world. Together, we'll look for ways to combine more and better observations of the real world with improved computer models of the weather and climate; which, over time, will lead to even more detailed and confident advice being issued.

**Julia Slingo, Met Office Chief Scientist**

# Introduction

Understanding the potential impacts of climate change is essential for informing both adaptation strategies and actions to avoid dangerous levels of climate change. A range of valuable national studies have been carried out and published, and the Intergovernmental Panel on Climate Change (IPCC) has collated and reported impacts at the global and regional scales. But assessing the impacts is scientifically challenging and has, until now, been fragmented. To date, only a limited amount of information about past climate change and its future impacts has been available at national level, while approaches to the science itself have varied between countries.

In April 2011, the Met Office Hadley Centre was asked by the United Kingdom's Secretary of State for Energy and Climate Change to compile scientifically robust and impartial information on the physical impacts of climate change for more than 20 countries. This was done using a consistent set of scenarios and as a pilot to a more comprehensive study of climate impacts. A report on the observations, projections and impacts of climate change has been prepared for each country. These provide up to date science on how the climate has already changed and the potential consequences of future changes. These reports complement those published by the IPCC as well as the more detailed climate change and impact studies published nationally.

Each report contains:

- A description of key features of national weather and climate, including an analysis of new data on extreme events.
- An assessment of the extent to which increases in greenhouse gases and aerosols in the atmosphere have altered the probability of particular seasonal temperatures compared to pre-industrial times, using a technique called 'fraction of attributable risk.'
- A prediction of future climate conditions, based on the climate model projections used in the Fourth Assessment Report from the IPCC.
- The potential impacts of climate change, based on results from the UK's Avoiding Dangerous Climate Change programme (AVOID) and supporting literature.  
For details visit: <http://www.avoid.uk.net>

The assessment of impacts at the national level, both for the AVOID programme results and the cited supporting literature, were mostly based on global studies. This was to ensure consistency, whilst recognising that this might not always provide enough focus on impacts of most relevance to a particular country. Although time available for the project was short, generally all the material available to the researchers in the project was used, unless there were good scientific reasons for not doing so. For example, some impacts areas were omitted, such as many of those associated with human health. In this case, these impacts are strongly dependant on local factors and do not easily lend themselves to the globally consistent framework used. No attempt was made to include the effect of future adaptation actions in the assessment of potential impacts. Typically, some, but not all, of the impacts are avoided by limiting global average warming to no more than 2 °C.

The Met Office Hadley Centre gratefully acknowledges the input that organisations and individuals from these countries have contributed to this study. Many nations contributed references to the literature analysis component of the project and helped to review earlier versions of these reports.

We welcome feedback and expect these reports to evolve over time. For the latest version of this report, details of how to reference it, and to provide feedback to the project team, please see the website at [www.metoffice.gov.uk/climate-change/policy-relevant/obs-projections-impacts](http://www.metoffice.gov.uk/climate-change/policy-relevant/obs-projections-impacts)

In the longer term, we would welcome the opportunity to explore with other countries and organisations options for taking forward assessments of national level climate change impacts through international cooperation.



# Summary

## Climate observations

- There has been a coherent warming trend during summer over Turkey since 1960 and in the annual regional average mean, minimum and maximum temperature since the 1990s.
- Since 1960 there have been widespread decreases in the frequency of cool nights and increases in the frequency of warm nights.
- Changes in precipitation are mixed with decreases in winter in the west and increases in autumn in the north.

## Climate change projections

- For the A1B emissions scenario projected temperature increases over Turkey are around 2.5-3°C in the north, 3-3.5°C over central and south-western regions, and 3.5-4.0°C in the east. There is consistently good agreement between the CMIP3 models over Turkey and the region in general.
- Turkey is projected to experience mainly decreases in precipitation, in common with the wider Mediterranean and majority of the Middle East. Decreases of over 20% are projected in the south of the country, with strong agreement across the CMIP3 ensemble. Smaller changes of between 0-10% are projected towards the north, but with more moderate agreement between the CMIP3 models.

## Climate change impacts projections

### Crop yields

- The majority of global- and regional-scale studies included here generally project declines in maize yields, one of the country's major crops.

- National-scale studies broadly concur with the global- and regional-scale projections of a decline in maize yields in the future.

### **Food security**

- Turkey is currently a country with extremely low levels of undernourishment. The majority of global-scale studies included here project a positive outlook for the impact of climate change on food security in Turkey. Considering land-based food production, Turkey is not projected to face severe food insecurity over the next 40 years.

### **Water stress and drought**

- Several global- and national-scale studies included here project that droughts in Turkey could increase in frequency and magnitude with climate change, with the greatest potential impacts projected for the south of the country.
- There is also consensus among global-, national- and sub-national-scale studies included here that water stress in Turkey could increase with climate change.
- Recent simulations by the AVOID programme project a median increase of around 45% of Turkey's population to be exposed to increases in water stress by 2100 under the A1B emissions scenario. Under an aggressive mitigation scenario, this increase is limited to 30%.

### **Fluvial Flooding**

- The consensus across the few published studies into the impact of climate change on fluvial flooding for Turkey suggests that extreme flood events could occur less frequently than present under climate change.
- Supporting this, recent simulations from the AVOID programme also indicate that flood risk in Turkey could decrease with climate change throughout the 21<sup>st</sup> century.

## **Coastal regions**

- A number of national-scale studies suggest that Turkey could experience appreciable coastal impacts from SLR.
- One study estimates that the population in Turkey exposed to SLR is around 428,000 along the Mediterranean coast, 208,000 along the Aegean coast, 842,000 in the Marmara region and 201,000 along the Black Sea coast.





# Table of Contents

<b>Chapter 1 – Climate Observations</b> .....	<b>9</b>
<b>Rationale</b> .....	<b>10</b>
<b>Climate overview</b> .....	<b>12</b>
Analysis of long-term features in the mean temperature .....	13
<b>Temperature extremes</b> .....	<b>16</b>
Recent extreme temperature events .....	17
Heat wave, Summer 2007.....	17
Cold spell, January 2008.....	17
Analysis of long-term features in moderate temperature extremes .....	17
Attribution of changes in likelihood of occurrence of seasonal temperatures.....	23
Summer 2007.....	23
Winter 2007/08.....	24
<b>Precipitation extremes</b> .....	<b>26</b>
Recent extreme precipitation events .....	27
Southeast floods, October 2006.....	27
Analysis of long-term features in precipitation .....	27
<b>Summary</b> .....	<b>31</b>
<b>Methodology annex</b> .....	<b>32</b>
Recent, notable extremes.....	32
Observational record .....	33
Analysis of seasonal mean temperature .....	33
Analysis of temperature and precipitation extremes using indices .....	34
Presentation of extremes of temperature and precipitation .....	44
Attribution.....	48
<b>References</b> .....	<b>51</b>
<b>Acknowledgements</b> .....	<b>54</b>
<b>Chapter 2 – Climate Change Projections</b> .....	<b>55</b>
<b>Introduction</b> .....	<b>56</b>
<b>Climate projections</b> .....	<b>58</b>
Summary of temperature change in Turkey .....	59
Summary of precipitation change in Turkey .....	59
<b>Chapter 3 – Climate Change Impact Projections</b> .....	<b>61</b>
<b>Introduction</b> .....	<b>62</b>
Aims and approach.....	62
Impact sectors considered and methods .....	62
Supporting literature .....	63
AVOID programme results.....	63
Uncertainty in climate change impact assessment.....	64
<b>Summary of findings for each sector</b> .....	<b>68</b>

<b>Crop yields</b> .....	<b>71</b>
Headline.....	71
Supporting literature .....	71
Introduction .....	71
Assessments that include a global or regional perspective .....	73
National-scale or sub-national scale assessments .....	79
AVOID programme results.....	80
Methodology.....	80
Results .....	81
<b>Food security</b> .....	<b>83</b>
Headline.....	83
Supporting literature .....	83
Introduction .....	83
Assessments that include a global or regional perspective .....	83
National-scale or sub-national scale assessments .....	92
<b>Water stress and drought</b> .....	<b>93</b>
Headline.....	93
Supporting literature .....	93
Introduction .....	93
Assessments that include a global or regional perspective .....	94
National-scale or sub-national scale assessments .....	101
AVOID Programme Results.....	102
Methodology.....	102
Results .....	103
<b>Pluvial flooding and rainfall</b> .....	<b>105</b>
Headline.....	105
Supporting literature .....	105
Assessments that include a global or regional perspective .....	105
National-scale or sub-national scale assessments .....	106
<b>Fluvial flooding</b> .....	<b>107</b>
Headline.....	107
Supporting literature .....	107
Introduction .....	107
Assessments that include a global or regional perspective .....	108
National-scale or sub-national scale assessments .....	108
AVOID programme results.....	109
Methodology.....	109
Results .....	110
<b>Tropical cyclones</b> .....	<b>112</b>
<b>Coastal regions</b> .....	<b>113</b>
Headline.....	113
Supporting literature .....	113
Assessments that include a global or regional perspective .....	113
National-scale or sub-national scale assessments .....	115

**References..... 117**



# **Chapter 1 – Climate Observations**

## Rationale

Present day weather and climate play a fundamental role in the day to day running of society. Seasonal phenomena may be advantageous and depended upon for sectors such as farming or tourism. Other events, especially extreme ones, can sometimes have serious negative impacts posing risks to life and infrastructure and significant cost to the economy. Understanding the frequency and magnitude of these phenomena, when they pose risks or when they can be advantageous and for which sectors

of society, can significantly improve societal resilience. In a changing climate it is highly valuable to understand possible future changes in both potentially hazardous events and those reoccurring seasonal events that are depended upon by sectors such as agriculture and tourism. However, in order to put potential future changes in context, the present day must first be well understood both in terms of common seasonal phenomena and extremes.

The purpose of this chapter is to summarise the weather and climate from 1960 to present day. This begins with a general climate overview including an up to date analysis of changes in surface mean temperature. These changes may be the result of a number of factors including climate change, natural variability and changes in land use. There is then a focus on extremes of temperature and precipitation selected from 2000 onwards, reported in the World Meteorological Organization (WMO) Annual Statement on the Status of the Global Climate and/or the Bulletin of the American Meteorological Society (BAMS) State of the Climate reports. This is followed by a discussion of changes in moderate extremes from 1960 onwards using an updated version of the HadEX extremes database (Alexander et al. 2006) which categorises extremes of temperature and precipitation. These are core climate variables which have received significant effort from the climate research community in terms of data acquisition and processing and for which it is possible to produce long high quality records for monitoring. For seasonal temperature extremes, an attribution analysis then puts the seasons with highlighted extreme events into context of the recent climate versus a hypothetical climate in the absence of anthropogenic emissions (Christidis et al., 2011). It is important to note that we carry out our attribution analyses on seasonal mean temperatures over the entire country. Therefore these analyses do not attempt to attribute



**Figure 1.** Location of boxes for the regional average time series (red dashed box) in Figures 3 and 4.

the changed likelihood of individual extreme events. The relationship between extreme events and the large scale mean temperature is likely to be complex, potentially being influenced by *inter alia* circulation changes, a greater expression of natural internal variability at smaller scales, and local processes and feedbacks.

Attribution of individual extreme events is an area of developing science. The work presented here is the foundation of future plans to systematically address the region's present and projected future weather and climate, and the associated impacts.

The methodology annex that follows provides details of the data shown here and of the scientific analyses underlying the discussions of changes in the mean temperature and in temperature and precipitation extremes. It also explains the methods used to attribute the likelihood of occurrence of seasonal mean temperatures.

## Climate overview

Turkey lies between latitudes 36-42°N and adjacent to the Mediterranean Sea and so might be expected to have a Mediterranean climate. This does apply to the southern and western coastal areas, but further to the east and north a number of factors make the climate more complex. These factors include extremely varied topography, an inland sea (the Black Sea) to the north and, beyond that, the vast Russian plain which, in winter, acts as a close source of very cold air. Contrastingly, the east of Turkey adjoins Syria and the Middle East which become very hot in summer and the southern coastline is only around 500km across the Mediterranean from the hot continent of Africa. Most of Turkey is high plateau and the terrain becomes increasingly mountainous towards the east. Even in the lower-lying west the terrain is mostly hilly.

In summer, southern coastal areas are mostly dry and sunny. However, in winter the northern hemisphere zone of eastward moving weather disturbances migrates southwards to affect these areas. Precipitation amounts to around 650 mm/year at Adana, most of it in the winter half of the year. Moving north and east across Turkey, most areas retain at least one or two summer months that are markedly drier than the rest of the year, albeit with occasional thunderstorms. However, the winter-summer contrast in precipitation amount becomes less pronounced and, inland, a double precipitation cycle emerges, peaking in both autumn and spring. Despite the higher altitude, inland areas have lower annual totals than on the coast – e.g. annual average precipitation only 382 mm at Ankara and 436mm at Erzurum. Along the Black Sea coast, precipitation increases eastwards from around 680mm at Istanbul, where there is still a clear winter peak, to 823mm at Trabzon, where the wettest season is autumn.

In general, Turkey is warm or hot in summer and cold or very cold in winter. However, coasts are much milder in winter than inland, especially the south and west coasts. Winter precipitation on the inland plateaux and mountains is often of snow which can lie for 3-4 months in the east. Annual mean temperatures are higher along the coasts and, inland, reduced by altitude. Examples, including the seasonal range in monthly mean temperature about the annual mean, are  $19\pm 10^{\circ}\text{C}$  at south coastal Adana,  $15\pm 8^{\circ}\text{C}$  at north coastal Trabzon,  $14\pm 9^{\circ}\text{C}$  at Istanbul,  $12\pm 11^{\circ}\text{C}$  at inland Ankara and  $6\pm 14^{\circ}\text{C}$  at inland Erzurum, which is 1750 m above mean sea level. These figures illustrate the quite large contrast between summer and winter temperatures, especially inland. Typical summer daily maxima range from  $\sim 26\text{-}28^{\circ}\text{C}$  along the Black Sea coastline to  $34^{\circ}\text{C}$  towards the east of the



Mediterranean coastline. Typical winter daytime maxima range dramatically from 15°C at Adana to below freezing inland in the east, e.g. only -4°C at Erzurum.

Weather hazards in Turkey include floods and, particularly, spells of extreme heat in summer or cold in winter.

## **Analysis of long-term features in the mean temperature**

CRUTEM3 data (Brohan et al., 2006) have been used to provide an analysis of mean temperatures from 1960 to 2010 over Turkey using the median of pairwise slopes method to fit the trend (Sen, 1968; Lanzante, 1996). The methods are fully described in the methodology section. Over the period 1960 to 2010, there is a mixed signal for temperature over Turkey as shown in Figure 2. There is a spatially consistent warming signal for summer (June to August) with higher confidence for all grid boxes in that the 5<sup>th</sup> to 95<sup>th</sup> percentiles of the slopes are of the same sign. This is consistent with reports from Turkey's First National Communication to the UNFCCC (UNFCCC 2007). For winter (December to February) there is a very mixed signal. Confidence is lower in all grid boxes over the region. Regionally averaged trends (over grid boxes included in the red dashed box in Figure 1) show warming with higher confidence only for summer and cooling over winter but with lower confidence in the signal. The trend is relatively large over summer at 0.34°C per decade (5<sup>th</sup> to 95<sup>th</sup> percentile of slopes: 0.21 to 0.48°C per decade). In winter the trend is very small at -0.01°C per decade (5<sup>th</sup> to 95<sup>th</sup> percentile of slopes: -0.21 to 0.26°C per decade).

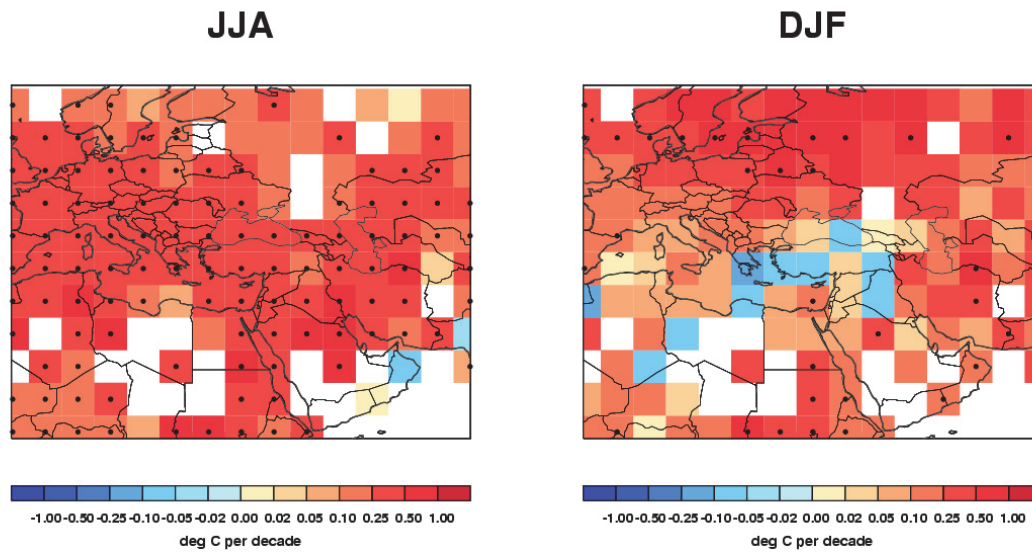


**Figure 2.** Decadal trends in seasonally averaged temperatures for Turkey and surrounding regions over the period 1960 to 2010. Monthly mean anomalies from CRUTEM3 (Brohan et al. 2006) are averaged over each 3 month season (June-July-August – JJA and December-January-February – DJF). Trends are fitted using the median of pairwise slopes method (Sen 1968, Lanzante 1996). There is higher confidence in the trends shown if the 5<sup>th</sup> to 95<sup>th</sup> percentiles of the pairwise slopes do not encompass zero because here the trend is considered to be significantly different from a zero trend (no change). This is shown by a black dot in the centre of the respective grid box.

Trends of annually and seasonally averaged mean temperature for Turkey are provided in Demir et al. 2008 for the period 1952 to 2006 and the annually averaged time series shown in Figure 3. The seasonal and annual trends are reported to show increases. For the annual time series there is no clear change over the full period but some warming is apparent from the 1990s.

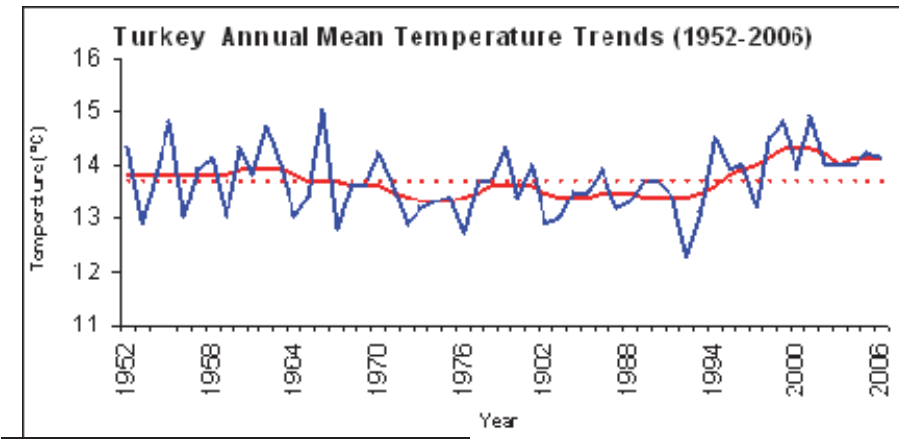


**Figure 3.** Interannual variations in the regionally averaged mean temperature series of 57 stations in Turkey, with a smoothed line provided by the binomial filter (from Demir et al., 2008).

## Temperature extremes

Both hot and cold temperature extremes can place many demands on society. While seasonal changes in temperature are normal and indeed important for a number of societal sectors (e.g. tourism, farming etc.), extreme heat or cold can have serious negative impacts. Importantly, what is 'normal' for one region may be extreme for another region that is less well adapted to such temperatures.

Table 1 shows selected extreme events since 2000 that are reported in WMO Statements on Status of the Global Climate and/or BAMS State of the Climate reports. Two recent events, the heat wave during summer 2007 and the cold spell during January 2008, are highlighted here as examples of recent extreme events in Turkey.

Year	Month	Event	Details	Source
2000	Jun-Jul	Heat wave	Temperatures exceeded 43°C, breaking many records and claiming numerous lives.	WMO (2001)
2007	Jun-Jul	Heat wave	For south-eastern Europe and Mediterranean area: June and July heat waves prompted record levels of electricity demand; about 40 deaths and over 130 fires blamed on the heat.	WMO (2008)
2008	Jan	Cold	Coldest January nights in nearly 50 years.	WMO (2009)

**Table 1.** Selected extreme temperature events reported in WMO Statements on Status of the Global Climate and/or BAMS State of the Climate reports since 2000.

## **Recent extreme temperature events**

### **Heat wave, Summer 2007**

Two extreme heat waves affected south-eastern Europe and the Mediterranean, including Turkey, in June and July. In Turkey, temperatures were significantly above average from May to October (Sensoy, 2008). The heat waves prompted record levels of electricity demand, and over south-eastern Europe and the Mediterranean area there were 40 deaths and over 130 fires due to the heat (WMO, 2008).

### **Cold spell, January 2008**

During January 2008, an exceptional cold outbreak occurred across Eurasia, from Turkey to China, resulting in many hundreds of deaths. In Turkey, mean monthly temperatures were as low as  $-8^{\circ}\text{C}$  and nearly 50 extreme events were recorded (Rogers et al., 2009). Some places experienced their coldest January nights in nearly 50 years (WMO, 2009). Snow cover across Eurasia was at record levels for the month of January (Rogers et al., 2009). Across Turkey, 49 extreme events, including heavy snowfall, storms and frosts were reported (Sensoy, 2009). This cold spell was thought to be due to the Siberian high-pressure system that affected Turkey, combined with prevailing La Nina conditions.

## **Analysis of long-term features in moderate temperature extremes**

HadEX extremes indices (Alexander et al., 2006) are used here for Turkey from 1960 to 2003 using daily maximum and minimum temperatures. Here we discuss changes in the frequency of cool days and nights and warm days and nights which are moderate extremes. Cool days/nights are defined as being below the 10<sup>th</sup> percentile of daily maximum/minimum temperature and warm days/nights are defined as being above the 90<sup>th</sup> percentile of the daily maximum/minimum temperature. The methods are fully described in the methodology section.

Between the late 1960s and 2003, the trend towards fewer cool nights and more warm nights and warm days is spatially consistent and in concert with the predominant pattern of increasing mean temperatures. There is a more mixed signal for changes in cool day frequency. The data presented here are annual totals, averaged across all seasons, and so

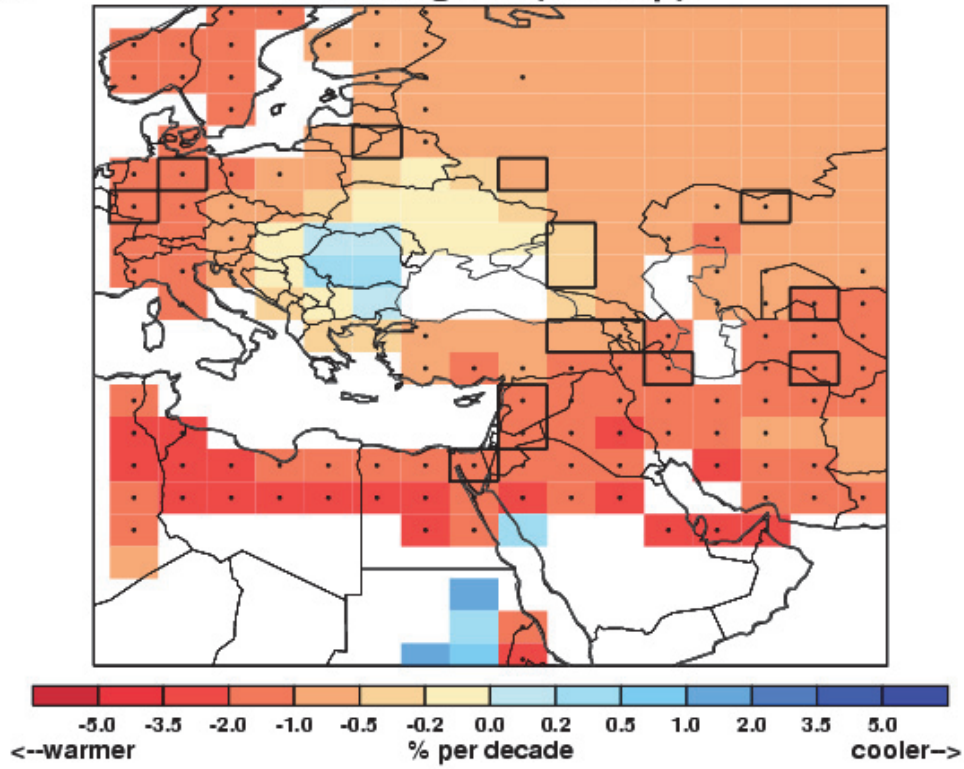
direct interpretation in terms of summertime heat waves and winter cold snaps is not possible.

Night time temperatures (daily minima) show widespread decreases in the frequency of cool nights and increases in the frequency of warm nights with widespread higher confidence, especially for the increase in warm nights (Figure 4 a,b,c,d). Regional averages show higher confidence in a trend of fewer cool nights and more warm nights. Local research (Demir et al., 2008) shows increasing daily minimum temperatures. This signal is statistically significant for the majority of stations assessed in Turkey. The regional average time series (Figure 5) shows warming from the 1990s but no clear change signal prior to that.

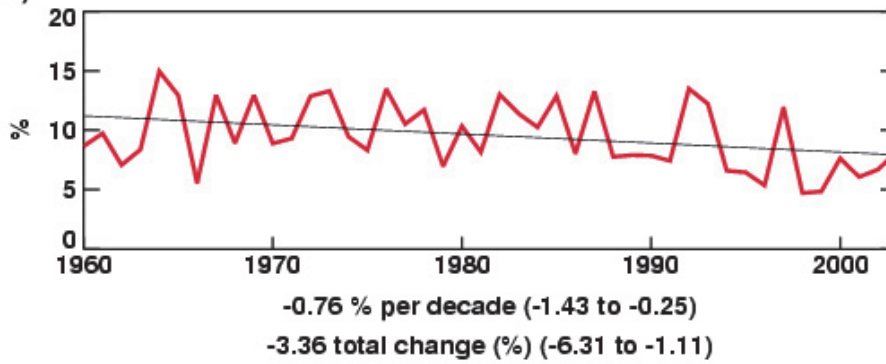
Daytime temperatures (daily maxima) show a mixed signal in frequency of cool days but a spatially consistent signal for increasing warm days (Figure 4 e,f,g,h). However, confidence is higher only for increases in the number of warm days over the east of Turkey. Confidence in the regional average trend of increasing warm days is higher. Local research (Demir et al., 2008) shows increasing daily maximum temperatures. As for minimum temperatures, the regional average time series (Figure 5) shows warming from the 1990s but no clear change signal prior to that.

In the HadEX data, the small numbers of stations present in most grid boxes means that even if there is higher confidence in the signals shown, uncertainty in the signal being representative of the wider grid box is large.

a) **cool nights (TN10p)**

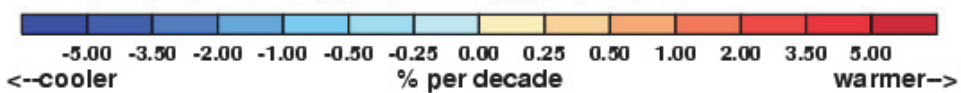
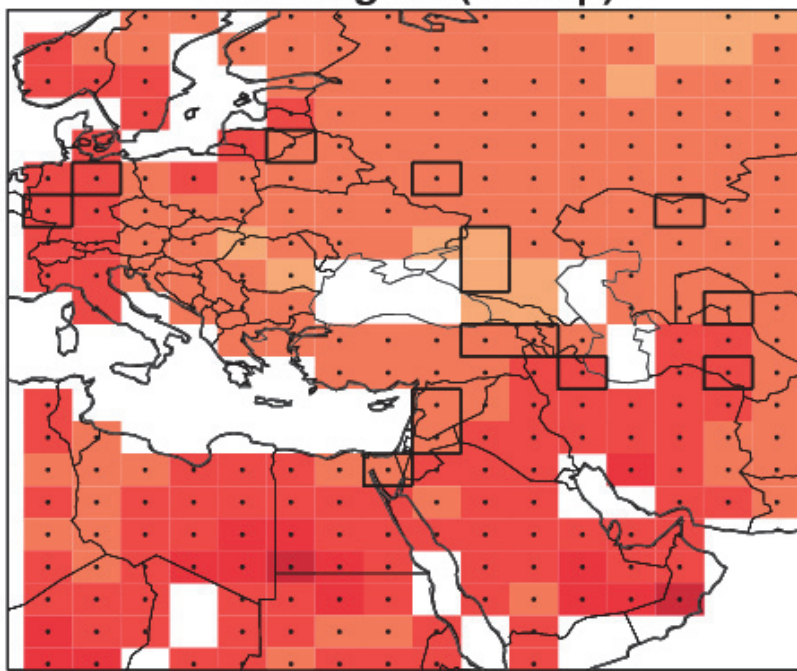


b)

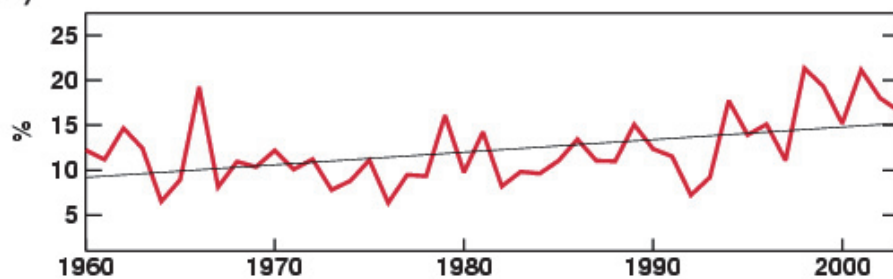


c)

### warm nights (TN90p)



d)

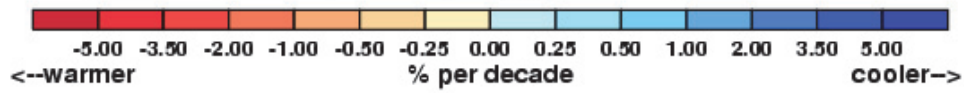
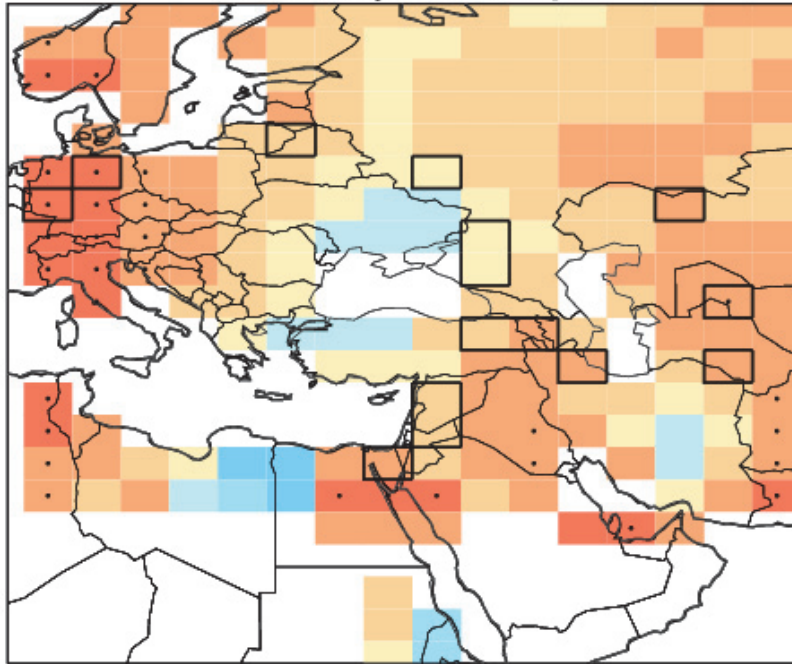


1.40 % per decade (0.47 to 2.29)  
6.18 total change (%) (2.05 to 10.07)

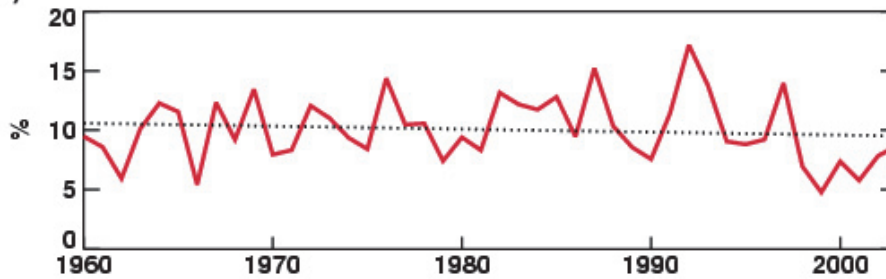


e)

### cool days (TX10p)



f)



-0.25 % per decade (-0.94 to 0.49)  
-1.10 total change (%) (-4.12 to 2.14)

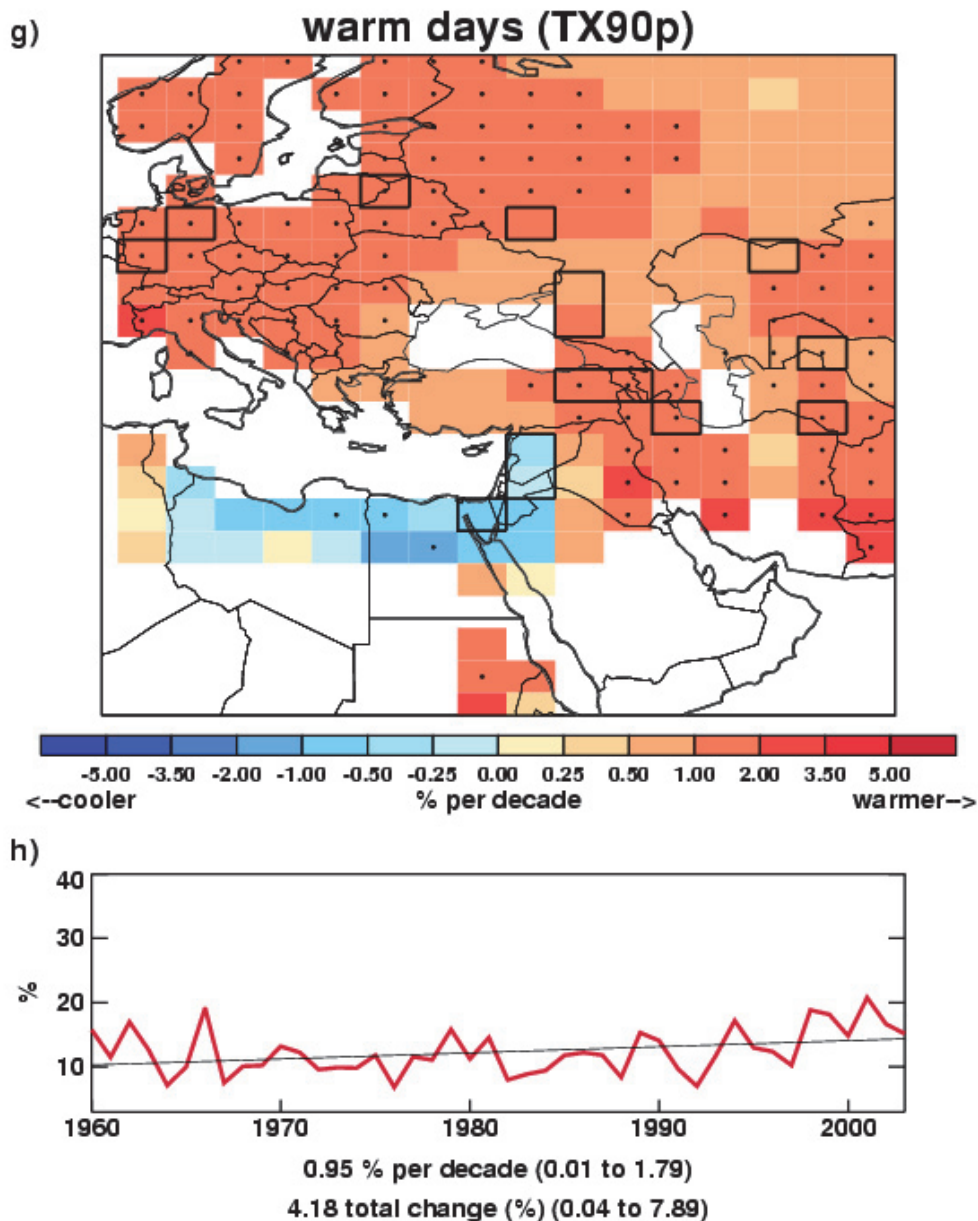


**Figure 4.** Percentage change in cool nights (a,b), warm nights (c,d), cool days (e,f) and warm days (g,h) for Turkey over the period 1960 to 2003 relative to 1961-1990 from HadEX (Alexander et al. 2006). a,c,e,g) Grid box decadal trends. Grid boxes outlined in solid black contain at least 3 stations and so are likely to be more representative of the wider grid box. Trends are fitted using the median of pairwise slopes method (Sen 1968, Lanzante 1996). High confidence in a long-term trend is shown by a black dot if the 5<sup>th</sup> to 95<sup>th</sup> percentile slopes are of the same sign. Differences in spatial coverage occur because each index has its own decorrelation length scale (see methodology section). b,d,f,h) Area averaged annual time series for 24.375 to 46.875° E, 36.25 to 43.75° N as shown in the red box in Figure 1. Trends are fitted as described above. The decadal trend and its 5<sup>th</sup> to 95<sup>th</sup> percentile pairwise slopes are stated below the time series plot, as well as the change over the period for which there are data. Higher confidence in the trends, as denoted above, is shown by a solid black line as opposed to a dotted one.

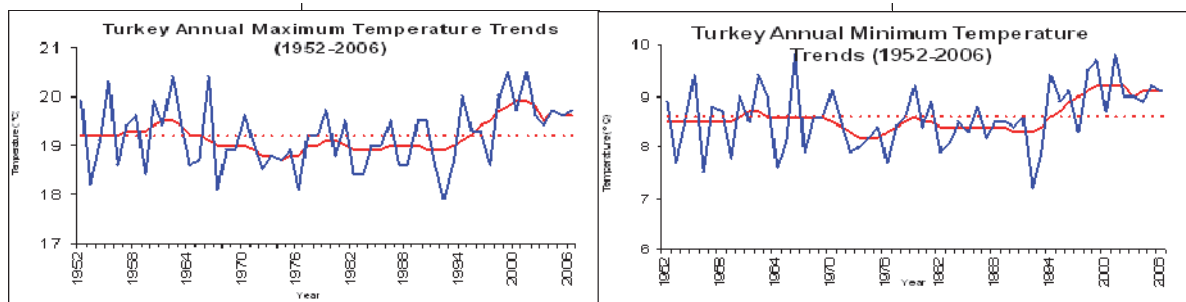


**Figure 5.** Interannual variations in the regional average of daily maximum and minimum temperature series for 57 stations in Turkey smoothed by the binomial filter (from Demir et al. 2008).

The annual number of frost days has evidently decreased at most of the stations with some observed regional differences. The decreasing trends are largest over Eastern Anatolia, the Marmara regions and along the Mediterranean coastline. The meteorological stations located in the continental northeast and the easternmost parts of the Anatolian Peninsula, including Ardahan, Iğdır and Van, show a negative linear trend with a rate of four days per decade (Erlat and Turkes, 2011).

## Attribution of changes in likelihood of occurrence of seasonal temperatures

Today's climate covers a range of likely extremes. Recent research has shown that the temperature distribution of seasonal means would likely be different in the absence of anthropogenic emissions (Christidis et al., 2011). Here we discuss the seasonal means, within which the highlighted extreme temperature events occur, in the context of recent climate and the influence of anthropogenic emissions on that climate. The methods are fully described in the methodology section.

### Summer 2007

The distributions of the June-July-August (JJA) mean regional temperature in recent years in the presence and absence of anthropogenic forcings are shown in Figure 6. Analyses with both models suggest that human influences on the climate have shifted the distribution to higher temperatures. Considering the average over the entire region, the summer of 2007 is hot, as it lies at the warm tail of the temperature distributions for the climate influenced by

anthropogenic forcings (red distributions) and is the hottest since 1900 in the CRUTEM3 dataset. In the absence of human influences on the climate (green distributions), the season would be even more extreme. It should be noted that the attribution results shown here refer to temperature anomalies over the entire region and over an entire season, whereas the actual extreme event had a shorter duration and affected a smaller region.

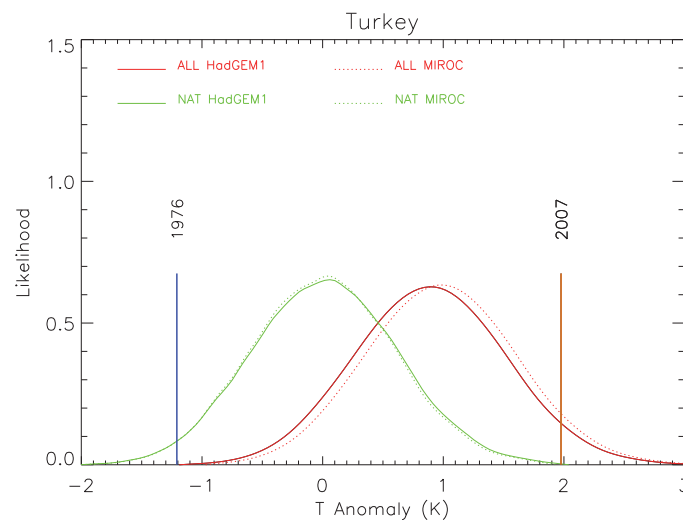


**Figure 6.** Distributions of the June-July-August mean temperature anomalies (relative to 1961-1990) averaged over an eastern Mediterranean region that encompasses Turkey (18-46E, 32-45N – as shown in Figure 1) including (red lines) and excluding (green lines) the influence of anthropogenic forcings. The distributions describe the seasonal mean temperatures expected in recent years (2000-2009) and are based on analyses with the HadGEM1 (solid lines) and MIROC (dotted lines) models. The vertical orange and blue lines correspond to the maximum and minimum anomaly in the CRUTEM3 dataset since 1900 respectively.

### Winter 2007/08

The distributions of the December-January-February (DJF) mean regional temperature in recent years in the presence and absence of anthropogenic forcings are shown in Figure 7. Analyses with both models suggest that human influences on the climate have shifted the distributions to higher temperatures. The winter of 2007/08 is cold, as shown in Figure 7, as it lies near the cold tail of the seasonal temperature distribution for the climate influenced by anthropogenic forcings (distributions plotted in red). It is considerably warmer than the winter of 1991/92, which is the coldest since 1900 in the CRUTEM3 dataset. In the absence of human influences (green distributions), the season lies nearer the central sector of the temperature distribution and would therefore be a less extreme season. The attribution results shown here refer to temperature anomalies over the entire region and over an entire season, whereas an extreme event has a shorter duration and affects a smaller region.

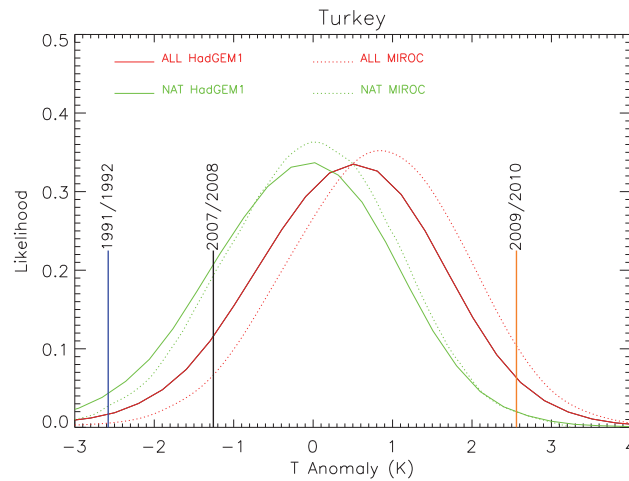


**Figure 7.** Distributions of the December-January-February mean temperature anomalies (relative to 1961-1990) averaged over an eastern Mediterranean region that encompasses Turkey (18-46E, 32-45N – as shown in Figure 1) including (red lines) and excluding (green lines) the influence of anthropogenic forcings. The distributions describe the seasonal mean temperatures expected in recent years (2000-2009) and are based on analyses with the HadGEM1 (solid lines) and MIROC (dotted lines) models. The vertical black line marks the observed anomaly in 2007/08 and the vertical orange and blue lines correspond to the maximum and minimum anomaly in the CRUTEM3 dataset since 1900 respectively.

## Precipitation extremes

Precipitation extremes, either excess or deficit, can be hazardous to human health, societal infrastructure, and livestock and agriculture. While seasonal fluctuations in precipitation are normal and indeed important for a number of societal sectors (e.g. tourism, farming etc.), flooding or drought can have serious negative impacts. These are complex phenomena and often the result of accumulated excesses or deficits or other compounding factors such as spring snow-melt, high tides/storm surges or changes in land use. The analysis section below deals purely with precipitation amounts.

Table 2 shows selected extreme events since 2000 that are reported in WMO Statements on Status of the Global Climate and/or BAMS State of the Climate reports. The flooding during October 2006 is highlighted below as an example of a recent extreme precipitation event that affected Turkey.

Year	Month	Event	Details	Source
2004	Feb	Storm	Widespread winter storm.	WMO (2005)
2006	Oct	Flooding	10 people died in Diyarbakir from flooding.	Sensoy (2007)
2009	Sep	Flooding	North-western Turkey received its heaviest rainfall in 80 years in a 48-hour period. Istanbul received 67mm of rain within one hour on 9 September.	WMO (2010), BAMS (Obregon et al., 2010)
2010	Aug	Flooding	Extreme rainfall in Rize, associated with floods and landslides. 13 people died and 168 houses were destroyed.	BAMS (Sensoy and Dermican, 2011)
2010	Oct	Flooding	1 in 200 year rainfall in Bursa, leading to 1 death.	BAMS (Sensoy and Dermican, 2011)

**Table 2.** Selected extreme precipitation events reported in WMO Statements on Status of the Global Climate and/or BAMS State of the Climate reports since 2000.

## **Recent extreme precipitation events**

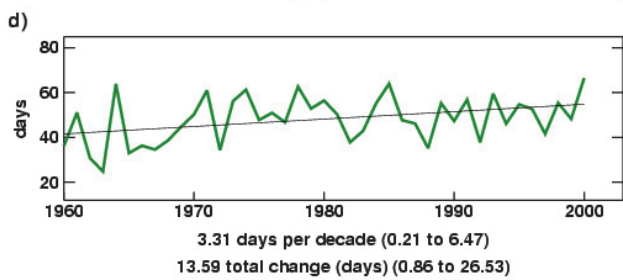
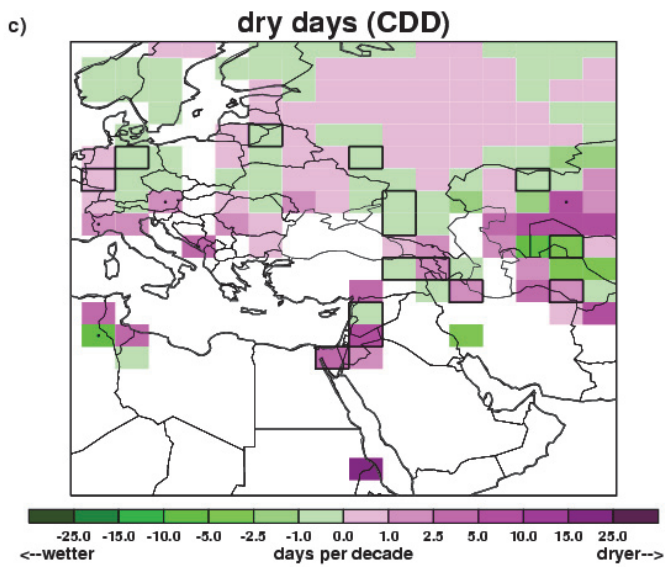
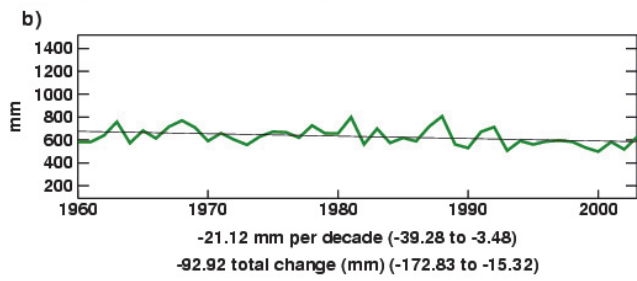
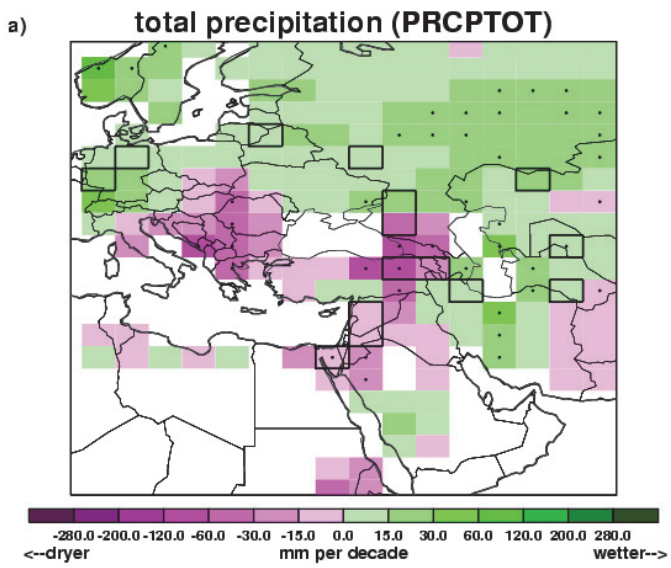
### **Southeast floods, October 2006**

In October 2006, there were severe flash floods in Turkey. The worst affected areas were the south-eastern provinces of Sanliurfa, Diyarbakir, Sirnak and Batman. In Diyarbakir 10 people died (Sensory, 2007). Across the whole region, according to the disaster report, about 40 people were killed, 1000 homes damaged and an estimated 63,000 people affected.

## **Analysis of long-term features in precipitation**

HadEX extremes indices (Alexander et al., 2006) are used here for Turkey from 1960 to 2003 using daily precipitation totals. Here we discuss changes in the annual total precipitation, and in the frequency of prolonged (greater than 6 days) wet and dry spells. The methods are fully described in the methodology section.

Between 1960 and 2003 there is a mixed signal in annual total precipitation over Turkey (Figure 8). Decreasing total precipitation is widespread with higher confidence in grid boxes over the northeast and for the regional average. There are very few grid boxes with data for changes in dry spells (Figure 8c) and wet spells (Figure 8e) over Turkey. This is due to the decorrelation length scale for precipitation, and over Turkey especially, being short.





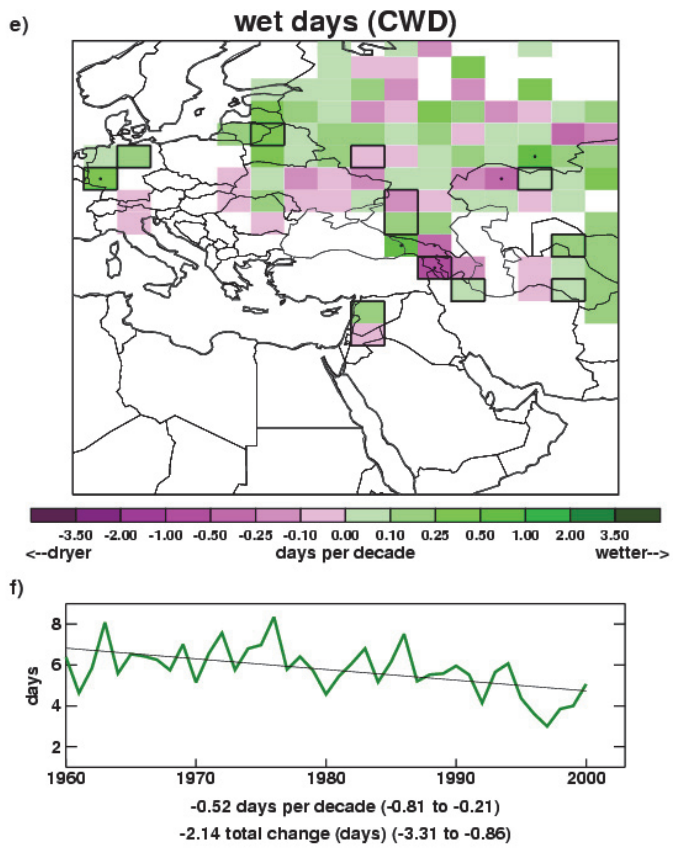


**Figure 8.** Change in total annual precipitation, continuous dry spell length and continuous wet spell length for Turkey over the period 1960 to 2003 relative to 1961-1990 from HadEX (Alexander et al., 2006). a) Decadal trends as described in Figure 4. b) Area average annual time-series for 24.375 to 46.875° E, 36.25 to 43.75° N as described in Figure 4.

Local research (UNFCCC 2007) shows changes in precipitation seasonally from 1951 to 2004 (Figure 9 a to d). Winter precipitation in the western provinces of Turkey has decreased significantly in the last five decades. Autumn (fall) precipitation, on the other hand, has increased at the stations that lie mostly in the northern parts of the Central Anatolia.

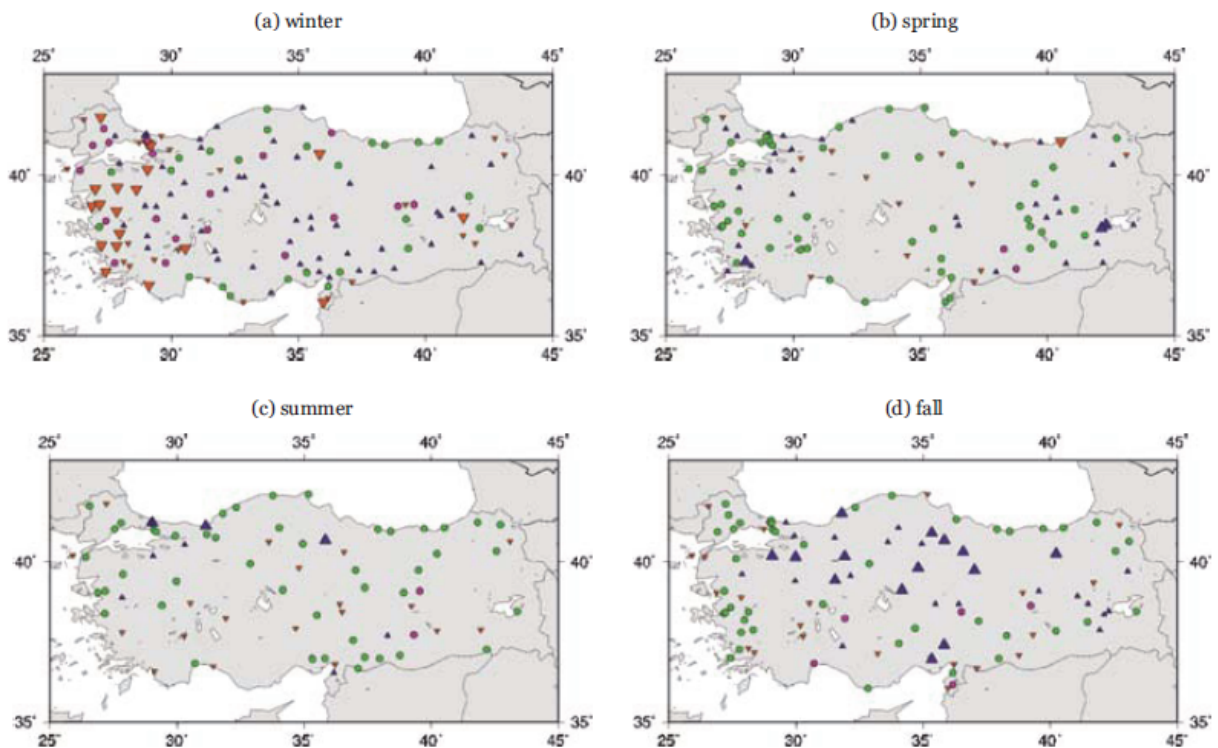


**Figure 9.** Seasonal precipitation trends using the Mann-Kendall test for the period 1951-2004. Large circles denote no trend. Large blue triangles denote significant increases while small blue triangles denote increases that are not significant. Large red inverted triangles denote significant decreases while small inverted red triangles denote decreases that are not significant (from UNFCCC 2007).

# Summary

**The main features seen in observed climate over Turkey in this analysis are:**

- There are coherent warming trends during summer over Turkey since 1960 and in the annual regional average mean, minimum and maximum temperature since the 1990s.
- Since 1960 there have been widespread decreases in the frequency of cool nights and increases in the frequency of warm nights.
- Changes in precipitation are mixed with decreases in winter in the west and increases in autumn in the north.

# Methodology annex

## Recent, notable extremes

In order to identify what is meant by 'recent' events the authors have used the period since 1994, when WMO Status of the Global Climate statements were available to the authors. However, where possible, the most notable events during the last 10 years have been chosen as these are most widely reported in the media, remain closest to the forefront of the memory of the country affected, and provide an example likely to be most relevant to today's society. By 'notable' the authors mean any event which has had significant impact either in terms of cost to the economy, loss of life, or displacement and long term impact on the population. In most cases the events of largest impact on the population have been chosen, however this is not always the case.

Tables of recent, notable extreme events have been provided for each country. These have been compiled using data from the World Meteorological Organisation (WMO) Annual Statements on the Status of the Global Climate. This is a yearly report which includes contributions from all the member countries, and therefore represents a global overview of events that have had importance on a national scale. The report does not claim to capture all events of significance, and consistency across the years of records available is variable. However, this database provides a concise yet broad account of extreme events per country. This data is then supplemented with accounts from the monthly National Oceanic and Atmospheric Administration (NOAA) State of the Climate reports which outline global extreme events of meteorological significance.

We give detailed examples of heat, precipitation and storm extremes for each country where these have had significant impact. Where a country is primarily affected by precipitation or heat extremes this is where our focus has remained. An account of the impact on human life, property and the economy has been given, based largely on media reporting of events, and official reports from aid agencies, governments and meteorological organisations. Some data has also been acquired from the Centre for Research on Epidemiological Disasters (CRED) database on global extreme events. Although media reports are unlikely to be completely accurate, they do give an indication as to the perceived impact of an extreme event, and so are useful in highlighting the events which remain in the national psyche.

Our search for data has not been exhaustive given the number of countries and events included. Although there are a wide variety of sources available, for many events, an official account is not available. Therefore figures given are illustrative of the magnitude of impact only (references are included for further information on sources). It is also apparent that the reporting of extreme events varies widely by region, and we have, where possible, engaged with local scientists to better understand the impact of such events.

The aim of the narrative for each country is to provide a picture of the social and economic vulnerability to the current climate. Examples given may illustrate the impact that any given extreme event may have and the recovery of a country from such an event. This will be important when considering the current trends in climate extremes, and also when examining projected trends in climate over the next century.

## **Observational record**

In this section we outline the data sources which were incorporated into the analysis, the quality control procedure used, and the choices made in the data presentation. As this report is global in scope, including 23 countries, it is important to maintain consistency of methodological approach across the board. For this reason, although detailed datasets of extreme temperatures, precipitation and storm events exist for various countries, it was not possible to obtain and incorporate such a varied mix of data within the timeframe of this project. Attempts were made to obtain regional daily temperature and precipitation data from known contacts within various countries with which to update existing global extremes databases. No analysis of changes in storminess is included as there is no robust historical analysis of global land surface winds or storminess currently available.

### **Analysis of seasonal mean temperature**

Mean temperatures analysed are obtained from the CRUTEM3 global land-based surface-temperature data-product (Brohan et al. 2006), jointly created by the Met Office Hadley Centre and Climatic Research Unit at the University of East Anglia. CRUTEM3 comprises of more than 4000 weather station records from around the world. These have been averaged together to create 5° by 5° gridded fields with no interpolation over grid boxes that do not contain stations. Seasonal averages were calculated for each grid box for the 1960 to 2010 period and linear trends fitted using the median of pairwise slopes (Sen 1968; Lanzante 1996). This method finds the slopes for all possible pairs of points in the data, and takes

their median. This is a robust estimator of the slope which is not sensitive to outlying points. High confidence is assigned to any trend value for which the 5<sup>th</sup> to 95<sup>th</sup> percentiles of the pairwise slopes are of the same sign as the trend value and thus inconsistent with a zero trend.

### **Analysis of temperature and precipitation extremes using indices**

In order to study extremes of climate a number of indices have been created to highlight different aspects of severe weather. The set of indices used are those from the World Climate Research Programme (WCRP) Climate Variability and Predictability (CLIVAR) Expert Team on Climate Change Detection and Indices (ETCCDI). These 27 indices use daily rainfall and maximum and minimum temperature data to find the annual (and for a subset of the indices, monthly) values for, e.g., the 'warm' days where daily maximum temperature exceeds the 90<sup>th</sup> percentile maximum temperature as defined over a 1961 to 1990 base period. For a full list of the indices we refer to the website of the ETCCDI (<http://cccma.seos.uvic.ca/ETCCDI/index.shtml>).

Index	Description	Shortname	Notes
Cool night frequency	Daily minimum temperatures lower than the 10 <sup>th</sup> percentile daily minimum temperature using the base reference period 1961-1990	TN10p	---
Warm night frequency	Daily minimum temperatures higher than the 90 <sup>th</sup> percentile daily minimum temperature using the base reference period 1961-1990	TN90p	---
Cool day frequency	Daily maximum temperatures lower than the 10 <sup>th</sup> percentile daily maximum temperature using the base reference period 1961-1990	TX10p	---
Warm day frequency	Daily maximum temperatures higher than the 90 <sup>th</sup> percentile daily maximum temperature using the base reference period 1961-1990	TX90p	---
Dry spell duration	Maximum duration of continuous days within a year with rainfall <1mm	CDD	Lower data coverage due to the requirement for a 'dry spell' to be at least 6 days long resulting in intermittent temporal coverage
Wet spell duration	Maximum duration of continuous days with rainfall >1mm for a given year	CWD	Lower data coverage due to the requirement for a 'wet spell' to be at least 6 days long resulting in intermittent temporal coverage
Total annual precipitation	Total rainfall per year	PRCPTOT	---

**Table 3.** Description of ETCCDI indices used in this document.

A previous global study of the change in these indices, containing data from 1951-2003 can be found in Alexander et al. 2006, (HadEX; see <http://www.metoffice.gov.uk/hadobs/hadex/>). In this work we aimed to update this analysis to the present day where possible, using the most recently available data. A subset of the indices is used here because they are most easily related to extreme climate events (Table 3).

### **Use of HadEX for analysis of extremes**

The HadEX dataset comprises all 27 ETCCDI indices calculated from station data and then smoothed and gridded onto a 2.5° x 3.75° grid, chosen to match the output from the Hadley Centre suite of climate models. To update the dataset to the present day, indices are calculated from the individual station data using the RClmDex/FClimDex software; developed and maintained on behalf of the ETCCDI by the Climate Research Branch of the

Meteorological Service of Canada. Given the timeframe of this project it was not possible to obtain sufficient station data to create updated HadEX indices to present day for a number of countries: Brazil; Egypt; Indonesia; Japan (precipitation only); South Africa; Saudi Arabia; Peru; Turkey; and Kenya. Indices from the original HadEX data-product are used here to show changes in extremes of temperature and precipitation from 1960 to 2003. In some cases the data end prior to 2003. Table 4 summarises the data used for each country. Below, we give a short summary of the methods used to create the HadEX dataset (for a full description see Alexander et al., 2006).

To account for the uneven spatial coverage when creating the HadEX dataset, the indices for each station were gridded, and a land-sea mask from the HadCM3 model applied. The interpolation method used in the gridding process uses a decorrelation length scale (DLS) to determine which stations can influence the value of a given grid box. This DLS is calculated from the e-folding distance of the individual station correlations. The DLS is calculated separately for five latitude bands, and then linearly interpolated between the bands. There is a noticeable difference in spatial coverage between the indices due to these differences in decorrelation length scales. This means that there will be some grid-box data where in fact there are no stations underlying it. Here we apply black borders to grid-boxes where at least 3 stations are present to denote greater confidence in representation of the wider grid-box area there. The land-sea mask enables the dataset to be used directly for model comparison with output from HadCM3. It does mean, however, that some coastal regions and islands over which one may expect to find a grid-box are in fact empty because they have been treated as sea

### **Data sources used for updates to the HadEX analysis of extremes**

We use a number of different data sources to provide sufficient coverage to update as many countries as possible to present day. These are summarised in Table 4. In building the new datasets we have tried to use exactly the same methodology as was used to create the original HadEX to retain consistency with a product that was created through substantial international effort and widely used, but there are some differences, which are described in the next section.

Wherever new data have been used, the geographical distributions of the trends were compared to those obtained from HadEX, using the same grid size, time span and fitting method. If the pattern of the trends in the temperature or precipitation indices did not match that from HadEX, we used the HadEX data despite its generally shorter time span. Differences in the patterns of the trends in the indices can arise because the individual



stations used to create the gridded results are different from those in HadEX, and the quality control procedures used are also very likely to be different. Countries where we decided to use HadEX data despite the existence of more recent data are Egypt and Turkey.

#### GHCND:

The Global Historical Climate Network Daily data has near-global coverage. However, to ensure consistency with the HadEX database, the GHCND stations were compared to those stations in HadEX. We selected those stations which are within 1500m of the stations used in the HadEX database and have a high correlation with the HadEX stations. We only took the precipitation data if its  $r > 0.9$  and the temperature data if one of its  $r$ -values  $> 0.9$ . In addition, we required at least 5 years of data beyond 2000. These daily data were then converted to the indices using the *fclimdex* software.

#### ECA&D and SACA&D:

The European Climate Assessment and Dataset and the Southeast Asian Climate Assessment and Dataset data are pre-calculated indices comprising the core 27 indices from the ETCCDI as well as some extra ones. We kindly acknowledge the help of Albert Klein Tank, the KNMI<sup>1</sup> and the BMKG<sup>2</sup> for their assistance in obtaining these data.

#### Mexico:

The station data from Mexico has been kindly supplied by the SMN<sup>3</sup> and Jorge Vazquez. These daily data were then converted to the required indices using the *Fclimdex* software. There are a total of 5298 Mexican stations in the database. In order to select those which have sufficiently long data records and are likely to be the most reliable ones we performed a cross correlation between all stations. We selected those which had at least 20 years of data post 1960 and have a correlation with at least one other station with an  $r$ -value  $> 0.95$ . This resulted in 237 stations being selected for further processing and analysis.

#### Indian Gridded:

The India Meteorological Department provided daily gridded data (precipitation 1951-2007, temperature 1969-2009) on a  $1^\circ \times 1^\circ$  grid. These are the only gridded daily data in our analysis. In order to process these in as similar a way as possible the values for each grid

---

<sup>1</sup> Koninklijk Nederlands Meteorologisch Instituut – The Royal Netherlands Meteorological Institute

<sup>2</sup> Badan Meteorologi, Klimatologi dan Geofisika – The Indonesian Meteorological, Climatological and Geophysical Agency

<sup>3</sup> Servicio Meteorológico Nacional de México – The Mexican National Meteorological Service

were assumed to be analogous to a station located at the centre of the grid. We keep these data separate from the rest of the study, which is particularly important when calculating the decorrelation length scale, which is on the whole larger for these gridded data.

Country	Region box (red dashed boxes in Fig. 1 and on each map at beginning of chapter)	Data source (T = temperature, P = precipitation)	Period of data coverage (T = temperature, P = precipitation)	Indices included (see Table 3 for details)	Temporal resolution available	Notes
Argentina	73.125 to 54.375 ° W, 21.25 to 56.25 ° S	Matilde Rusticucci (T,P)	1960-2010 (T,P)	TN10p, TN90p, TX10p, TX90p, PRCPTOT, CDD, CWD	annual	
Australia	114.375 to 155.625 ° E, 11.25 to 43.75 ° S	GHCND (T,P)	1960-2010 (T,P)	TN10p, TN90p, TX10p, TX90p, PRCPTOT, CDD, CWD	monthly, seasonal and annual	Land-sea mask has been adapted to include Tasmania and the area around Brisbane
Bangladesh	88.125 to 91.875 ° E, 21.25 to 26.25 ° N	Indian Gridded data (T,P)	1960-2007 (P), 1970-2009 (T)	TN10p, TN90p, TX10p, TX90p, PRCPTOT, CDD, CWD	monthly, seasonal and annual	Interpolated from Indian Gridded data
Brazil	73.125 to 31.875 ° W, 6.25 ° N to 33.75 ° S	HadEX (T,P)	1960-2000 (P) 2002 (T)	TN10p, TN90p, TX10p, TX90p, PRCPTOT, CDD, CWD	annual	Spatial coverage is poor
China	73.125 to 133.125 ° E, 21.25 to 53.75 ° N	GHCND (T,P)	1960-1997 (P) 1960-2003 (T <sub>min</sub> ) 1960-2010 (T <sub>max</sub> )	TN10p, TN90p, TX10p, TX90p, PRCPTOT, CDD, CWD	monthly, seasonal and annual	Precipitation has very poor coverage beyond 1997 except in 2003-04, and no data at all in 2000-02, 2005-11
Egypt	24.375 to 35.625 ° E, 21.25 to 31.25 ° N	HadEX (T,P)	No data	TN10p, TN90p, TX10p, TX90p, PRCPTOT,	annual	There are no data for Egypt so all grid-box values have been interpolated from stations in Jordan, Israel, Libya and Sudan
France	5.625 ° W to 9.375 ° E, 41.25 to 51.25 ° N	ECA&D (T,P)	1960-2010 (T,P)	TN10p, TN90p, TX10p, TX90p, PRCPTOT, CDD, CWD	monthly, seasonal and annual	

Germany	5.625 to 16.875 ° E, 46.25 to 56.25 ° N	ECA&D (T,P)	1960-2010 (T,P)	TN10p, TN90p, TX10p, TX90p, PRCPTOT, CDD, CWD	monthly, seasonal and annual	
India	69.375 to 99.375 ° E, 6.25 to 36.25 ° N	Indian Gridded data (T,P)	1960-2003 (P), 1970-2009 (T)	TN10p, TN90p, TX10p, TX90p, PRCPTOT, CDD, CWD	monthly, seasonal and annual	
Indonesia	95.625 to 140.625 ° E, 6.25 ° N to 11.25 ° S	HadEX (T,P)	1968-2003 (T,P)	TN10p, TN90p, TX10p, TX90p, PRCPTOT,	annual	Spatial coverage is poor
Italy	5.625 to 16.875 ° E, 36.25 to 46.25 ° N	ECA&D (T,P)	1960-2010 (T,P)	TN10p, TN90p, TX10p, TX90p, PRCPTOT, CDD, CWD	monthly, seasonal and annual	Land-sea mask has been adapted to improve coverage of Italy
Japan	129.375 to 144.375 ° E, 31.25 to 46.25 ° N	HadEX (P) GHCND (T)	1960-2003 (P) 1960-2000 (T <sub>min</sub> ) 1960-2010 (T <sub>max</sub> )	TN10p, TN90p, TX10p, TX90p, PRCPTOT,	monthly, seasonal and annual (T), annual (P)	
Kenya	31.875 to 43.125 ° E, 6.25 ° N to 6.25 ° S	HadEX (T,P)	1960-1999 (P)	TN10p, TN90p, TX10p, TX90p, PRCPTOT	annual	There are no temperature data for Kenya and so grid-box values have been interpolated from neighbouring Uganda and the United Republic of Tanzania. Regional averages include grid-boxes from outside Kenya that enable continuation to 2003
Mexico	118.125 to 88.125 ° W, 13.75 to 33.75 ° N	Raw station data from the Servicio Meteorológico Nacional (SMN) (T,P)	1960-2009 (T,P)	TN10p, TN90p, TX10p, TX90p, PRCPTOT, CDD, CWD	monthly, seasonal and annual	237/5298 stations selected. Non uniform spatial coverage. Drop in T and P coverage in 2009.
Peru	84.735 to 65.625 ° W, 1.25 ° N to 18.75 ° S	HadEX (T,P)	1960-2002 (T,P)	TN10p, TN90p, TX10p, TX90p, PRCPTOT, CDD, CWD	annual	Intermittent coverage in TX90p, CDD and CWD

Russia	West Russia 28.125 to 106.875 ° E, 43.75 to 78.75 ° N, East Russia 103.125 to 189.375 ° E, 43.75 to 78.75 ° N	ECA&D (T,P)	1960-2010 (T,P)	TN10p, TN90p, TX10p, TX90p, PRCPTOT, CDD, CWD	monthly, seasonal and annual	Country split for presentation purposes only.
Saudi Arabia	31.875 to 54.375 ° E, 16.25 to 33.75 ° N	HadEX (T,P)	1960-2000 (T,P)	TN10p, TN90p, TX10p, TX90p, PRCPTOT	annual	Spatial coverage is poor
South Africa	13.125 to 35.625 ° W, 21.25 to 36.25 ° S	HadEX (T,P)	1960-2000 (T,P)	TN10p, TN90p, TX10p, TX90p, PRCPTOT, CDD, CWD	annual	---
Republic of Korea	125.625 to 129.375 ° E, 33.75 to 38.75 ° N	HadEX (T,P)	1960-2003 (T,P)	TN10p, TN90p, TX10p, TX90p, PRCPTOT, CDD	annual	There are too few data points for CWD to calculate trends or regional timeseries
Spain	9.375 ° W to 1.875 ° E, 36.25 to 43.75 ° N	ECA&D (T,P)	1960-2010 (T,P)	TN10p, TN90p, TX10p, TX90p, PRCPTOT, CDD, CWD	monthly, seasonal and annual	
Turkey	24.375 to 46.875 ° E, 36.25 to 43.75 ° N	HadEX (T,P)	1960-2003 (T,P)	TN10p, TN90p, TX10p, TX90p, PRCPTOT, CDD, CWD	annual	Intermittent coverage in CWD and CDD with no regional average beyond 2000
United Kingdom	9.375 ° W to 1.875 ° E, 51.25 to 58.75 ° N	ECA&D (T,P)	1960-2010 (T,P)	TN10p, TN90p, TX10p, TX90p, PRCPTOT, CDD, CWD	monthly, seasonal and annual	
United States of America	125.625 to 65.625 ° W, 23.75 to 48.75 ° N	GHCND (T,P)	1960-2010 (T,P)	TN10p, TN90p, TX10p, TX90p, PRCPTOT, CDD, CWD	monthly, seasonal and annual	

**Table 4. Summary of data used for each country**

## **Quality control and gridding procedure used for updates to the HadEX analysis of extremes**

In order to perform some basic quality control checks on the index data, we used a two-step process on the indices. Firstly, internal checks were carried out, to remove cases where the 5 day rainfall value is less than the 1 day rainfall value, the minimum T<sub>min</sub> is greater than the minimum T<sub>max</sub> and the maximum T<sub>min</sub> is greater than the maximum T<sub>max</sub>.

Although these are physically impossible, they could arise from transcription errors when creating the daily dataset, for example, a misplaced minus sign, an extra digit appearing in the record or a column transposition during digitisation. During these tests we also require that there are at least 20 years of data in the period of record for the index for that station, and that some data is found in each decade between 1961 and 1990, to allow a reasonable estimation of the climatology over that period.

Weather conditions are often similar over many tens of kilometres and the indices calculated in this work are even more coherent. The correlation coefficient between each station-pair combination in all the data obtained is calculated for each index (and month where appropriate), and plotted as a function of the separation. An exponential decay curve is fitted to the data, and the distance at which this curve has fallen by a factor  $1/e$  is taken as the decorrelation length scale (DLS). A DLS is calculated for each dataset separately. For the GHCND, a separate DLS is calculated for each hemisphere. We do not force the fitted decay curve to show perfect correlation at zero distance, which is different to the method employed when creating HadEX. For some of the indices in some countries, no clear decay pattern was observed in some data sets or the decay was so slow that no value for the DLS could be determined. In these cases a default value of 200km was used.

We then perform external checks on the index data by comparing the value for each station with that of its neighbours. As the station values are correlated, it is therefore likely that if one station measures a high value for an index for a given month, its neighbours will also be measuring high. We exploit this coherence to find further bad values or stations as follows. Although raw precipitation data shows a high degree of localisation, using indices which have monthly or annual resolution improves the coherence across wider areas and so this neighbour checking technique is a valid method of finding anomalous stations.

We calculate a climatology for each station (and month if appropriate) using the mean value for each index over the period 1961-1990. The values for each station are then anomalised using this climatology by subtracting this mean value from the true values, so that it is clear if the station values are higher or lower than normal. This means that we do not need to take

differences in elevation or topography into account when comparing neighbours, as we are not comparing actual values, but rather deviations from the mean value.

All stations which are within the DLS distance are investigated and their anomalised values noted. We then calculate the weighted median value from these stations to take into account the decay in the correlation with increasing distance. We use the median to reduce the sensitivity to outliers.

If the station value is greater than 7.5 median-absolute-deviations away from the weighted median value (this corresponds to about 5 standard deviations if the distribution is Gaussian, but is a robust measure of the spread of the distribution), then there is low confidence in the veracity of this value and so it is removed from the data.

To present the data, the individual stations are gridded on a  $3.75^\circ \times 2.5^\circ$  grid, matching the output from HadCM3. To determine the value of each grid box, the DLS is used to calculate which stations can reasonably contribute to the value. The value of each station is then weighted using the DLS to obtain a final grid box value. At least three stations need to have valid data and be near enough (within 1 DLS of the gridbox centre) to contribute in order for a value to be calculated for the grid point. As for the original HadEX, the HadCM3 land-sea mask is used. However, in three cases the mask has been adjusted as there are data over Tasmania, eastern Australia and Italy that would not be included otherwise (Figure 10).

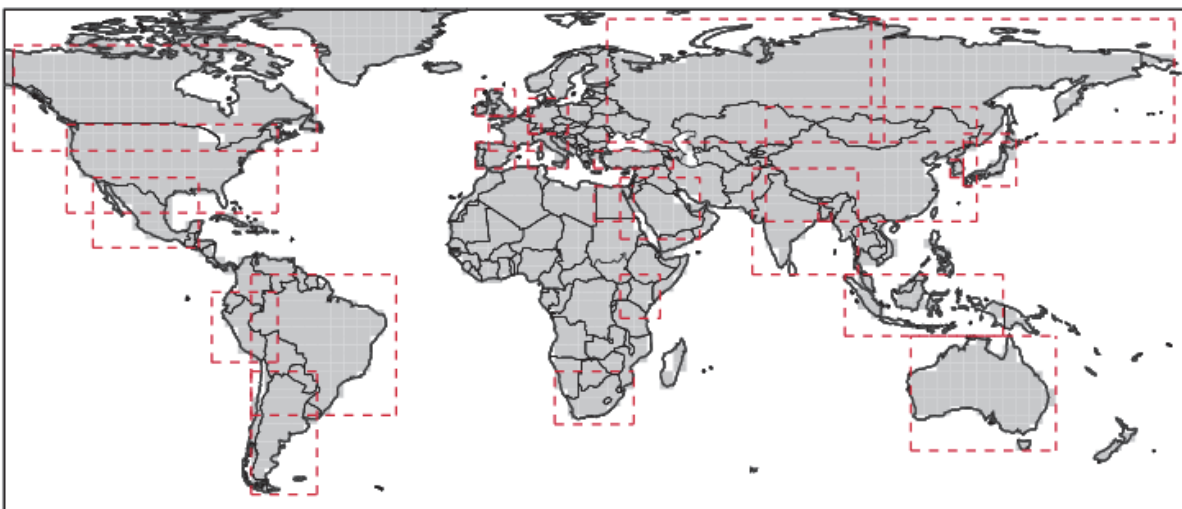


**Figure 10.** Land-sea mask used for gridding the station data and regional areas allocated to each country as described in Table 4.

## **Presentation of extremes of temperature and precipitation**

Indices are displayed as regional gridded maps of decadal trends and regional average time-series with decadal trends where appropriate. Trends are fitted using the median of pairwise slopes method (Sen 1968, Lanzante 1996). Trends are considered to be significantly different from a zero trend if the 5<sup>th</sup> to 95<sup>th</sup> percentiles of the pairwise slopes do not encompass zero. This is shown by a black dot in the centre of the grid-box or by a solid line on time-series plots. This infers that there is high confidence in the sign (positive or negative) of the sign. Confidence in the trend magnitude can be inferred by the spread of the 5<sup>th</sup> to 95<sup>th</sup> percentiles of the pairwise slopes which is given for the regional average decadal trends. Trends are only calculated when there are data present for at least 50% of years in the period of record and for the updated data (not HadEX) there must be at least one year in each decade.

Due to the practice of data-interpolation during the gridding stage (using the DLS) there are values for some grid boxes when no actually station lies within the grid box. There is more confidence in grid boxes for which there are underlying data. For this reason, we identify those grid boxes which contain at least 3 stations by a black contour line on the maps. The DLS differs with region, season and index which leads to large differences in the spatial coverage. The indices, by their nature of being largely threshold driven, can be intermittent over time which also effects spatial and temporal coverage (see Table 3).

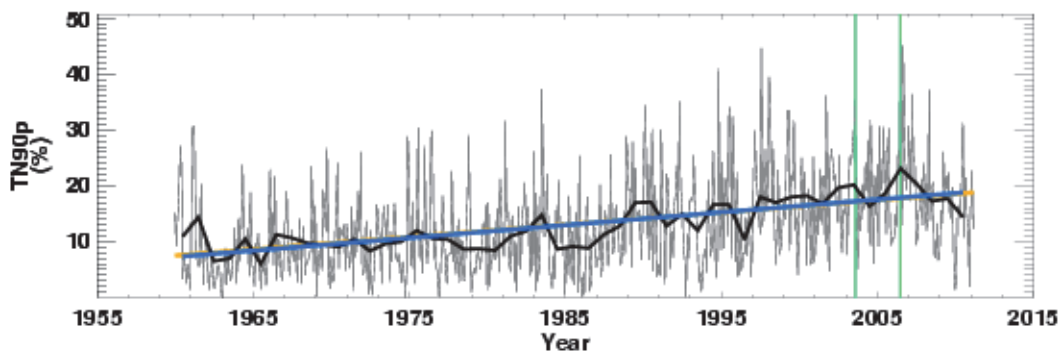
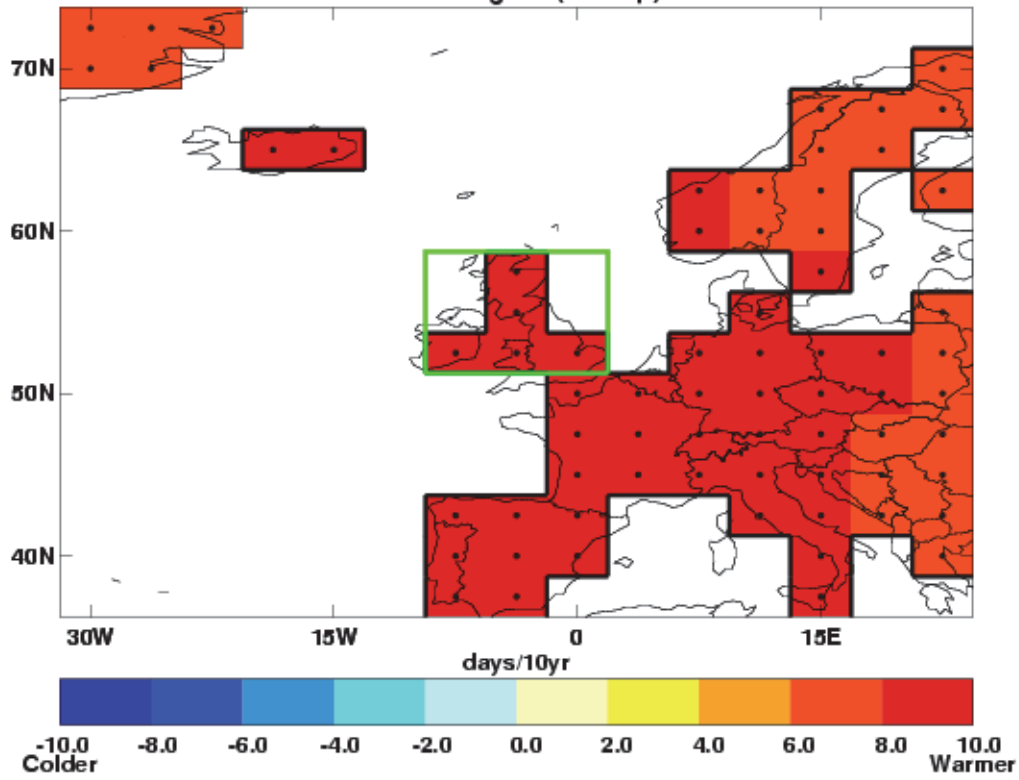
Each index (and each month for the indices for which there is monthly data) has a different DLS, and so the coverage between different indices and datasets can be different. The restrictions on having at least 20 years of data present for each input station, at least 50% of years in the period of record and at least one year in each decade for the trending calculation, combined with the DLS, can restrict the coverage to only those regions with a dense station network reporting reliably.

Each country has a rectangular region assigned as shown by the red dashed box on the map in Figure 1 and listed in Table 2, which is used for the creation of the regional average. This is sometimes identical to the attribution region shown in grey on the map in Figure 1. This region is again shown on the maps accompanying the time series of the regional averages as a reminder of the region and grid boxes used in the calculation. Regional averages are created by weighting grid box values by the cosine of their grid box centre latitude. To ensure consistency over time a regional average is only calculated when there are a sufficient number of grid boxes present. The full-period median number of grid-boxes present is calculated. For regions with a median of more than six grid-boxes there must be at least 80%



of the median number of grid boxes present for any one year to calculate a regional average. For regions with six or fewer median grid boxes this is relaxed to 50%. These limitations ensure that a single station or grid box which has a longer period of record than its neighbours cannot skew the timeseries trend. So sometimes there may be grid-boxes present but no regional average time series. The trends for the regional averages are calculated in the same way as for the individual grid boxes, using the median of pairwise slopes method (Sen 1968, Lanzante 1996). Confidence in the trend is also determined if the 5<sup>th</sup> to 95<sup>th</sup> percentiles of the pairwise slopes are of the same sign and thus inconsistent with a zero trend. As well as the trend in quantity per decade, we also show the full change in the quantity from 1960 to 2010 that this fitted linear trend implies.

### Warm Nights (TN90p)



Monthly: 2.20% per decade (1.80 to 2.61)  
 Total change of 11.02% from 1960 to 2011 (9.00% to 13.06%)  
 Annual: 2.28% per decade (1.69 to 2.86)  
 Total change of 11.41% from 1960 to 2010 (8.43% to 14.28%)

### warm nights (TN90p)

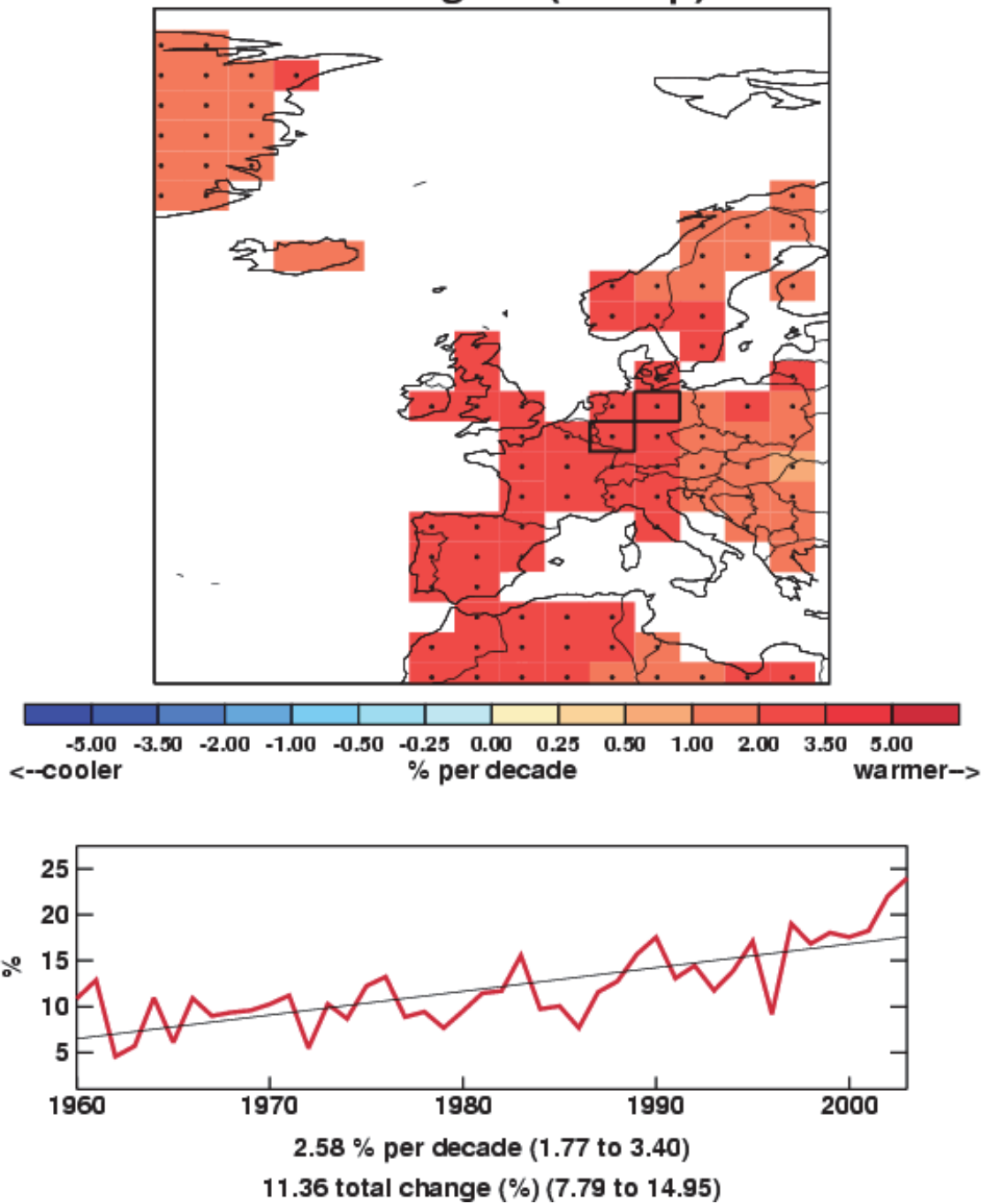


**Figure 11.** Examples of the plots shown in the data section. Left: From ECA&D data between 1960-2010 for the number of warm nights, and Right: from HadEX data (1960-2003) for the total precipitation. A full explanation of the plots is given in the text below.

The results are presented in the form of a map and a time series for each country and index. The map shows the grid box decadal trend in the index over the period for which there are data. High confidence, as determined above, is shown by a black dot in the grid box centre. To show the variation over time, the values for each year (and month if available) are shown in a time series for a regional average. The values of the indices have been normalised to a

base period of 1961-1990 (except the Indian gridded data which use a 1971 to 1990 period), both in HadEX and in the new data acquired for this project. Therefore, for example, the percentage of nights exceeding the 90<sup>th</sup> percentile for a temperature is 10% for that period.

There are two influences on whether a grid box contains a value or not – the land-sea mask, and the decorrelation length scale. The land-sea mask is shown in Figure 10. There are grid boxes which contain some land but are mostly sea and so are not considered. The decorrelation length scale sets the maximum distance a grid box can be from stations before no value is assigned to it. Grid boxes containing three or more stations are highlighted by a thick border. This indicates regions where the value shown is likely to be more representative of the grid box area mean as opposed to a single station location.

On the maps for the new data there is a box indicating which grid boxes have been extracted to calculate the area average for the time series. This box is the same as shown in Figure 1 at the beginning of each country's document. These selected grid boxes are combined using area (cosine) weighting to calculate the regional average (both annual [thick lines] and monthly [thin lines] where available). Monthly (orange) and annual (blue) trends are fitted to these time series using the method described above. The decadal trend and total change over the period where there are data are shown with 5<sup>th</sup> to 95<sup>th</sup> percentile confidence intervals in parentheses. High confidence, as determined above, is shown by a solid line as opposed to a dotted one. The green vertical lines on the time series show the dates of some of the notable events outlined in each section.

## **Attribution**

Regional distributions of seasonal mean temperatures in the 2000s are computed with and without the effect of anthropogenic influences on the climate. The analysis considers temperatures averaged over the regions shown in Figure 12. These are also identified as grey boxes on the maps in Figure 1. The coordinates of the regions are given in Table 5. The methodology combines information from observations and model simulations using the approach originally introduced in Christidis et al., 2010 and later extended in Christidis et al., 2011, where more details can be found. The analysis requires spatial scales greater than about 2,500 km and for that reason the selected regions (Fig.12 and Table 5) are often larger than individual countries, or include several smaller countries in a single region (for example UK, Germany and France are grouped in one region).

Observations of land temperature come from the CRUTEM3 gridded dataset (Brohan et al., 2006) and model simulations from two coupled GCMs, namely the Hadley Centre HadGEM1 model (Martin et al., 2006) and version 3.2 of the MIROC model (K-1 Developers, 2004). The use of two GCMs helps investigate the sensitivity of the results to the model used in the analysis. Ensembles of model simulations from two types of experiments are used to partition the temperature response to external forcings between its anthropogenic and natural components. The first experiment (ALL) simulates the combined effect of natural and anthropogenic forcings on the climate system and the second (ANTHRO) includes anthropogenic forcings only. The difference of the two gives an estimate of the effect of the natural forcings (NAT). Estimates of the effect of internal climate variability are derived from long control simulations of the unforced climate. Distributions of the regional summer mean temperature are computed as follows:

- a) A global optimal fingerprinting analysis (Allen and Tett, 1999; Allen and Stott, 2003) is first carried out that scales the global simulated patterns (fingerprints) of climate change attributed to different combinations of external forcings to best match them to the observations. The uncertainty in the scaling that originates from internal variability leads to samples of the scaled fingerprints, i.e. several realisations that are plausibly consistent with the observations. The 2000-2009 decade is then extracted from the scaled patterns and two samples of the decadal mean temperature averaged over the reference region are then computed with and without human influences, which provide the Probability Density Functions (PDFs) of the decadal mean temperature attributable to ALL and NAT forcings.
- b) Model-derived estimates of noise are added to the distributions to take into account the uncertainty in the simulated fingerprints.
- c) In the same way, additional noise from control model simulations is introduced to the distributions to represent the effect of internal variability in the annual values of the seasonal mean temperatures. The result is a pair of estimated distributions of the annual values of the seasonal mean temperature in the region with and without the effect of human activity on the climate. The temperatures throughout the analysis are expressed as anomalies relative to period 1961-1990.

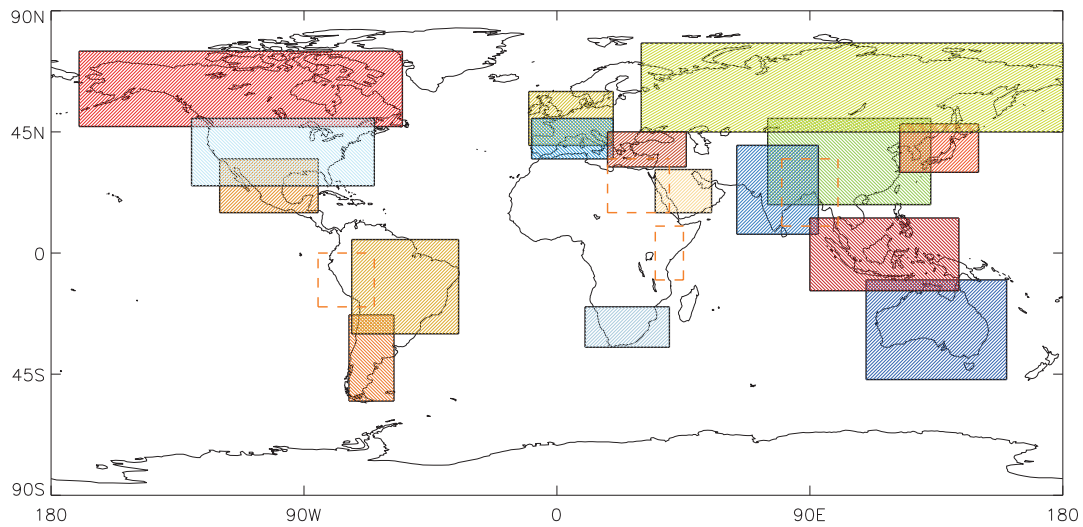


**Figure 12.** The regions used in the attribution analysis. Regions marked with dashed orange boundaries correspond to non-G20 countries that were also included in the analysis

Region	Region Coordinates
Argentina	74-58W, 55-23S
Australia	110-160E, 47-10S
Bangladesh	80-100E, 10-35N
Brazil	73-35W, 30S-5N
Canada-Alaska	170-55W, 47-75N
China	75-133E, 18-50N
Egypt	18-40E, 15-35N
France-Germany-UK	10W-20E, 40-60N
India	64-93E, 7-40N
Indonesia	90-143E, 14S-13N
Italy-Spain	9W-20E, 35-50N
Japan-Republic of Korea	122-150E, 30-48N
Kenya	35-45E, 10S-10N
Mexico	120-85W, 15-35N
Peru	85-65W, 20-0S
Russia	30-185E, 45-78N
Saudi Arabia	35-55E, 15-31N
South Africa	10-40E, 35-20S
Turkey	18-46E, 32-45N

**Table 5.** The coordinates of the regions used in the attribution analysis.

## References

ALEXANDER, L. V., ZHANG, X., PETERSON, T. C., CAESAR, J., GLEASON, B., KLEIN TANK, A. M. G., HAYLOCK, M., COLLINS, D., TREWIN, B., RAHIMZADEH, F., TAGIPOUR, A., RUPA KUMAR, K., REVADEKAR, J., GRIFFITHS, G., VINCENT, L., STEPHENSON, D. B., BURN, J., AGUILAR, E., BRUNET, M., TAYLOR, M., NEW, M., ZHAI, P., RUSTICUCCI, M. and VAZQUEZ-AGUIRRE, J. L. 2006. Global observed changes in daily climate extremes of temperature and precipitation. *J. Geophys. Res.* 111, D05109. doi:10.1029/2005JD006290.

ALLEN, M. R., TETT S. F. B. 1999. Checking for model consistency in optimal fingerprinting. *Clim Dyn* 15: 419-434.

ALLEN M. R., STOTT P. A. 2003. Estimating signal amplitudes in optimal fingerprinting, part I: theory. *Clim Dyn* 21: 477-491.

BROHAN, P., KENNEDY, J.J., HARRIS, I., TETT, S.F.B. and JONES, P.D. 2006. Uncertainty estimates in regional and global observed temperature changes: a new dataset from 1850. *J. Geophys. Res.* 111, D12106. doi:10.1029/2005JD006548.

CHRISTIDIS N., STOTT. P A., ZWIERS, F. W., SHIOGAMA, H., NOZAWA, T. 2010. Probabilistic estimates of recent changes in temperature: a multi-scale attribution analysis. *Clim Dyn* 34: 1139-1156.

CHRISTIDIS, N., STOTT, P. A., ZWIERS, F. W., SHIOGAMA, H., NOZAWA, T. 2011. The contribution of anthropogenic forcings to regional changes in temperature during the last decade. *Climate Dynamics* in press.

DEMİR, I., KILIÇ, G., COSKUN, M., SÜMER, U.M. 2008. Türkiye’de maksimum, minimum ve ortalama hava sıcaklıkları ile yağış dizilerinde gözlenen değişiklikler ve eğilimler. TMMOB İklim Değişimi Sempozyumu, Bildiriler Kitabı, 69-84. TMMOB Meteoroloji Mühendisleri Odası, 13-14 Mart 2008, Ankara.

ERLAT E, TÜRKEŞ M.2011. Analysis of observed variability and trends in numbers of frost days in Turkey for the period 1950–2010. *International Journal Of Climatology* doi: 10.1002/joc.2403.

K-1 MODEL DEVELOPERS (2004) K-1 coupled GCM (MIROC) description, K-1 Tech Rep, H Hasumi and S Emori (eds), Centre for Clim Sys Res, Univ of Tokyo.

LANZANTE, J. R. 1996. Resistant, robust and non-parametric techniques for the analysis of climate data: theory and examples, including applications to historical radiosonde station data. *Int. J. Clim.* 16, 1197–226.

MARTIN G.M., RINGER. M. A., POPE V. D., JONES, A., DEARDEN, C., HINTON, T. 2006. The physical properties of the atmosphere in the new Hadley Centre Global Environmental Model (HadGEM1). Part I: Model description and global climatology. *J Clim* 19: 1274-1301.

OBREGÓN, A., BISSOLLI, P., KENNEDY, J. J., PARKER, D. E., and SENSOY, S. 2010: Mediterranean, Italian, and Balkan Peninsulas in State of The Climate in 2009. *Bulletin of the American Metrological Society* 91(6). S167-S168 available online:  
<http://www1.ncdc.noaa.gov/pub/data/cmb/bams-sotc/climate-assessment-2009-lo-rez.pdf>.

ROGERS M, SENSOY S, BULGINA O, RAHIMZADEH F, GUO Y, ATTAHER S and WATKINS AB. 2009. The Eurasian cold event of January 2008 in State of the Climate in 2008. *Bulletin of the American Metrological Society* 90, S156.

SEN, P. K. 1968. Estimates of the regression coefficient based on Kendall's tau. *J. Am. Stat. Assoc.*, 63, 1379–89.

SENSOY, S. 2007. Turkey in State of the Climate in 2006. Arguez, A., ed. *Bulletin of the American Meteorological Society* 88, S102.

SENSOY, S. 2008. Turkey in State of the Climate in 2007. Levinson, D.H., and J.H. Lawrimore eds. *Bulletin of the American Meteorological Society* 89, S139-S140.

SENSOY, S. 2009. Turkey in State of the Climate in 2008. *Bulletin of the American Meteorological Society* 90, S163.

SENSOY, S. and DEMIRCAN, M. 2011. Turkey in State of the Climate in 2010. *Bulletin of the American Meteorological Society* 92, S221-S222.

UNFCCC. 2007. First national report by the government of the Turkish Republic to the United Nations Framework Convention on Climate Change. available online:  
[http://unfccc.int/essential\\_background/library/items/3599.php?rec=j&preref=5834](http://unfccc.int/essential_background/library/items/3599.php?rec=j&preref=5834)

WMO WORLD METEOROLOGICAL ORGANIZATION. 2001. Statement on Status of the Global Climate in 2000, WMO-No. 920.  
[http://www.wmo.int/pages/prog/wcp/wcdmp/statement/wmostatement\\_en.html](http://www.wmo.int/pages/prog/wcp/wcdmp/statement/wmostatement_en.html)



WMO WORLD METEOROLOGICAL ORGANIZATION. 2005. Statement on Status of the Global Climate in 2004, WMO-No. 983.

[http://www.wmo.int/pages/prog/wcp/wcdmp/statement/wmostatement\\_en.html](http://www.wmo.int/pages/prog/wcp/wcdmp/statement/wmostatement_en.html)

WMO WORLD METEOROLOGICAL ORGANIZATION. 2008. Statement on Status of the Global Climate in 2007, WMO-No. 1031.

[http://www.wmo.int/pages/prog/wcp/wcdmp/statement/wmostatement\\_en.html](http://www.wmo.int/pages/prog/wcp/wcdmp/statement/wmostatement_en.html)

WMO WORLD METEOROLOGICAL ORGANIZATION. 2009. Statement on Status of the Global Climate in 2008, WMO-No. 1039.

[http://www.wmo.int/pages/prog/wcp/wcdmp/statement/wmostatement\\_en.html](http://www.wmo.int/pages/prog/wcp/wcdmp/statement/wmostatement_en.html)

WMO WORLD METEOROLOGICAL ORGANIZATION. 2010. Statement on Status of the Global Climate in 2009, WMO-No. 1055.

[http://www.wmo.int/pages/prog/wcp/wcdmp/statement/wmostatement\\_en.html](http://www.wmo.int/pages/prog/wcp/wcdmp/statement/wmostatement_en.html)

## **Acknowledgements**

We thank Lisa Alexander and Markus Donat (University of New South Wales) for their help and advice. We also thank reviewers from Turkey for their valuable advice and input.

|

# **Chapter 2 – Climate Change Projections**

## Introduction

Climate models are used to understand how the climate will evolve over time and typically represent the atmosphere, ocean, land surface, cryosphere, and biogeochemical processes, and solve the equations governing their evolution on a geographical grid covering the globe. Some processes are represented explicitly within climate models, large-scale circulations for instance, while others are represented by simplified parameterisations. The use of these parameterisations is sometimes due to processes taking place on scales smaller than the typical grid size of a climate model (a Global Climate Model (GCM) has a typical horizontal resolution of between 250 and 600km) or sometimes to the current limited understanding of these processes. Different climate modelling institutions use different plausible representations of the climate system, which is why climate projections for a single greenhouse gas emissions scenario differ between modelling institutes. This gives rise to “climate model structural uncertainty”.

In response to a proposed activity of the World Climate Research Programme's (WCRP's; <http://www.wcrp-climate.org/>) Working Group on Coupled Modelling (WGCM), the Program for Climate Model Diagnosis and Intercomparison (PCMDI; <http://www-pcmdi.llnl.gov/>) volunteered to collect model output contributed by leading climate modelling centres around the world. Climate model output from simulations of the past, present and future climate was collected by PCMDI mostly during the years 2005 and 2006, and this archived data constitutes phase 3 of the Coupled Model Intercomparison Project (CMIP3). In part, the WGCM organised this activity to enable those outside the major modelling centres to perform research of relevance to climate scientists preparing the IPCC Fourth Assessment Report (AR4). This unprecedented collection of recent model output is commonly known as the “CMIP3 multi-model dataset”. The GCMs included in this dataset are referred to regularly throughout this review, although not exclusively.

The CMIP3 multi-model ensemble has been widely used in studies of regional climate change and associated impacts. Each of the constituent models was subject to extensive testing by the contributing institute, and the ensemble has the advantage of having been constructed from a large pool of alternative model components, therefore sampling alternative structural assumptions in how best to represent the physical climate system. Being assembled on an opportunity basis, however, the CMIP3 ensemble was not designed to represent model uncertainties in a systematic manner, so it does not, in isolation, support robust estimates of the risk of different levels of future climate change, especially at a regional level.

Since CMIP3, a new (CMIP5) generation of coupled ocean-atmosphere models has been developed, which is only just beginning to be available and is being used for new projections for the IPCC Fifth Assessment Report (AR5).

These newer models typically feature higher spatial resolution than their CMIP3 counterparts, including in some models a more realistic representation of stratosphere-troposphere interactions. The CMIP5 models also benefit from several years of development in their parameterisations of small scale processes, which, together with resolution increases, are expected to result in a general improvement in the accuracy of their simulations of historical climate, and in the credibility of their projections of future changes. The CMIP5 programme also includes a number of comprehensive Earth System Models (ESMs) which explicitly simulate the earth's carbon cycle and key aspects of atmospheric chemistry, and also contain more sophisticated representations of aerosols compared to CMIP3 models.

The CMIP3 results should be interpreted as a useful interim set of plausible outcomes. However, their neglect of uncertainties, for instance in carbon cycle feedbacks, implies that higher levels of warming outside the CMIP3 envelope cannot be ruled out. In future, CMIP5 coupled model and ESM projections can be expected to produce improved advice on future regional changes. In particular, ensembles of ESM projections will be needed to provide a more comprehensive survey of possible future changes and their relative likelihoods of occurrence. This is likely to require analysis of the CMIP5 multi-model ESM projections, augmented by larger ensembles of ESM simulations in which uncertainties in physical and biogeochemical feedback processes can be explored more systematically, for example via ensembles of model runs in which key aspects of the climate model are slightly adjusted. Note that such an exercise might lead to the specification of wider rather than narrower uncertainties compared to CMIP3 results, if the effects of representing a wider range of earth system processes outweigh the effects of refinements in the simulation of physical atmosphere-ocean processes already included in the CMIP3 models.

# Climate projections

The Met Office Hadley Centre is currently producing perturbed parameter ensembles of a single model configuration known as HadCM3C, to explore uncertainties in physical and biogeochemical feedback processes. The results of this analysis will become available in the next year and will supplement the CMIP5 multi-model ESM projections, providing a more comprehensive set of data to help progress understanding of future climate change. However, many of the studies covered in the chapter on climate impacts have used CMIP3 model output. For this reason, and because it is still the most widely used set of projections available, the CMIP3 ensemble output for temperature and precipitation, for the A1B emission scenario, for Turkey and the surrounding region is shown below.

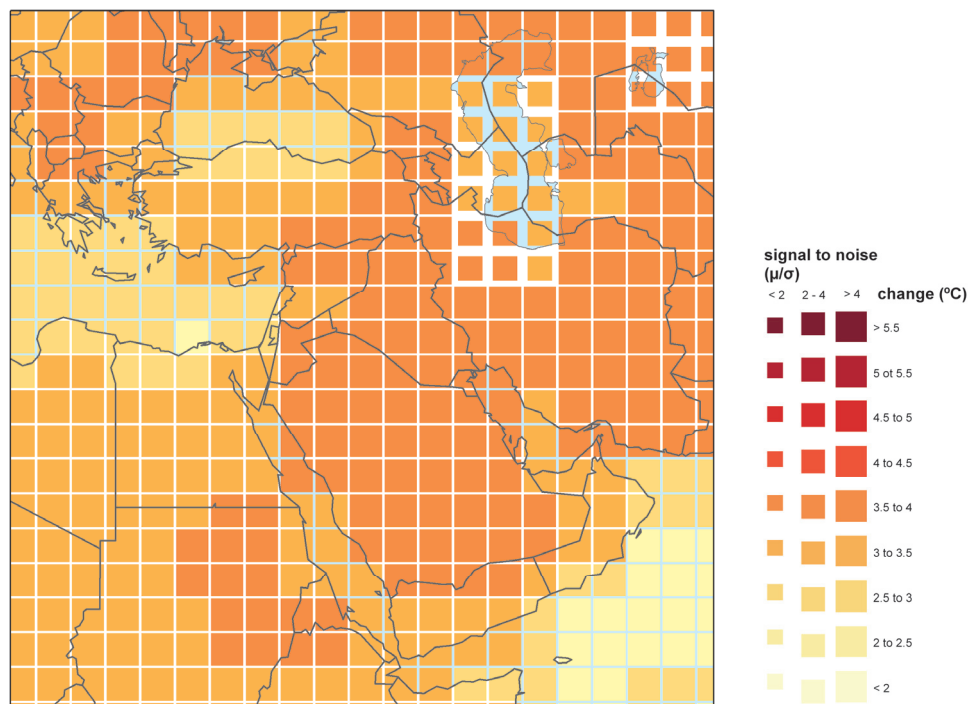


**Figure 1.** Percentage change in average annual temperature by 2100 from 1960-1990 baseline climate, averaged over 21 CMIP3 models. The size of each pixel represents the level of agreement between models on the magnitude of the change.

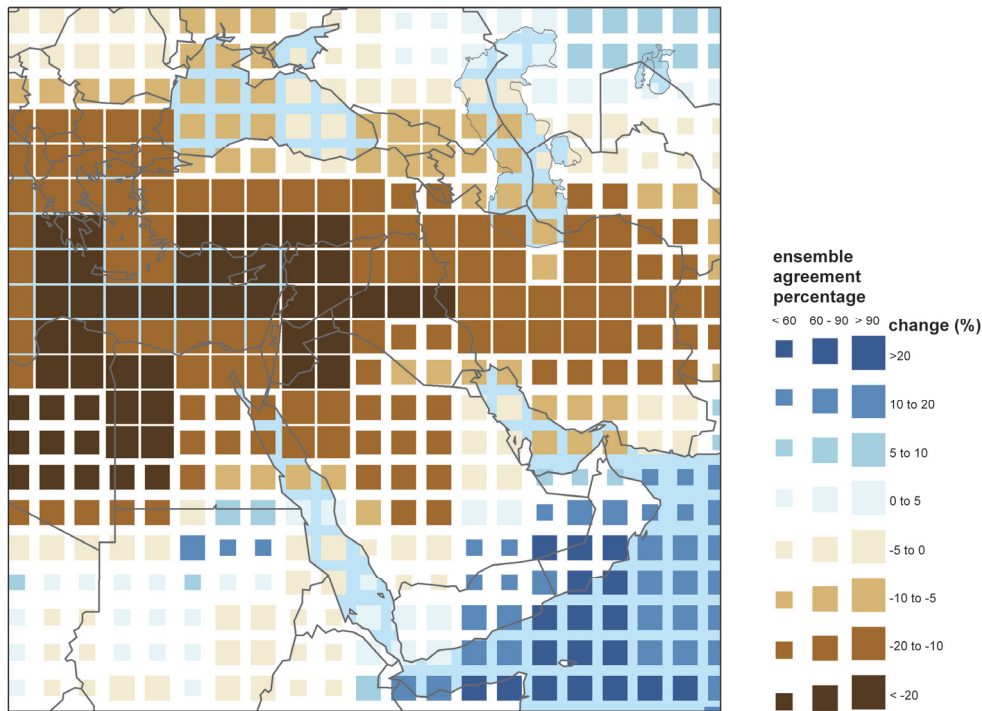


**Figure 2.** Percentage change in average annual precipitation by 2100 from 1960-1990 baseline climate, averaged over 21 CMIP3 models. The size of each pixel represents the level of agreement between models on the sign of the change.

## Summary of temperature change in Turkey

Figure 1 shows the percentage change in average annual temperature by 2100 from 1960-1990 baseline climate, averaged over 21 CMIP3 models. All of the models in the CMIP3 ensemble project increased temperatures in the future, but the size of each pixel indicates how well the models agree over the magnitude of the increase.

Projected temperature increases over Turkey are around 2.5-3°C in the north, 3-3.5°C over central and south-western regions, and 3.5-4.0°C in the east. There is consistently good agreement between the models over Turkey and this region in general.

## Summary of precipitation change in Turkey

Figure 2 shows the percentage change in average annual precipitation by 2100 from 1960-1990 baseline climate, averaged over 21 CMIP3 models. Unlike for temperature, the models sometimes disagree over whether precipitation is increasing or decreasing over a region, so

in this case the size of each pixel indicates the percentage of the models in the ensemble that agree on the sign of the change in precipitation.

Turkey is projected to experience mainly decreases in precipitation, in common with the wider Mediterranean and majority of the Middle East. Decreases of over 20% are projected in the south of the country, with strong ensemble agreement. Smaller changes are projected towards the north, between 0-10%, but with more moderate agreement between the models.



# **Chapter 3 – Climate Change Impact Projections**

# Introduction

## Aims and approach

This chapter looks at research on a range of projected climate change impacts, with focus on results for Turkey. It includes projections taken from the AVOID programme, for some of the impact sectors.

The aim of this work is to take a ‘top down’ approach to assessing global impacts studies, both from the literature and from new research undertaken by the AVOID programme. This project covers 23 countries, with summaries from global studies provided for each of these. This global approach allows some level of comparison between countries, whilst presenting information on a scale most meaningful to inform international policy.

The literature covered in this chapter focuses on research published since the Fourth Assessment Report (AR4) of the Intergovernmental Panel on Climate Change (IPCC) and should be read in conjunction with IPCC AR4 WG1 and WG2 reports. For some sectors considered, an absence of research developments since the IPCC AR4, means earlier work is cited as this helps describe the current level of scientific understanding. This report focuses on assessing scientific research about climate change impacts within sectors; it does not present an integrated analysis of climate change adaptation policies.

Some national and sub-national scale literature is reported to a limited extent to provide some regional context.

## Impact sectors considered and methods

This report reviews the evidence for the impact of climate change on a number of sectors, for Turkey. The following sectors are considered in turn in this report:

- Crop yields
- Food security
- Water stress and drought
- Pluvial flooding and rainfall
- Fluvial flooding

- Tropical cyclones (where applicable)
- Coastal regions

## **Supporting literature**

Literature searches were conducted for each sector with the Thomson Reuters Web of Science (WoS., 2011) and Google Scholar academic search engines respectively. Furthermore, climate change impact experts from each of the 23 countries reviewed were contacted. These experts were selected through a combination of government nomination and from experts known to the Met Office. They were asked to provide literature that they felt would be of relevance to this review. Where appropriate, such evidence has been included. A wide range of evidence was considered, including; research from international peer-reviewed journal papers; reports from governments, non-governmental organisations, and private businesses (e.g. reinsurance companies), and research papers published in national journals.

For each impact sector, results from assessments that include a global- or regional-scale perspective are considered separately from research that has been conducted at the national- or sub-national-scale. The consideration of global- and regional-scale studies facilitates a comparison of impacts across different countries, because such studies apply a consistent methodology for each country. While results from national- and sub-national-scale studies are not easily comparable between countries, they can provide a level of detail that is not always possible with larger-scale studies. However, the national- and sub-national scale literature included in this project does not represent a comprehensive coverage of regional-based research and cannot, and should not, replace individual, detailed impacts studies in countries. The review aims to present an up-to-date assessment of the impact of climate change on each of the sectors considered.

## **AVOID programme results**

Much of the work in this report is drawn from modelling results and analyses coming out of the AVOID programme. The AVOID programme is a research consortium funded by DECC and Defra and led by the UK Met Office and also comprises the Walker Institute at the University of Reading, the Tyndall Centre represented through the University of East Anglia,

and the Grantham Institute for Climate Change at Imperial College. The expertise in the AVOID programme includes climate change research and modelling, climate change impacts in natural and human systems, socio-economic sciences, mitigation and technology. The unique expertise of the programme is in bringing these research areas together to produce integrated and policy-relevant results. The experts who work within the programme were also well suited to review the literature assessment part of this report. In this report the modelling of sea level rise impacts was carried out for the AVOID programme by the University of Southampton.

The AVOID programme uses the same emissions scenarios across the different impact sectors studied. These are a business as usual (IPCC SRES A1B) and an aggressive mitigation (the AVOID A1B-2016-5-L) scenario. Model output for both scenarios was taken from more than 20 GCMs and averaged for use in the impact models. The impact models are sector specific, and frequently employ further analytical techniques such as pattern scaling and downscaling in the crop yield models.

Data and analysis from AVOID programme research is provided for the following impact sectors:

- Crop yields
- Water stress and drought
- Fluvial flooding
- Coastal regions

## **Uncertainty in climate change impact assessment**

There are many uncertainties in future projections of climate change and its impacts. Several of these are well-recognised, but some are not. One category of uncertainty arises because we don't yet know how mankind will alter the climate in the future. For instance, uncertainties in future greenhouse gas emissions depends on the future socio-economic pathway, which, in turn, depends on factors such as population, economic growth, technology development, energy demand and methods of supply, and land use. The usual approach to dealing with this is to consider a range of possible future scenarios.

Another category of uncertainties relate to our incomplete understanding of the climate system, or an inability to adequately model some aspects of the system. This includes:

- Uncertainties in translating emissions of greenhouse gases into atmospheric concentrations and radiative forcing. Atmospheric CO<sub>2</sub> concentrations are currently rising at approximately 50% of the rate of anthropogenic emissions, with the remaining 50% being offset by a net uptake of CO<sub>2</sub> into the oceans and land biosphere. However, this rate of uptake itself probably depends on climate, and evidence suggests it may weaken under a warming climate, causing more CO<sub>2</sub> to remain in the atmosphere, warming climate further. The extent of this feedback is highly uncertain, but it not considered in most studies. The phase 3 of the Coupled Model Intercomparison Project (CMIP3), which provided the future climate projections for the IPCC Fourth Assessment Report (AR4), used a single estimate of CO<sub>2</sub> concentration rise for each emissions scenario, so the CMIP3 projections (which were used in most studies presented here, including AVOID) do not account for this uncertainty.
- Uncertainty in climate response to the forcing by greenhouse gases and aerosols. One aspect of this is the response of global mean temperature (“climate sensitivity”), but a more relevant aspect for impacts studies is the response of regional climates, including temperature, precipitation and other meteorological variables. Different climate models can give very different results in some regions, while giving similar results in other regions. Confidence in regional projections requires more than just agreement between models: physical understanding of the relevant atmospheric, ocean and land surface processes is also important, to establish whether the models are likely to be realistic.
- Additional forcings of regional climate. Greenhouse gas changes are not the only anthropogenic driver of climate change; atmospheric aerosols and land cover change are also important, and unlike greenhouse gases, the strength of their influence varies significantly from place to place. The CMIP3 models used in most impacts studies generally account for aerosols but not land cover change.
- Uncertainty in impacts processes. The consequences of a given changes in weather or climatic conditions for biophysical impacts such as river flows, drought, flooding, crop yield or ecosystem distribution and functioning depend on many other processes which are often poorly-understood, especially at large scales. In particular, the extent to which different biophysical impacts interact with each other has been hardly studied, but may be crucial; for example, impacts of climate change on crop

yield may depend not only on local climate changes affecting rain-fed crops, but also remote climate changes affecting river flows providing water for irrigation.

- Uncertainties in non-climate effects of some greenhouse gases. As well as being a greenhouse gas, CO<sub>2</sub> exerts physiological influences on plants, affecting photosynthesis and transpiration. Under higher CO<sub>2</sub> concentrations, and with no other limiting factors, photosynthesis can increase, while the requirements of water for transpiration can decrease. However, while this has been extensively studied under experimental conditions, including in some cases in the free atmosphere, the extent to which the ongoing rise in ambient CO<sub>2</sub> affects crop yields and natural vegetation functioning remains uncertain and controversial. Many impacts projections assume CO<sub>2</sub> physiological effects to be significant, while others assume it to be non-existent. Studies of climate change impacts on crops and ecosystems should therefore be examined with care to establish which assumptions have been made.

In addition to these uncertainties, the climate varies significantly through natural processes from year-to-year and also decade-to-decade, and this variability can be significant in comparison to anthropogenic forcings on shorter timescales (the next few decades) particularly at regional scales. Whilst we can characterise the natural variability it will not be possible to give a precise forecast for a particular year decades into the future.

A further category of uncertainty in projections arises as a result of using different methods to correct for uncertainties and limitations in climate models. Despite being painstakingly developed in order to represent current climate as closely as possible, current climate models are nevertheless subject to systematic errors such as simulating too little or too much rainfall in some regions. In order to reduce the impact of these, '*bias correction*' techniques are often employed, in which the climate model is a source of information on the *change* in climate which is then applied to the observed present-day climate state (rather than using the model's own simulation of the present-day state). However, these bias-corrections typically introduce their own uncertainties and errors, and can lead to inconsistencies between the projected impacts and the driving climate change (such as river flows changing by an amount which is not matched by the original change in precipitation). Currently, this source of uncertainty is rarely considered

When climate change projections from climate models are applied to climate change impact models (e.g. a global hydrological model), the climate model structural uncertainty carries through to the impact estimates. Additional uncertainties include changes in future emissions

and population, as well as parameterisations within the impact models (this is rarely considered). Figure 1 highlights the importance of considering climate model structural uncertainty in climate change impacts assessment. Figure 1 shows that for 2°C prescribed global-mean warming, the magnitude of, and sign of change in average annual runoff from present, simulated by an impacts model, can differ depending upon the GCM that provides the climate change projections that drive the impact model. This example also shows that the choice of impact model, in this case a global hydrological model (GHM) or catchment-scale hydrological model (CHM), can affect the magnitude of impact and sign of change from present (e.g. see IPSL CM4 and MPI ECHAM5 simulations for the Xiangxi). To this end, throughout this review, the number of climate models applied in each study reviewed, and the other sources of uncertainty (e.g. emissions scenarios) are noted. Very few studies consider the application of multiple impacts models and it is recommended that future studies address this.

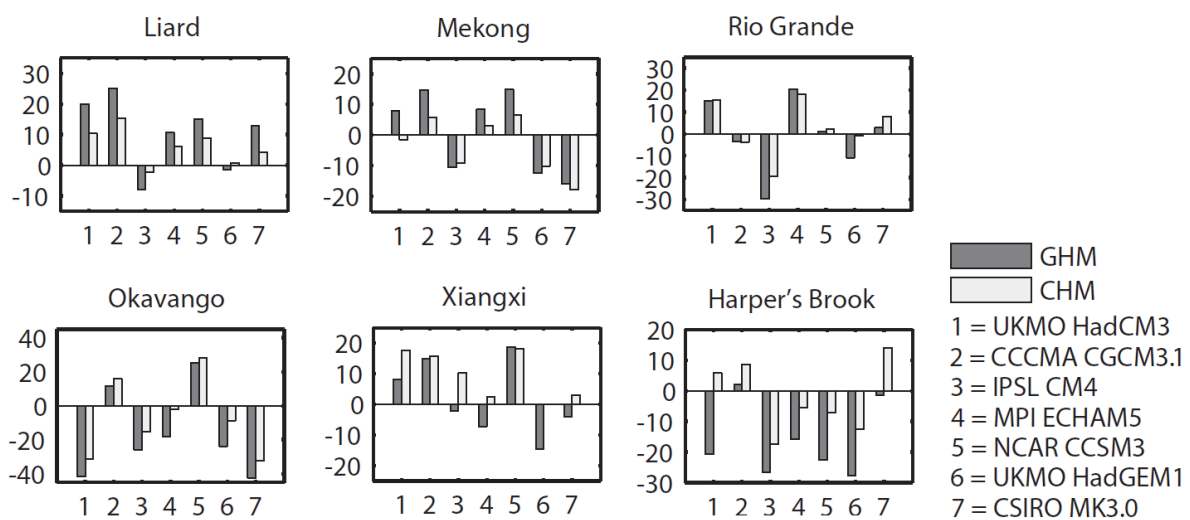


**Figure 1.** Change in average annual runoff relative to present (vertical axis; %), when a global hydrological model (GHM) and a catchment-scale hydrological model (CHM) are driven with climate change projections from 7 GCMs (horizontal axis), under a 2°C prescribed global-mean warming scenario, for six river catchments. The figure is from Gosling et al. (2011).

# Summary of findings for each sector

## Crop yields

- Quantitative crop yield projections under climate change scenarios for Turkey vary across studies due to the application of different models, assumptions and emissions scenarios.
- However, the majority of global- and regional-scale studies included here generally project declines in maize yields, one of the country's major crops, with climate change.
- National-scale studies broadly concur with the global- and regional-scale projections of a decline in maize yields in the future. However, it is more difficult to draw a conclusion on the impact of climate change on wheat yields in Turkey, the country's major crop.
- Important knowledge gaps and key uncertainties include the quantification of yield increases due to CO<sub>2</sub> fertilisation, quantification of yield reductions due to ozone damage and the extent to which crop diseases might affect crop yields with climate change.

## Food security

- Turkey is currently a country of extremely low undernourishment. The majority of global-scale studies included here project a positive outlook for the impact of climate change on food security in Turkey. Considering land-based food production, Turkey is not projected to face severe food insecurity over the next 40 years.
- The outlook is less optimistic when considering marine based fisheries. One study concluded that Turkey's economy is projected to be highly vulnerable to the impact of climate change on fisheries by the 2050s.



## **Water stress and drought**

- Several global- and national-scale studies included here project that droughts in Turkey could increase in frequency and magnitude with climate change, with the greatest potential impacts projected for the south of the country.
- There is also consensus among global-, national- and sub-national-scale studies included here that water stress in Turkey could increase with climate change.
- Recent simulations by the AVOID programme project a median increase of around 45% of Turkey's population to be exposed to increases in water stress by 2100 under SRES A1B. Under an aggressive mitigation scenario, this is 30%.

## **Pluvial flooding and rainfall**

- The IPCC AR4 stated that annual precipitation could decrease across most of the Mediterranean area, including Turkey.
- A number of recent studies confirm this.

## **Fluvial flooding**

- Few studies have explored the impact of climate change on fluvial flooding for Turkey.
- However, the consensus across the few published studies available suggests that extreme flood events could occur less frequently than present under climate change.
- Supporting this, is recent simulations from the AVOID programme, which show high agreement across 21 models that flood risk in Turkey could decrease with climate change throughout the 21<sup>st</sup> century.

## **Tropical cyclones**

- Turkey is not impacted by tropical cyclones.

## Coastal regions

- There are no global-scale assessments of the impacts of sea level rise (SLR) on coastal regions that provide national-scale estimates for Turkey.
- However, a number of national-scale studies suggest that Turkey could experience appreciable coastal impacts from SLR.
- One study estimates that the population in Turkey exposed to SLR is around 428,000 along the Mediterranean coast, 208,000 along the Aegean coast, 842,000 in the Marmara region and 201,000 along the Black Sea coast.

# Crop yields

## Headline

Crop yield projections under climate change scenarios for Turkey vary across studies due to the application of different models, assumptions and emissions scenarios. The majority of studies simulate declines in maize yields with climate change.

Results from the AVOID programme for Turkey indicate that model projections implied only up to 2%-13% of current Turkish cropland areas to undergo an improvement of suitability of cultivation, for both scenarios. This changed very little across the entire 21<sup>st</sup> century, with the model consensus indicating only a small decrease in areas of increased suitability by 2100, particularly in the A1B scenario. In contrast, the models showed a very high degree of consensus towards a large proportion of current Turkish croplands undergoing declining suitability from 2030 onwards. In 2030, approximately 75%-95% of current croplands experienced declining suitability in both scenarios. By 2100 this had remained similar under the mitigation scenario, but risen to 86%-100% under A1B. So for Turkey, there is a strong consensus between models of climate change giving declining suitability for cultivation over most current croplands.

## Supporting literature

### Introduction

The impacts of climate change on crop productivity are highly uncertain due to the complexity of the processes involved. Most current studies are limited in their ability to capture the uncertainty in regional climate projections, and often omit potentially important aspects such as extreme events and changes in pests and diseases. Importantly, there is a lack of clarity on how climate change impacts on drought are best quantified from an agricultural perspective, with different metrics giving very different impressions of future risk. The dependence of some regional agriculture on remote rainfall, snowmelt and glaciers adds to the complexity - these factors are rarely taken into account, and most studies focus solely on the impacts of local climate change on rain-fed agriculture. However, irrigated agricultural land produces approximately 40-45 % of the world's food (Doll and Siebert 2002), and the

water for irrigation is often extracted from rivers which can depend on climatic conditions far from the point of extraction. Hence, impacts of climate change on crop productivity often need to take account of remote as well as local climate changes. Indirect impacts via sea-level rise, storms and diseases have also not been quantified. Perhaps most seriously, there is high uncertainty in the extent to which the direct effects of CO<sub>2</sub> rise on plant physiology will interact with climate change in affecting productivity. Therefore, at present, the aggregate impacts of climate change on large-scale agricultural productivity cannot be reliably quantified (Gornall et al, 2010). This section summarises findings from a range of post IPCC AR4 assessments to inform and contextualise the analysis performed by AVOID programme for this project. The results from the AVOID work are discussed in the next section.

Wheat is the most important cereal crop grown in Turkey, followed by barley and maize (see Table 1) (FAO, 2008). Other important crops typical of the Mediterranean climate are cotton, grapes and olives.

Harvested area (ha)		Quantity (Metric ton)		Value (\$1000)	
Wheat	8090000	Wheat	17700000	Wheat	2420000
Barley	2730000	Sugar beet	15400000	Tomatoes	2210000
Olives	707000	Tomatoes	10900000	Grapes	1810000
Maize	593000	Barley	5920000	Cotton lint	999000
Sunflower seed	577000	Maize	4270000	Hazelnuts, with shell	782000
Seed cotton	494000	Potatoes	4190000	Olives	732000
Chick peas	486000	Watermelons	4000000	Apples	719000

**Table 1.** The top 7 crops by harvested area, quantity and value according to the FAO (2008) in Turkey. Crops that feature in all lists are shaded green; crops that feature in two top 7 lists are shaded amber. Data is from FAO (2008) and has been rounded down to three significant figures.

A number of global, regional, national and sub-national impact model studies, which include results for some of the main crops in Turkey, have been conducted. They applied a variety of methodological approaches, including using different climate model inputs and treatment of other factors that might affect yield, such as impact of increased CO<sub>2</sub> in the atmosphere on plant growth and adaption of agricultural practises to changing climate conditions. These different models, assumptions and emissions scenarios mean that there are a range of crop yield projections for Turkey. However, the majority of studies explored in this report show that yields of maize decline with climate change.

Important knowledge gaps, which are applicable to Turkey as well as at the global-scale, include; the quantification of yield reductions due to ozone damage (Ainsworth and McGrath, 2010, Iglesias et al., 2009), and the extent crop diseases could affect crop yields with climate change (Luck et al., 2011). Most crop simulation models do not include the direct effect of extreme temperatures on crop development and growth, thus only changes in mean climate conditions are considered to affect crop yields for the studies included here.

## Assessments that include a global or regional perspective

### Recent Past

Crop yield changes could be due to a variety of factors, which might include, but not be confined to, a changing climate. In order to assess the impact of recent climate change (1980-2008) on wheat, maize, rice and soybean, Lobell et al. (2011) looked at how the overall yield trend in these crops changed in response to changes in climate over the period studied. The study was conducted at the global-scale but national estimates for Turkey were also calculated. Lobell et al. (2011) divided the climate-induced yield trend by the overall yield trend for 1980–2008, to produce a simple metric of the importance of climate relative to all other factors. The ratio produced indicates the influence of climate on the productivity trend overall. So for example a value of  $-0.1$  represents a 10% reduction in yield gain due to climate change, compared to the increase that could have been achieved without climate change, but with technology and other gains. This can also be expressed as 10 years of climate trend being equivalent to the loss of roughly 1 year of technology gains. For Turkey, a positive effect on rice yield but a strong negative effect on wheat yield was estimated relative to what could have been achieved without the climate trends (see Table 2).

Crop	Trend
Maize	n/a
Rice	0.1 – 0.2
Wheat	-0.4 to -0.3
Soybean	n/a

**Table 2.** The estimated net impact of climate trends for 1980-2008 on crop yields. Climate-induced yield trend divided by overall yield trend. 'n/a' infers zero or insignificant crop production or unavailability of data. Data is from Lobell et al. (2011).

### Climate change studies

Included in this section are results from recent studies that have applied climate projections from Global Climate Models (GCMs) to crop yield models to assess the global-scale impact of climate change on crop yields, and which include impact estimates at the national-scale

for Turkey (Avnery et al., 2011, Iglesias and Rosenzweig, 2009, Giannakopoulos et al., 2005, Giannakopoulos et al., 2009). The process of CO<sub>2</sub> fertilisation of some crops is usually included in climate impact studies of yields. However, other gases can influence crop growth, and are not always included in impact model projections. An example of this is ozone, (O<sub>3</sub>) and so a study which attempts to quantify the potential impact of changes in the atmospheric concentration of this gas is also included Avnery et al., (2011).

In addition to these studies, the AVOID programme analysed the patterns of climate change for 21 GCMs to establish an index of 'climate suitability' of agricultural land. Climate suitability is not directly equivalent to crop yields, but is a means of looking at a standard metric across all countries included in this project, and of assessing the level of agreement on variables that affect crop production between all 21 GCMs.

Iglesias and Rosenzweig (2009) repeated an earlier study presented by Parry et al. (2004) by applying climate projections from the HadCM3 GCM (instead of HadCM2, which was applied by Parry et al. (2004)), under seven SRES emissions scenarios and for three future time periods. This study used consistent crop simulation methodology and climate change scenarios globally, and weighted the model site results by their contribution to regional and national, rain-fed and irrigated production. The study also applied a quantitative estimation of physiological CO<sub>2</sub> effects on crop yields and considered the affect of adaptation by assessing the potential of the country or region to reach optimal crop yield. The results from the study are presented in Table 3 and Table 4. The simulations showed contrasting responses for wheat and maize. Wheat yield steadily increased with climate change whereas maize decreased until 2050, after which yields increased modestly. These impacts were generally consistent across emissions scenarios.

Scenario	Year	Wheat	Maize
A1FI	2020	2.69	-3.07
	2050	7.36	-3.70
	2080	5.79	-0.75
A2a	2020	3.64	-2.80
	2050	6.94	-3.47
	2080	9.90	-1.63
A2b	2020	2.14	-2.02
	2050	7.27	-3.84
	2080	10.83	-1.36
A2c	2020	1.60	-2.67
	2050	6.85	-4.12
	2080	12.27	-2.01
B1a	2020	-0.82	-3.27
	2050	3.19	-4.77
	2080	4.84	-5.43
B2a	2020	2.18	-4.43
	2050	3.11	-5.17
	2080	3.68	-3.68
B2b	2020	1.18	-3.92
	2050	3.27	-5.35
	2080	7.01	-3.64

**Table 3.** Wheat and maize yield changes (%) relative to baseline scenario (1970-2000) for different emission scenarios and future time periods. Some emissions scenarios were run in an ensemble simulation (e.g. A2a, A2b, A2c). Data is from Iglesias and Rosenzweig (2009).

	Wheat		Maize	
	Up	Down	Up	Down
<b>Baseline to 2020</b>	6	1	0	7
<b>Baseline to 2050</b>	7	0	0	7
<b>Baseline to 2080</b>	7	0	0	7
<b>2020 to 2050</b>	7	0	0	7
<b>2050 to 2080</b>	6	1	6	1

**Table 4.** The number of emission scenarios that predict yield gains (“Up”) or yield losses (“Down”) for wheat and maize between two points in time. Data is from Iglesias and Rosenzweig (2009).

Giannakopoulos et al. (2005, 2009) applied climate projections with the HadCM3 GCM under the SRES A2 and B2 emissions scenarios to assess climate change impacts for the Mediterranean basin for the period 2031-2060 under the A2 and B2 emissions scenarios. Climate data were used as input to the CROPSYST (Cropping Systems Simulation Model) (Stockle et al. 2003) crop model to project crop productivity changes (compared to 1961-1990) for a range of different crop types. The crop types were divided into ‘C4’ summer crop, ‘C3’ summer crop, legumes, tuber crops and cereals, where ‘C4’ and ‘C3’ refer to two plant physiology types that affect the way plants take up CO<sub>2</sub> from the atmosphere. ‘C3’ crops are

able to benefit from CO<sub>2</sub> enrichment of the atmosphere, whereas 'C4' crops are not. This process is simulated by CROPSYST. The process is important because the benefit from CO<sub>2</sub> enrichment can potentially off-set some of the negative impacts of climate change for that crop. For Turkey the 'C4' summer crop studied was irrigated maize, the 'C3' summer crop was rain-fed sunflowers, the legume was rain-fed lentil, the tuber crop was irrigated potato and the cereal was rain-fed wheat. The study indicated that rain-fed wheat in particular could be positively affected by climate change under either scenario, although particularly under B2 (see Figure 2).

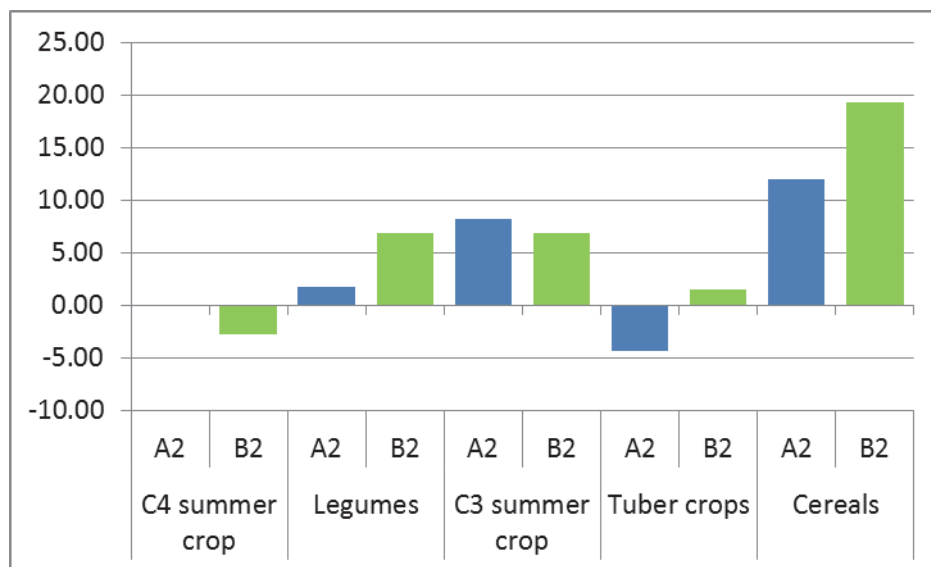


**Figure 2.** Impact of climate change on crop productivity for different types of crops for Turkey. The Y-axis is expressed as percentage difference between future (A2 and B2 scenarios respectively) and present yields. After Giannakopoulos et al. (2005, 2009).

Elsewhere, recent studies have assessed the impact of climate change on a global-scale and include impact estimates for West Asia as a whole (Tatsumi et al., 2011, Lobell et al., 2008, Fischer, 2009). Whilst these studies provide a useful indicator of crop yields under climate change for the *region*, it should be noted that the crop yields presented in such cases are not definitive *national* estimates. This is because the yields are averaged over the entire region, which includes other countries as well as Turkey.

Tatsumi et al. (2011) applied an improved version of the GAEZ crop model (iGAEZ) to simulate crop yields on a global scale for wheat, potato, cassava, soybean, rice, sweet potato, maize, green beans. The impact of global warming on crop yields from the 1990s to 2090s was assessed by projecting five GCM outputs under the SRES A1B scenario and



comparing the results for crop yields as calculated using the iGAEZ model for the period of 1990-1999. The results for West Asia, which includes Turkey, are displayed in Table 5.

Wheat	Potato	Cassava	Soybean	Rice	Sweet potato	Maize	Green beans
22.91	1.46	-	-18.67	4.35	-4.18	-19.32	16.23

**Table 5.** Average change in yield (%), during 1990s-2090s in Southeast Asia. Data is from Tatsumi et al. (2011).

Lobell et al. (2008) conducted an analysis of climate risks for the major crops in 12 food-insecure regions to identify adaptation priorities. Statistical crop models were used in combination with climate projections for 2030 from 20 GCMs that have contributed to the World Climate Research Programme’s Coupled Model Intercomparison Project phase 3. The results from the study for West Asia, are presented in Figure 3. Lobell et al. (2008) found that in West Asia (the region Turkey was included in), climate change had an adverse impact in 2030 on crop yield for maize, sugarcane, rice, soybean and sunflowers, and a modest positive impact was projected for potato.

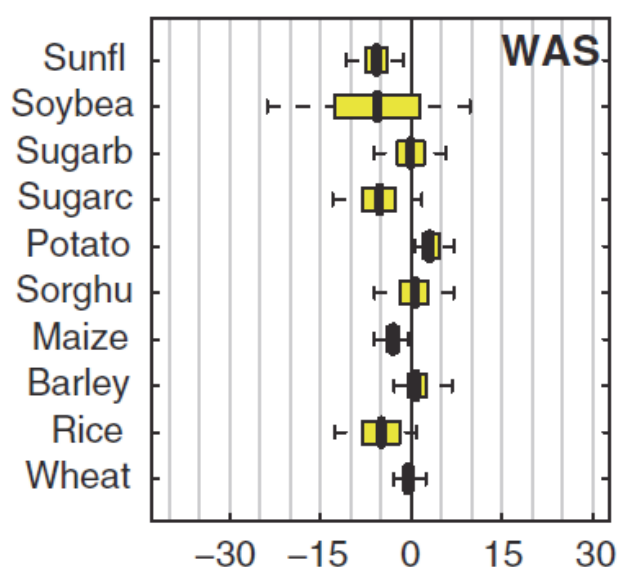


**Figure 3.** Probabilistic projections of production impacts in 2030 from climate change (expressed as a percentage of 1998 to 2002 average yields) for West Asia. Red, orange, and yellow indicate a Hunger Importance Ranking of 1 to 30 (more important), 31 to 60 (important), and 61 to 94 (less important), respectively. Dashed lines extend from 5th to 95th percentile of projections, boxes extend from 25th to 75th percentile, and the middle vertical line within each box indicates the median projection. Figure is from Lobell et al. (2008).

Fischer (2009) projected global 'production potential' changes for 2050 using the GAEZ (Global Agro-Ecological Zones) crops model with climate change scenarios from the HadCM3 and CSIRO GCMs respectively, under SRES A2 emissions. The impact of future climate on crop yields of rain-fed cereals are presented in Table 6 (relative to yield realised under current climate) for West Asia, the region in which Turkey was included.

	CO <sub>2</sub> fert.	2020s		2050s		2080s	
		CSIRO	HADCM3	CSIRO	HADCM3	CSIRO	HADCM3
<b>Rain-fed wheat</b>	Yes	3	2	-3	2	9	-6
	No	0	n/a	-9	n/a	-17	n/a
<b>Rain-fed maize</b>	Yes	33	12	38	25	26	31
	No	32	n/a	34	n/a	21	n/a
<b>Rain-fed cereals</b>	Yes	n/a	2	n/a	1	n/a	-5
	No	n/a	n/a	n/a	n/a	n/a	n/a
<b>Rain-fed sorghum</b>	Yes	11	n/a	12	n/a	9	n/a
	No	9	n/a	8	n/a	5	n/a

**Table 6.** Impacts of climate change on the production potential of rain-fed cereals in current cultivated land (% change with respect to yield realised under current climate), with two GCMs and with and without CO<sub>2</sub> fertilisation ("CO<sub>2</sub> fert.") under SRES A2 emissions. Data is from Fischer (2009).

In addition to the studies looking at the effect of changes in climate and CO<sub>2</sub> concentrations on crop yield, Avnery et al. (2011) investigated the effects of ozone surface exposure on crop yield losses for soybeans, maize and wheat under the SRES A2 and B1 scenarios respectively. Two metrics of ozone exposure were investigated; seasonal daytime (08:00-19:59) mean O<sub>3</sub> ("M12") and accumulated O<sub>3</sub> above a threshold of 40 ppbv ("AOT40"). The results for Turkey are presented in Table 7.

	A2		B1	
	M12	AOT40	M12	AOT40
<b>Soybeans</b>	30-45	25-30	20-25	25-30
<b>Maize</b>	10-15	6-8	8-10	4-6
<b>Wheat</b>	6-8	30-45	4-6	15-20

**Table 7.** National relative crop yield losses (%) for 2030 under A2 and B1 emission scenarios according to the M12 (seasonal daytime (08:00–19:59) mean) and AOT40 (accumulated O<sub>3</sub> above a threshold of 40 ppbv) metrics of O<sub>3</sub> exposure. Data is from Avnery et al. (2011).

## **National-scale or sub-national scale assessments**

### **Climate change studies**

Included in this section are results from recent studies that have applied crop models, alongside meteorological models and information from global climate models, to produce national or sub-national scale projections of future crop yields in Turkey

Yano et al. (2007) applied climate change projections from two climate models under the SRES A2 emissions scenario in the year 2079 to the SWAP (Soil-Water-Atmosphere-Plant) model, to investigate the impact of climate change on water demand and on wheat and maize yields. Both climate models simulated a shortening of the growing period of maize and wheat (9 and 24 days for maize and wheat respectively, for the first model; 3 and 9 days for maize and wheat respectively for the second model). The combination of shorter growth duration and a higher temperature reduced the biomass accumulation of both crops regardless of CO<sub>2</sub>-fertilization effect. The simulations under the combined effect of CO<sub>2</sub>-fertilisation and increased temperature suggested an increase of 16% and 36% in grain yield of wheat with the two climate models respectively, and a decrease by about 25% and an increase by 3% in maize yield, respectively.

Özdoğan (2011) investigated the impacts of elevated atmospheric CO<sub>2</sub> concentrations and associated changes in climate on winter wheat yields in north-western Turkey. Climate change scenarios were applied from four GCMs (CSIRO Mk3.5, NCAR CCSM3, UKMO HadCM3, GFDL CM2.1) and three SRES emissions scenarios (A2, A1B, B1), for three time horizons (2021–2040, 2041–2060, and 2061–2080), to the wheat crop model AFRC2. The simulations indicated that increased atmospheric CO<sub>2</sub> concentrations in the absence of changing climatic conditions had a slightly positive effect on yields. However, a significant decline in yields was simulated when temperature and precipitation were allowed to vary with increased atmospheric CO<sub>2</sub> concentrations. Under these conditions, winter wheat yields were estimated to decline between 5-35% by 2061-2080, depending upon GCM. When the multi-model ensemble mean GCM climate projections were applied, wheat yields were estimated to decline by 20% (A2), 19% (A1B) and 17% (B1) by 2061-2080.

## **AVOID programme results**

To further quantify the impact of climate change on crops, the AVOID programme simulated the effect of climate change on the suitability of land for crop cultivation for all countries reviewed in this literature assessment based upon the patterns of climate change from 21 GCMs (Warren et al., 2010). This ensures a consistent methodological approach across all countries and takes consideration of climate modelling uncertainties.

### **Methodology**

The effect of climate change on the suitability of land for crop cultivation is characterised here by an index which defines the percentage of cropland in a region with 1) a decrease in suitability or 2) an increase in suitability. A threshold change of 5% is applied here to characterise decrease or increase in suitability. The crop suitability index is calculated at a spatial resolution of  $0.5^{\circ} \times 0.5^{\circ}$ , and is based on climate and soil properties (Ramankutty et al., 2002). The baseline crop suitability index, against which the future changes are measured, is representative of conditions circa 2000. The key features of the climate for the crop suitability index are temperature and the availability of water for plants. Changes in these were derived from climate model projections of future changes in temperature and precipitation, with some further calculations then being used to estimate actual and potential evapotranspiration as an indicator of water availability. It should be noted that changes in atmospheric  $\text{CO}_2$  concentrations can decrease evapotranspiration by increasing the efficiency of water use by plants (Ramankutty et al., 2002), but that aspect of the index was not included in the analysis here. Increased  $\text{CO}_2$  can also increase photosynthesis and improve yield to a small extent, but again these effects are not included. Exclusion of these effects may lead to an overestimate of decreases in suitability.

The index here is calculated only for grid cells which contain cropland circa 2000, as defined in the global crop extent data set described by Ramankutty et al. (2008) which was derived from satellite measurements. It is assumed that crop extent does not change over time. The crop suitability index varies significantly for current croplands across the world (Ramankutty et al., 2002), with the suitability being low in some current cropland areas according to this index. Therefore, while climate change clearly has the potential to decrease suitability for cultivation if temperature and precipitation regimes become less favourable, there is also scope for climate change to increase suitability in some existing cropland areas if conditions become more favourable in areas where the suitability index is not at its maximum value of 1. It should be noted that some areas which are not currently croplands may already be

suitable for cultivation or may become suitable as a result of future climate change, and may become used as croplands in the future either as part of climate change adaptation or changes in land use arising for other reasons. Such areas are not included in this analysis.

## **Results**

Crop suitability was estimated under the pattern of climate change from 21 GCMs with two emissions scenarios; 1) SRES A1B and 2) an aggressive mitigation scenario where emissions follow A1B up to 2016 but then decline at a rate of 5% per year thereafter to a low emissions floor (denoted A1B-2016-5-L). The application of 21 GCMs is an attempt to quantify the uncertainty due to climate modelling, although it is acknowledged that only one crop suitability impacts model is applied. Simulations were performed for the years 2030, 2050, 2080 and 2100. The results for Turkey are presented in Figure 4.

The model projections implied only up to 2%-13% of current Turkish cropland areas to undergo an improvement of suitability of cultivation, for both scenarios, over the 21st century with little variation in this range through the years. The models showed a very high degree of consensus towards a large proportion of current Turkish croplands undergoing declining suitability from 2030 onwards. In 2030, approximately 75%-95% of current croplands experienced declining suitability in both scenarios. By 2100 this had remained similar under the mitigation scenario, but risen to 86%-100% under A1B. So for Turkey, there is a strong consensus between models of climate change giving declining suitability for cultivation over most current croplands.

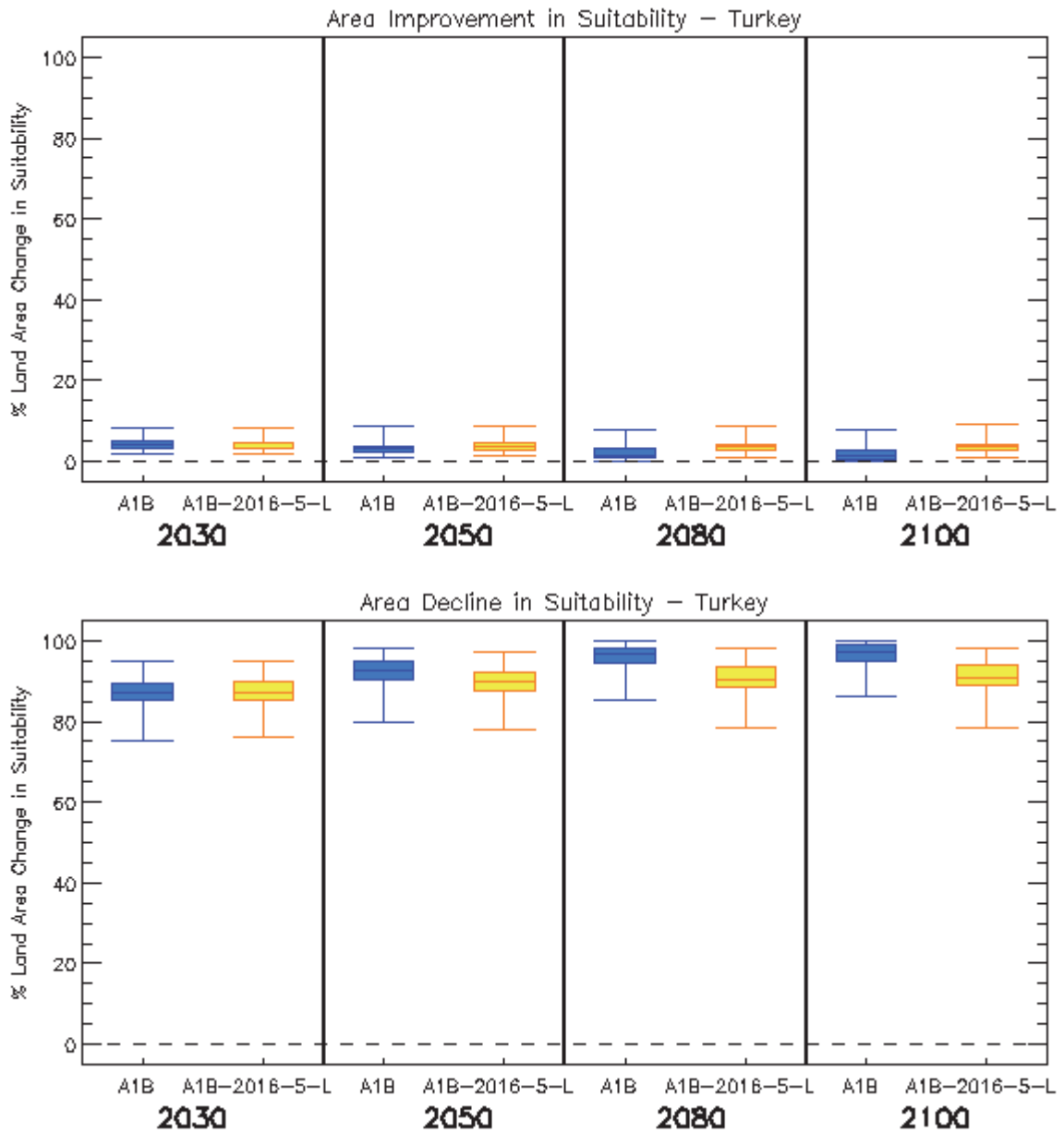


**Figure 4.** Box and whisker plots for the impact of climate change on increased crop suitability (top panel) and decreased crop suitability (bottom panel) for Turkey, from 21 GCMs under two emissions scenarios (A1B and A1B-2016-5-L), for four time horizons. The plots show the 25th, 50th, and 75th percentiles (represented by the boxes), and the maximum and minimum values (shown by the extent of the whiskers).

# Food security

## Headline

Recent global-scale studies suggest that Turkey may not face major food-insecurity under climate change scenarios, when food supply production from terrestrial biomes is considered (Falkenmark et al., 2009, Wu et al., 2011). However, if food supply from marine capture fisheries is considered, then the outlook is less optimistic (Cheung et al., 2010). Further research should seek to understand how changes in capture fisheries and land-based food production combine to affect total food security for Turkey under climate change scenarios.

## Supporting literature

### Introduction

Food security is a concept that encompasses more than just crop production, but is a complex interaction between food availability and socio-economic, policy and health factors that influence access to food, utilisation and stability of food supplies. In 1996 the World Food Summit defined food security as existing 'when all people, at all times, have physical and economic access to sufficient, safe and nutritious food to meet their dietary needs, and their food preferences are met for an active and healthy life'.

As such this section cannot be a comprehensive analysis of all the factors that are important in determining food security, but does attempt to assess a selection of the available literature on how climate change, combined with projections of global and regional population and policy responses, may influence food security.

### Assessments that include a global or regional perspective

Turkey is not presently a country of high concern in terms of food security, particularly in a global context. According to the FAO's *Food Security Country Profiles* (FAO, 2010) an extremely low proportion (<5%) of Turkey's population are currently undernourished.

## **Climate change studies**

A study on food security by Wu et al. (2011) simulated crop yields with the GIS-based Environmental Policy Integrated Climate (EPIC) model. This was combined with crop areas simulated by a crop choice decision model to calculate total food production and per capita food availability across the globe, which was used to represent the status of food availability and stability. The study focussed on the SRES A1 scenario and applied climate change simulations for the 2000s (1991–2000) and 2020s (2011–2020). The climate simulations were performed by MIROC (Model for Interdisciplinary Research on Climate) version 3.2., which means the effects of climate model uncertainty were not considered. Downscaled population and GDP data from the International Institute for Applied Systems Analysis (IIASA) were applied in the simulations. Wu et al. (2011) conclude that Turkey is not likely to face severe food insecurity in the next 20 years.

A global analysis of food security under climate change scenarios for the 2050s by Falkenmark et al. (2009) considered the importance of water availability for ensuring global food security. The study is largely supportive of the optimistic assessment presented by Wu et al. (2011). The study presents an analysis of water constraints and opportunities for global food production on current croplands and assesses five main factors:

- 1) how far improved land and water management might go towards achieving global food security,
- 2) the water deficits that would remain in regions currently experiencing water scarcity and which are aiming at food self-sufficiency,
- 3) how the water deficits above may be met by importing food,
- 4) the cropland expansion required in low income countries without the needed purchasing power for such imports, and
- 5) the proportion of that expansion pressure which will remain unresolved due to potential lack of accessible land.

Similar to the study presented by Wu et al. (2011), there is no major treatment of modelling uncertainty; simulations were generated by only the LPJml dynamic global vegetation and water balance model (Gerten et al. 2004) with population growth and climate change under the SRES A2 emission scenario. Falkenmark et al. (2009) summarise the impacts of future improvements (or lack thereof) in water productivity for each country across the globe and show that this generates either a deficit or a surplus of water in relation to food water



requirements in each country. These can be met either by trade or by horizontal expansion (by converting other terrestrial ecosystems to crop land). The study estimated that in 2050 around one third of the world's population will live in each of three regions: those that export food, those that import food, and those that have to expand their croplands at the expense of other ecosystems because they do not have enough purchasing power to import their food. The simulations demonstrated that Turkey was a food exporting country in 2050.

The International Food Policy Research Institute (IFPRI) have produced a report and online tool that describes the possible impact of climate change on two major indicators of food security; 1) the number of children aged 0-5 malnourished, and 2) the average daily kilocalorie availability (Nelson et al., 2010, IFPRI, 2010). The study considered three broad socio-economic scenarios; 1) a 'pessimistic' scenario, which is representative of the lowest of the four GDP growth rate scenarios from the Millennium Ecosystem Assessment GDP scenarios and equivalent to the UN high variant of future population change, 2) a 'baseline' scenario, which is based on future GDP rates estimated by the World Bank and a population change scenario equivalent to the UN medium variant, and 3) an 'optimistic' scenario that is representative of the highest of the four GDP growth rate scenarios from the Millennium Ecosystem Assessment GDP scenarios and equivalent to the UN low variant of future population change. Nelson et al. (2010) also considered climate modelling and emission uncertainty and included a factor to account for CO<sub>2</sub> fertilisation in their work. The study applied two GCMs, the CSIRO GCM and the MIROC GCM, and forced each GCM with two SRES emissions scenarios (A1B and B1). They also considered a no climate change emissions scenario, which they called 'perfect mitigation' (note that in most other climate change impact studies that this is referred to as the baseline). The perfect mitigation scenario is useful to compare the effect of climate change against what might have happened without, but is not a realistic scenario itself. Estimates for both indicators of food security from 2010 to 2050, for Turkey, are presented in Table 8 and Table 9. Figure 5 displays the effect of climate change, calculated by comparing the 'perfect mitigation' scenario with each baseline, optimistic and pessimistic scenario. The results show that under the baseline and pessimistic socio-economic scenarios, average kilocalorie availability declines during 2010-2050, and this is compounded by climate change. Up to a 10% decline in kilocalorie availability is attributable to climate change. Only under the optimistic scenario does availability improve by 2050, but still, climate change has a negative effect on calorific availability. The projections for child undernourishment are generally more optimistic, although climate change remains a mitigating factor. Climate change is attributable for up to a 19% increase in child malnourishment in 2050. Figure 6 and Figure 7 show how the

changes projected for Turkey compare with the projections for the rest of the globe (IFPRI, 2010).

Scenario	2010	2050
Baseline CSI A1B	3160	2983
Baseline CSI B1	3165	3009
Baseline MIR A1B	3140	2903
Baseline MIR B1	3153	2965
Baseline Perfect Mitigation	3212	3217
Pessimistic CSI A1B	3131	2820
Pessimistic CSI B1	3136	2844
Pessimistic MIR A1B	3111	2740
Pessimistic MIR B1	3120	2782
Pessimistic Perfect Mitigation	3183	3037
Optimistic CSI A1B	3123	3290
Optimistic CSI B1	3128	3311
Optimistic MIR A1B	3103	3194
Optimistic MIR B1	3112	3238
Optimistic Perfect Mitigation	3175	3545

**Table 8.** Average daily kilocalorie availability simulated under different climate and socioeconomic scenarios, for Turkey (IFPRI, 2010).

Scenario	2010	2050
Baseline CSI A1B	1.42	1.1
Baseline CSI B1	1.42	1.08
Baseline MIR A1B	1.43	1.14
Baseline MIR B1	1.43	1.1
Baseline Perfect Mitigation	1.39	0.98
Pessimistic CSI A1B	1.44	1.35
Pessimistic CSI B1	1.44	1.34
Pessimistic MIR A1B	1.45	1.4
Pessimistic MIR B1	1.45	1.38
Pessimistic Perfect Mitigation	1.41	1.23
Optimistic CSI A1B	1.44	0.82
Optimistic CSI B1	1.44	0.81
Optimistic MIR A1B	1.45	0.86
Optimistic MIR B1	1.45	0.84
Optimistic Perfect Mitigation	1.41	0.72

**Table 9.** Number of malnourished children (aged 0-5; millions) simulated under different climate and socioeconomic scenarios, for Turkey (IFPRI, 2010).

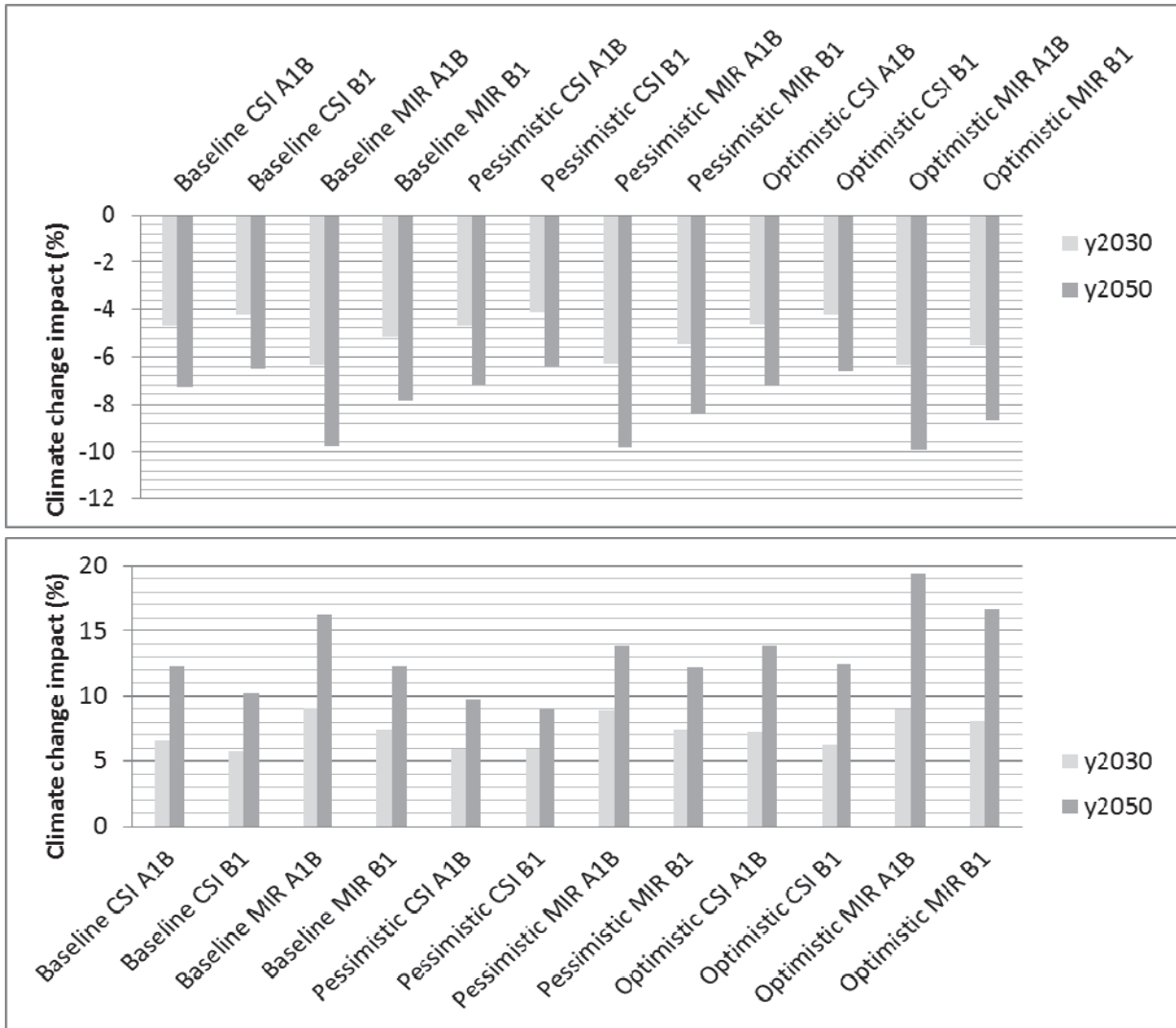


**Figure 5.** The impact of climate change on average daily kilocalorie availability (top panel) and number of malnourished children (bottom) (IFPRI, 2010).

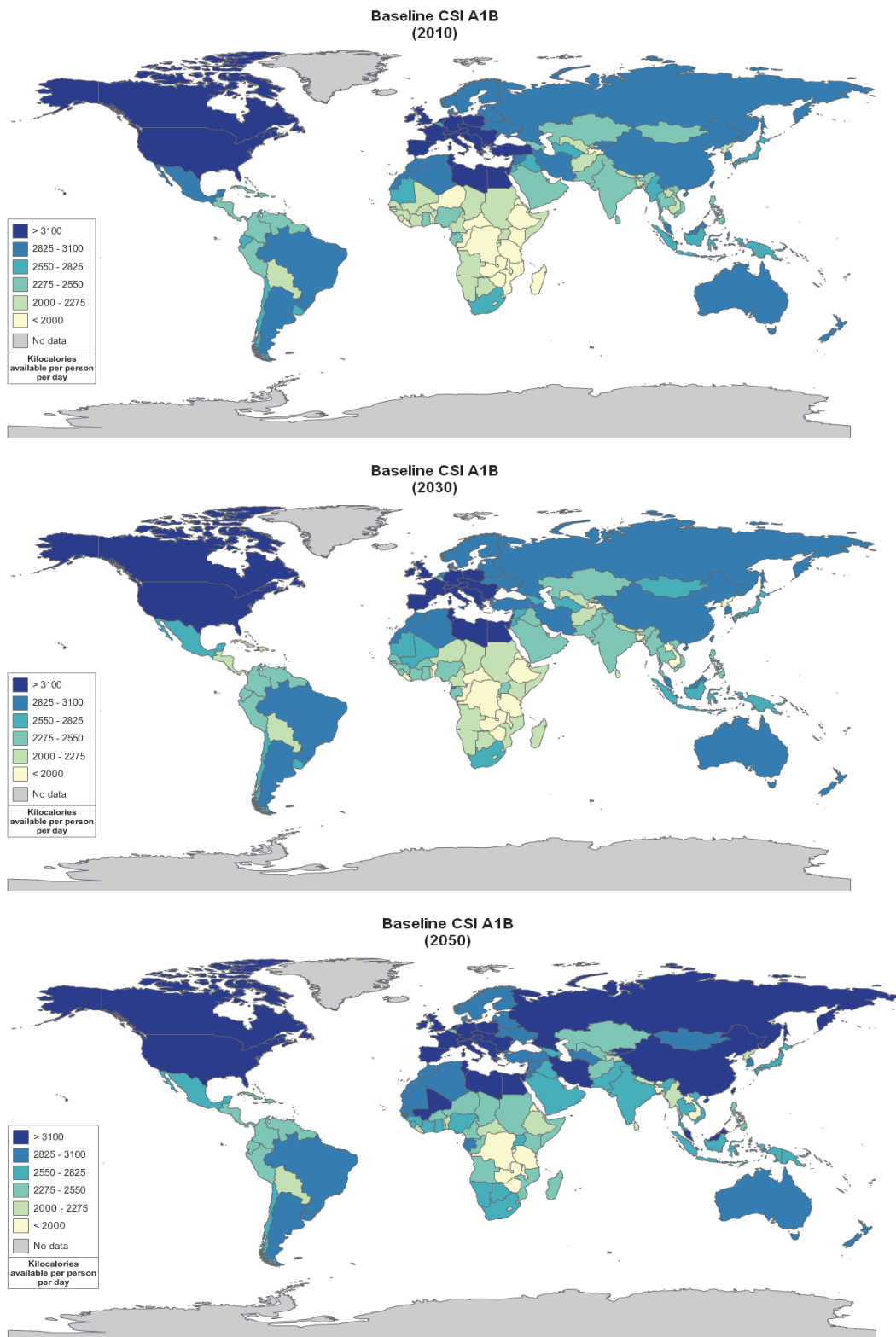


**Figure 6.** Average daily kilocalorie availability simulated by the CSIRO GCM (CSI) under an A1B emissions scenario and the baseline socioeconomic scenario, for 2010 (top panel), 2030 (middle panel) and 2050 (bottom panel). Figure is from IFPRI (2010). The changes show the combination of both climate change and socio-economic changes.

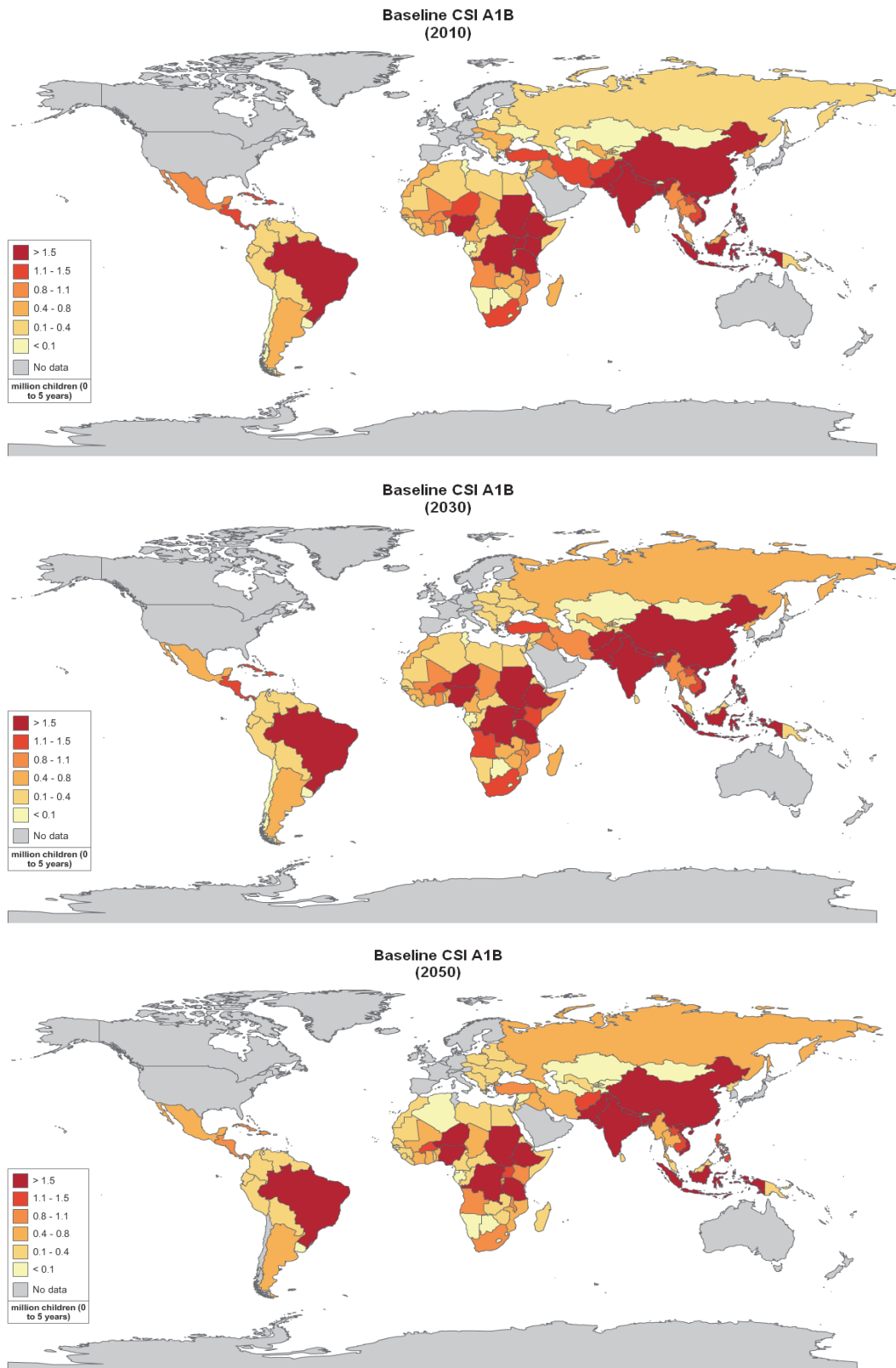


**Figure 7.** Number of malnourished children (aged 0-5; millions) simulated by the CSIRO GCM (CSI) under an A1B emissions scenario and the baseline socioeconomic scenario, for 2010 (top panel), 2030 (middle panel) and 2050 (bottom panel). Figure is from IFPRI (2010). The changes show the combination of both climate change and socio-economic changes.

It is important to note that up until recently, projections of climate change impacts on global food supply have tended to focus solely on production from terrestrial biomes, with the large contribution of animal protein from marine capture fisheries often ignored. However, recent studies have addressed this knowledge gap. In addition to the direct affects of climate change, changes in the acidity of the oceans, due to increases in CO<sub>2</sub> levels, could also have an impact of marine ecosystems, which could also affect fish stocks. However, this relationship is complex and not well understood, and studies today have not been able to begin to quantify the impact of ocean acidification on fish stocks.

Allison et al. (2009) present a global analysis that compares the vulnerability of 132 national economies to potential climate change impacts on their capture fisheries. The study considered a country's vulnerability to be a function of the combined effect of projected climate change, the relative importance of fisheries to national economies and diets, and the national societal capacity to adapt to potential impacts and opportunities. Climate change projections from a single GCM under two emissions scenarios (SRES A1FI and B2) were used in the analysis. Allison et al. (2009) concluded that the national economy of Turkey presented a high vulnerability to climate change impacts on fisheries (see Figure 8). It should be noted, however, that results from studies that have applied only a single climate model or climate change scenario should be interpreted with caution. This is because they do not consider other possible climate change scenarios which could result in a different impact outcome, in terms of magnitude and in some cases sign of change.

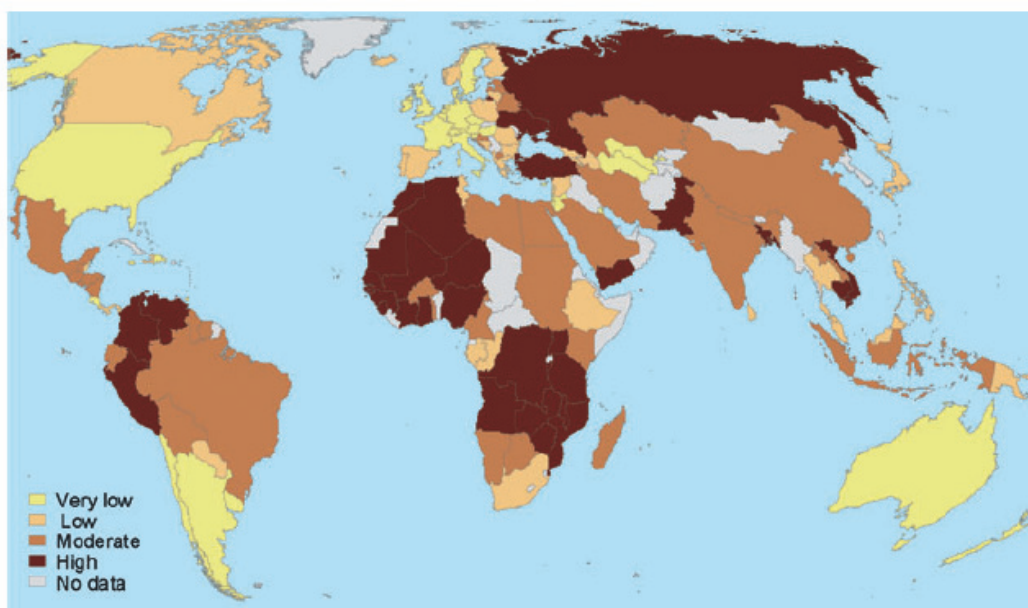


**Figure 8.** Vulnerability of national economies to potential climate change impacts on fisheries under SRES B2 (Allison et al., 2009). Colours represent quartiles with dark brown for the upper quartile (highest index value), yellow for the lowest quartile, and grey where no data were available.

## **National-scale or sub-national scale assessments**

Literature searches yielded no results for national-scale or sub-national scale studies for this impact sector.



# Water stress and drought

## Headline

Studies generally agree that Turkey currently experiences a high degree of water stress. Several global-scale and national-scale assessments indicate that droughts could increase in frequency and magnitude with climate change. There is also consensus among several studies that water stress could increase for Turkey. This is supported in recent simulations by the AVOID programme. The greatest potential effects of climate change on drought are reported for the south of the country.

## Supporting literature

### Introduction

For the purposes of this report droughts are considered to be extreme events at the lower bound of climate variability; episodes of prolonged absence or marked deficiency of precipitation. Water stress is considered as the situation where water stores and fluxes (e.g. groundwater and river discharge) are not replenished at a sufficient rate to adequately meet water demand and consumption.

A number of impact model studies looking at water stress and drought for the present (recent past) and future (climate change scenario) have been conducted. These studies are conducted at global or national scale and include the application of global water 'availability' or 'stress' models driven by one or more climate change scenario from one or more GCM. The approaches variously include other factors and assumptions that might affect water availability, such as the impact of changing demographics and infrastructure investment, etc. These different models (hydrological and climate), assumptions and emissions scenarios mean that there are a range of water stress projections for Turkey. This section summarises findings from these studies to inform and contextualise the analysis performed by the AVOID programme for this project. The results from the AVOID work and discussed in the next section.

Important knowledge gaps and key uncertainties which are applicable to Turkey as well as at the global-scale, include; the appropriate coupling of surface water and groundwater in hydrological models, including the recharge process, improved soil moisture and evaporation dynamics, inclusion of water quality, inclusion of water management (Wood et al. 2011) and further refinement of the down-scaling methodologies used for the climate driving variables (Harding et al. 2011).

## **Assessments that include a global or regional perspective**

### **Recent Past**

Recent research presented by Vörösmarty et al. (2010) describes the calculation of an 'Adjusted Human Water Security Threat' (HWS) indicator. The indicator is a function of the cumulative impacts of 23 biophysical and chemical drivers simulated globally across 46,517 grid cells representing 99.2 million km<sup>2</sup>. With a digital terrain model at its base, the calculations in each of the grid boxes of this model take account of the multiple pressures on the environment, and the way these combine with each other, as water flows in river basins. The level of investment in water infrastructure is also considered. This infrastructure measure (the *investment benefits factor*) is based on actual existing built infrastructure, rather than on the financial value of investments made in the water sector, which is a very unreliable and incomplete dataset. The analysis described by Vörösmarty et al. (2010) represents the current state-of-the-art in applied policy-focussed water resource assessment. In this measure of water security, the method reveals those areas where this is lacking, which is a representation of human water stress. One drawback of this method is that no analysis is provided in places where there is 'no appreciable flow', where rivers do not flow, or only do so for such short periods that they cannot be reliably measured. This method also does not address places where water supplies depend wholly on groundwater or desalination, being piped in, or based on wastewater reuse. It is based on what is known from all verified peer reviewed sources about surface water resources as generated by natural ecosystem processes and modified by river and other hydraulic infrastructure ( Vörösmarty ey al., 2010).

Here, the present day HWS is mapped for Turkey. The model applied operates at 50km resolution, so, larger countries appear to have smoother coverage than smaller countries, but all are mapped and calculated on the same scale, with the same data and model, and thus comparisons between places are legitimate. It is important to note that this analysis is a comparative one, where each place is assessed *relative* to the rest of the globe. In this way, this presents a realistic comparison of conditions across the globe. As a result of this,

however, some places may seem to be less stressed than may be originally considered. One example is Australia, which is noted for its droughts and long dry spells, and while there are some densely populated cities in that country where water stress is a real issue, for most of the country, *relative to the rest of the world*, the measure suggests water stress (as measured by HWS defined by Vörösmarty et al. (2010)), is not a serious problem.

Figure 9 presents the results of this analysis for Turkey. Turkey is shown to be some of the highest levels of water security threat of the countries in Europe. It is densely populated and most areas of the country face high or very high levels of water stress. This problem is likely to increase with the rapidly rising population and the potential drying associated with rising temperatures.

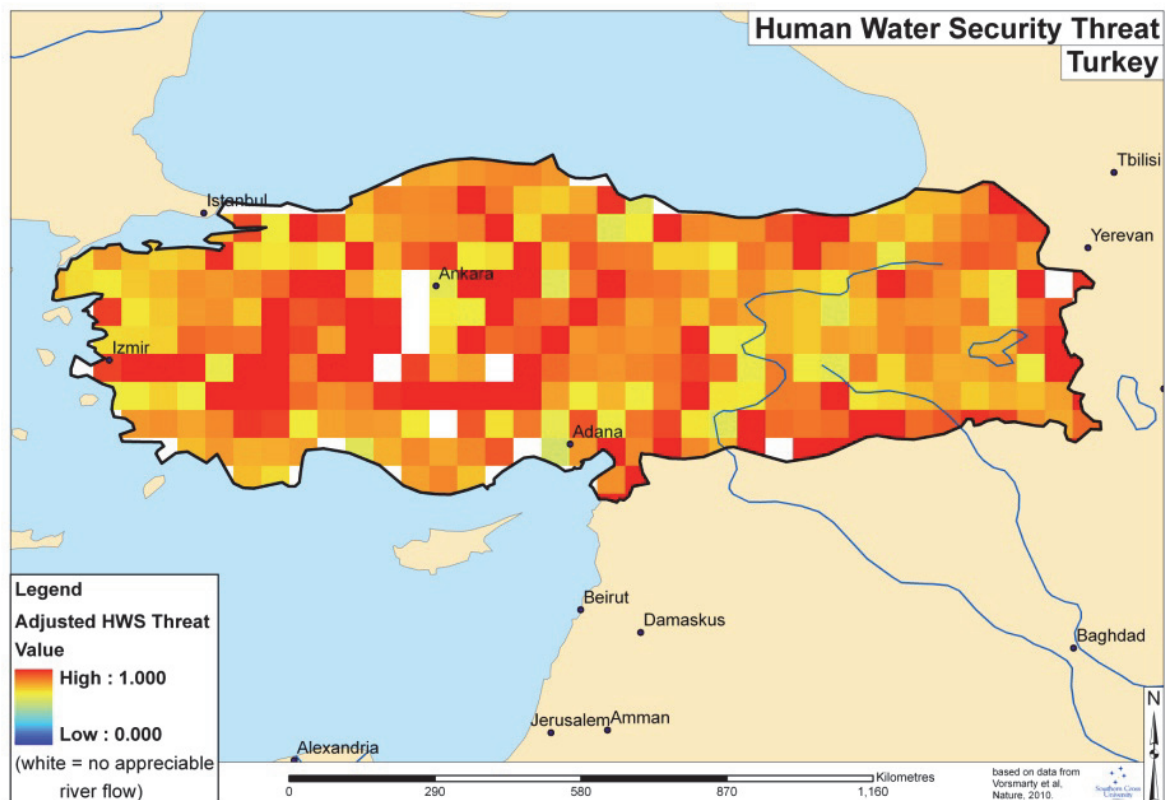


**Figure 9.** Present Adjusted Human Water Security Threat (HWS) for Turkey, calculated following the method described by Vörösmarty et al. (2010).

Smakhtin et al. (2004) describe a first attempt to estimate the volume of water required for the maintenance of freshwater-dependent ecosystems at the global scale. This total environmental water requirement (EWR) consists of ecologically relevant low-flow and high-

flow components. The authors argue that the relationship between water availability, total use and the EWR may be described by the water stress indicator (WSI). If WSI exceeds 1.0, the basin is classified as “environmentally water scarce”. In such a basin, the discharge has already been reduced by total withdrawals to such levels that the amount of water left in the basin is less than EWR. Smaller index values indicate progressively lower water resources exploitation and lower risk of “environmental water scarcity.” Basins where WSI is greater than 0.6 but less than 1.0 are arbitrarily defined as heavily exploited or “environmentally water stressed” and basins where WSI is greater than 0.3 but less than 0.6 are defined as moderately exploited. In these basins, 0-40% and 40-70% of the utilizable water respectively is still available before water withdrawals come in conflict with the EWR. Environmentally “safe” basins are defined as those where WSI is less than 0.3. The global distribution of WSI for the 1961-1990 time horizon is shown in Figure 10. The results show that for the basins considered, much of Turkey presents a high WSI.

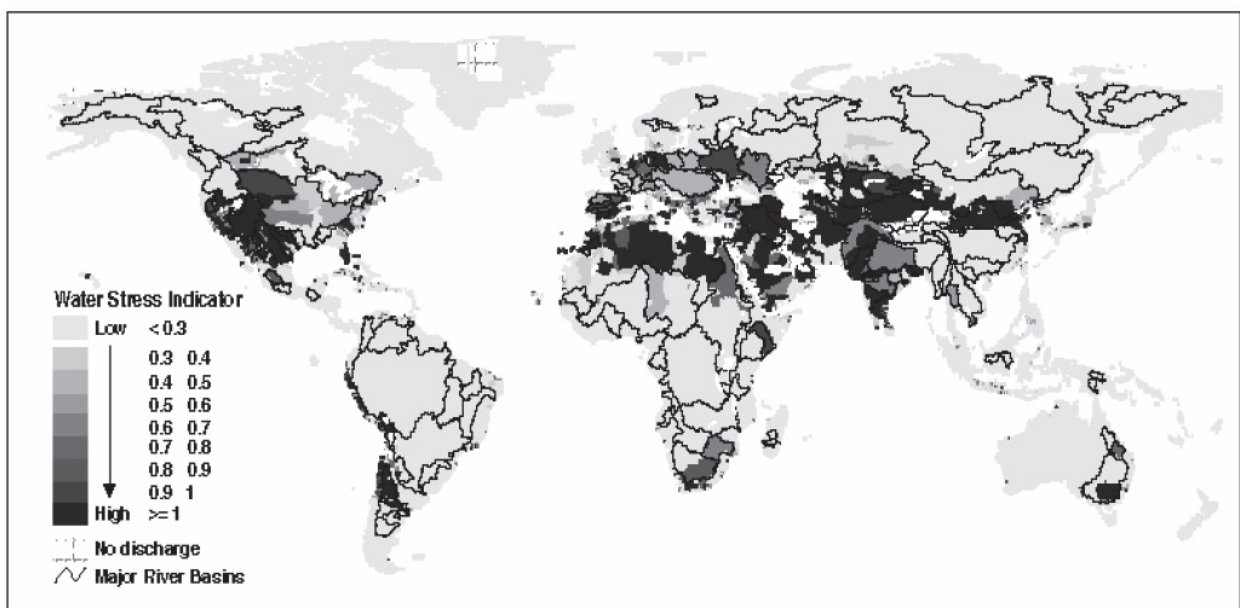


**Figure 10.** A map of the major river basins across the globe and the water stress indicator (WSI) for the 1961-1990 time horizon. The figure is from Smakhtin et al. (2004).

### Climate Change Studies

Rockstrom et al. (2009) applied the LPJml vegetation and water balance model to assess green-blue water availability and requirements. The authors applied observed climate data from the CRU TS2.1 gridded dataset for a present-day simulation, and climate change projections from the HadCM2 GCM under the SRES A2 scenario to represent the climate change scenario for the year 2050. The study assumed that if water availability was less

than 1,300m<sup>3</sup>/capita/year, then the country was considered to present insufficient water for food self-sufficiency. The simulations presented by Rockstrom et al. (2009) should not be considered as definitive, however, because the study only applied one climate model, which means climate modelling uncertainty was overlooked. The results from the two simulations are presented in Figure 11. Rockstrom et al. (2009) found that globally in 2050 and under the SRES A2 scenario, around 59% of the world's population could be exposed to "blue water shortage" (i.e. irrigation water shortage), and 36% exposed to "green water shortages" (i.e. infiltrated rain shortage). For Turkey, Rockstrom et al. (2009) found that blue-green water availability was well above the 1,300m<sup>3</sup>/capita/year threshold in the present climate but with climate change, this reduced to 1,300-1,700 m<sup>3</sup>/capita/year, which implies that Turkey's water resource requirements could be compromised by 2050.

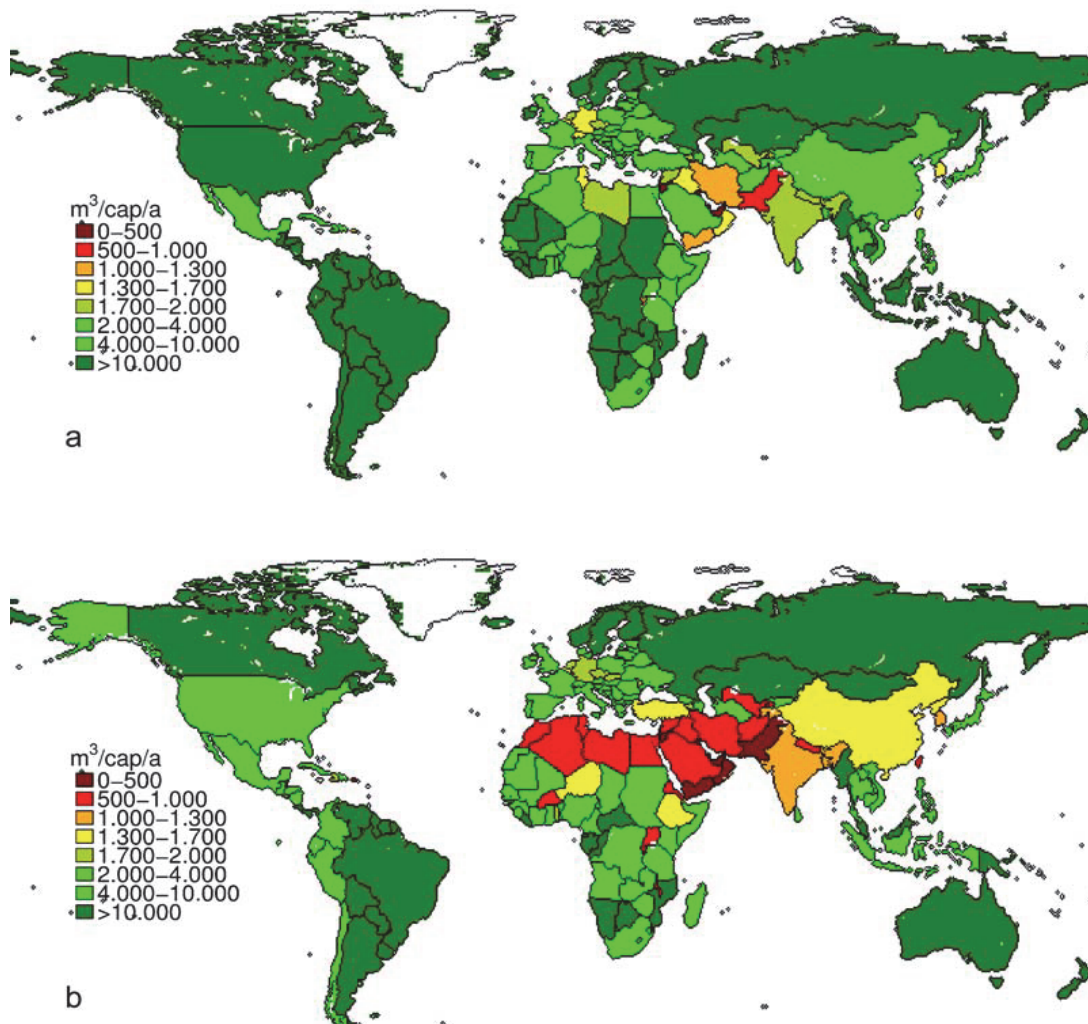


**Figure 11.** Simulated blue-green water availability (m<sup>3</sup>/capita/year) for present climate (top panel) and including both demographic and climate change under the SRES A2 scenario in 2050 (bottom panel). The study assumed that if water availability was less than 1,300m<sup>3</sup>/capita/year, then the country was considered to present insufficient water for food self-sufficiency. The figure is from Rockstrom et al. (2009).

Doll (2009) presents updated estimates of the impact of climate change on groundwater resources by applying a new version of the WaterGAP hydrological model. The study accounted for the number of people affected by changes in groundwater resources under climate change relative to present (1961-1990). To this end, the study provides an assessment of the vulnerability of humans to decreases in available groundwater resources (GWR). This indicator was termed the "Vulnerability Index" (VI), defined as;  $VI = -\% \text{ change GWR} * \text{Sensitivity Index (SI)}$ . The SI component was a function of three more specific sensitivity indicators that include an indicator of water scarcity (calculated from the ratio between consumptive water use to low flows), an indicator for the dependence upon groundwater supplies, and an indicator for the adaptive capacity of the human system. Doll (2009) applied climate projections from two GCMs (ECHAM4 and HadCM3) to WaterGAP, for two scenarios (SRES A2 and B2), for the 2050s. Figure 12 presents each of these four simulations respectively. There is variation across scenarios and GCMs. For Turkey, the simulations with both GCMs indicate that parts of Turkey present a very high VI, especially in the south of the country; one of the highest in Europe with southern Italy and southern Spain.

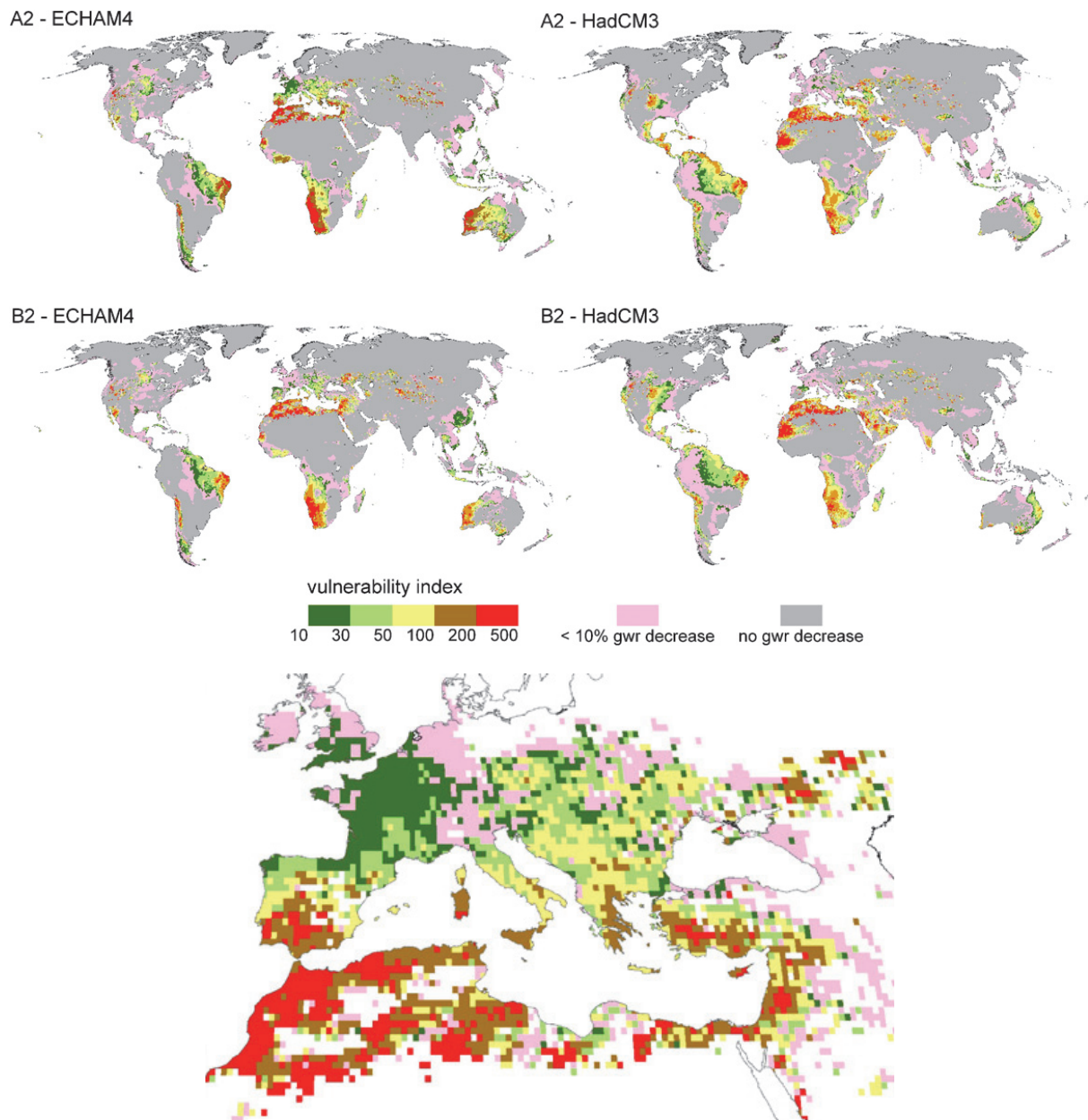


**Figure 12.** Vulnerability index (VI) showing human vulnerability to climate change induced decreases of renewable groundwater resources (GWR) by the 2050s under two emissions scenarios for two GCMs. VI is only defined for areas with a GWR decrease of at least 10% relative to present (1961-1990). Also shown is VI for the Mediterranean region with ECHAM4 under A2 emissions. The figure is from Doll (2009).

Lehner et al. (2006) assessed the impact of climate change on European drought risk. The authors accounted for future human water use and assessed future flood and drought frequencies by applying the WaterGAP hydrological model, driven by climate projections from the HadCM3 and ECHAM4 GCMs, under a 1%/year CO<sub>2</sub> increase emissions scenario. The simulations are presented in Figure 13 and Figure 14. The results reflect the general consensus from other studies that southern and south-eastern Europe could experience increased drought frequencies, leading to water stress. This in part due to increased water

use but the impacts are much more pronounced and wide spread when climate change is factored in (Lehner et al., 2006). Long term projections indicate those drought events expected to occur once every 100 years could become much more frequent, to around every 40 years in the most extreme areas, including much of the Mediterranean. For Turkey, both GCMs simulated that the current 100-year drought could be expected to occur more frequently with climate change. Moreover, the results show that the 100-year drought could become more intense with climate change, increasing in intensity by over 10% from present magnitude.

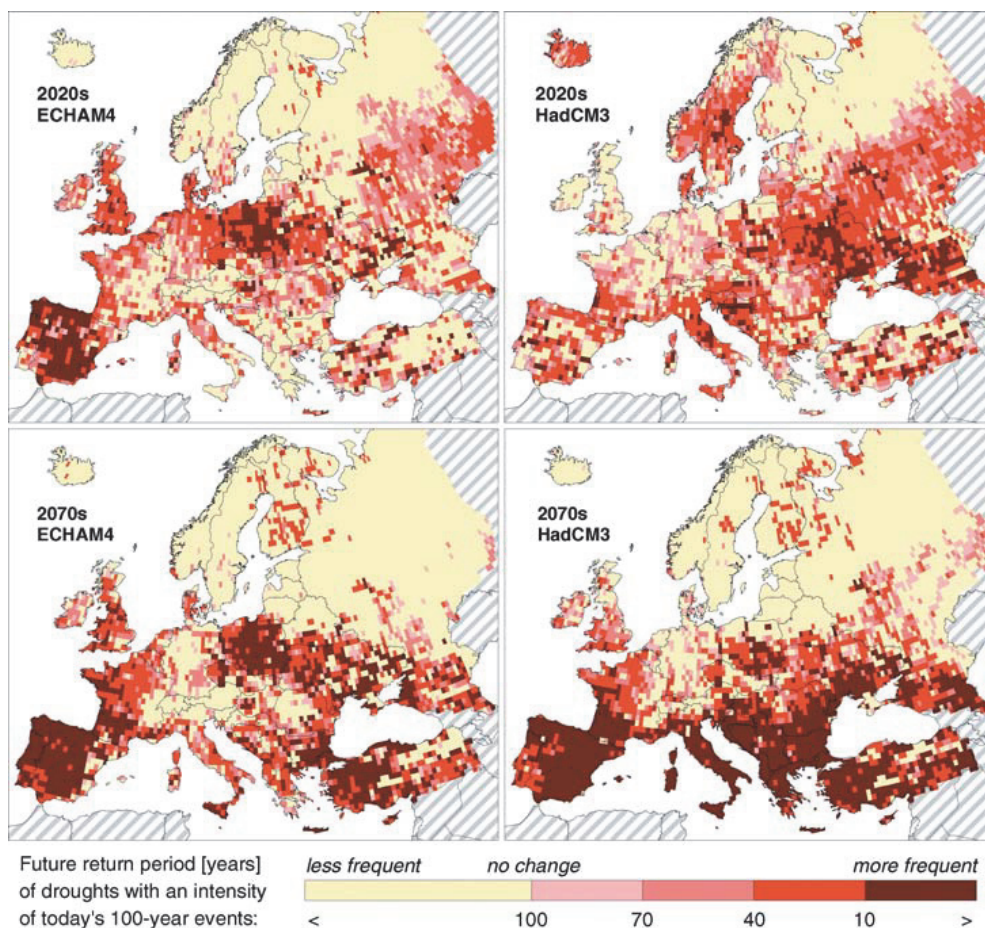


**Figure 13.** Change in recurrence of 100-year droughts, based on comparisons between today's climate and water use (1961–1990) and simulations for the 2020s and 2070s (ECHAM4 and HadCM3 GCMs), under a 1%/year CO<sub>2</sub> increase emissions scenario. The figure is from Lehner et al. (2006).



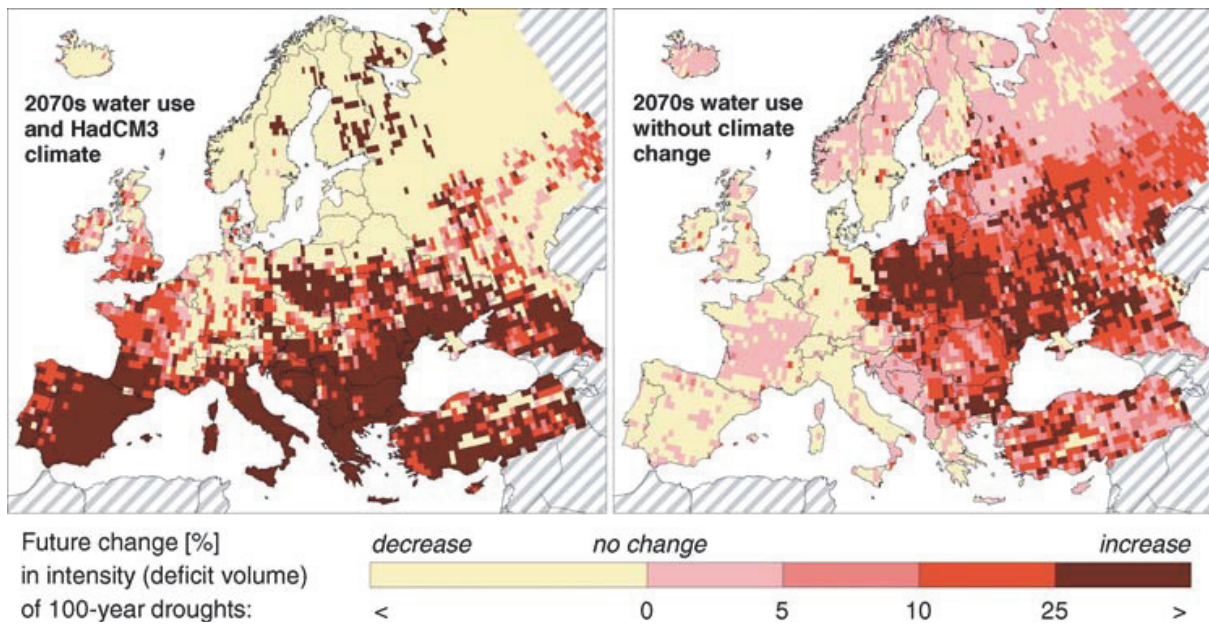


**Figure 14.** Change in intensity of 100-year droughts, based on comparison between today's climate and water use (1961–1990) and simulations for the 2070s (left map: HadCM3 GCM; right map: only water use scenario, no climate change), under a 1%/year CO<sub>2</sub> increase emissions scenario.

## National-scale or sub-national scale assessments

### Climate change studies

Smaller-scale assessments point towards increases in water stress with climate change for Turkey, which supports the results from larger-scale studies (Doll, 2009, Lehner et al., 2006). Fujihara et al. (2008b) applied climate change simulations from the MRI-CGMM2 and CCSR GCMs under an SRES A2 emissions scenario to explore the impact of climate change on water security in Turkey. The authors simulated average annual changes in temperature of between +2°C and +2.7°C, evapotranspiration of between -9% and -10%, and runoff of between -52% and -61% respectively. Water budget model simulations presented by Ozkul (2009) reveal that surface waters in the Turkish basins they considered could reduce by nearly 20% in 2030. This reduction was projected to continue so that reductions of 35% and 50% could be experienced by 2050 and 2100 respectively. Gao and Giorgi (2008) calculated aridity indices for climate simulations under A2 and B2 emissions scenarios. Results indicated that by 2100 Turkey could experience an expansion of arid areas that could lead to increased water stress around the southern Mediterranean areas.

## AVOID Programme Results

To further quantify the impact of climate change on water stress and the inherent uncertainties, the AVOID programme calculated water stress indices for all countries reviewed in this literature assessment based upon the patterns of climate change from 21 GCMs (Warren et al., 2010), following the method described by Gosling et al. (2010) and Arnell (2004). This ensures a consistent methodological approach across all countries and takes consideration of climate modelling uncertainties.

### Methodology

The indicator of the effect of climate change on exposure to water resources stress has two components. The first is the number of people within a region with an *increase in exposure to stress*, calculated as the sum of 1) people living in water-stressed watersheds with a significant reduction in runoff due to climate change and 2) people living in watersheds which become water-stressed due to a reduction in runoff. The second is the number of people within a region with a *decrease in exposure to stress*, calculated as the sum of 1) people living in water-stressed watersheds with a significant increase in runoff due to climate change and 2) people living in watersheds which cease to be water-stressed due to an increase in runoff. It is not appropriate to calculate the net effect of “increase in exposure” and “decrease in exposure”, because the consequences of the two are not equivalent. A water-stressed watershed has an average annual runoff less than 1000m<sup>3</sup>/capita/year, a widely used indicator of water scarcity. This indicator may underestimate water stress in watersheds where per capita withdrawals are high, such as in watersheds with large withdrawals for irrigation.

Average annual runoff (30-year mean) is simulated at a spatial resolution of 0.5x0.5° using a global hydrological model, MacPDM (Gosling and Arnell, 2011), and summed to the watershed scale. Climate change has a “significant” effect on average annual runoff when the change from the baseline is greater than the estimated standard deviation of 30-year mean annual runoff: this varies between 5 and 10%, with higher values in drier areas.

The pattern of climate change from 21 GCMs was applied to MacPDM, under two emissions scenarios; 1) SRES A1B and 2) an aggressive mitigation scenario where emissions follow A1B up to 2016 but then decline at a rate of 5% per year thereafter to a low emissions floor (denoted A1B-2016-5-L). Both scenarios assume that population changes through the 21<sup>st</sup> century following the SRES A1 scenario as implemented in IMAGE 2.3 (van Vuuren et al., 2007). The application of 21 GCMs is an attempt to quantify the uncertainty due to climate

modelling, although it is acknowledged that only one impacts model is applied (MacPDM). Simulations were performed for the years 2030, 2050, 2080 and 2100. Following Warren et al. (2010), changes in the population affected by increasing or decreasing water stress represent the additional percentage of population affected due to climate change, not the absolute change in the percentage of the affected population relative to present day.

## **Results**

The results for Turkey are presented in Figure 15. None of the 21 GCMs are associated with simulated decreases in water stress under climate change. By 2100 and under A1B, the median population across 21 GCMs exposed to an increase in water stress due to climate change is 45%. Under the mitigation scenario, this is 30%. The simulations show that Turkey's population could experience a large increase in water stress with climate change, which supports the results from other large-scale assessments (Doll, 2009, Lehner et al., 2006).

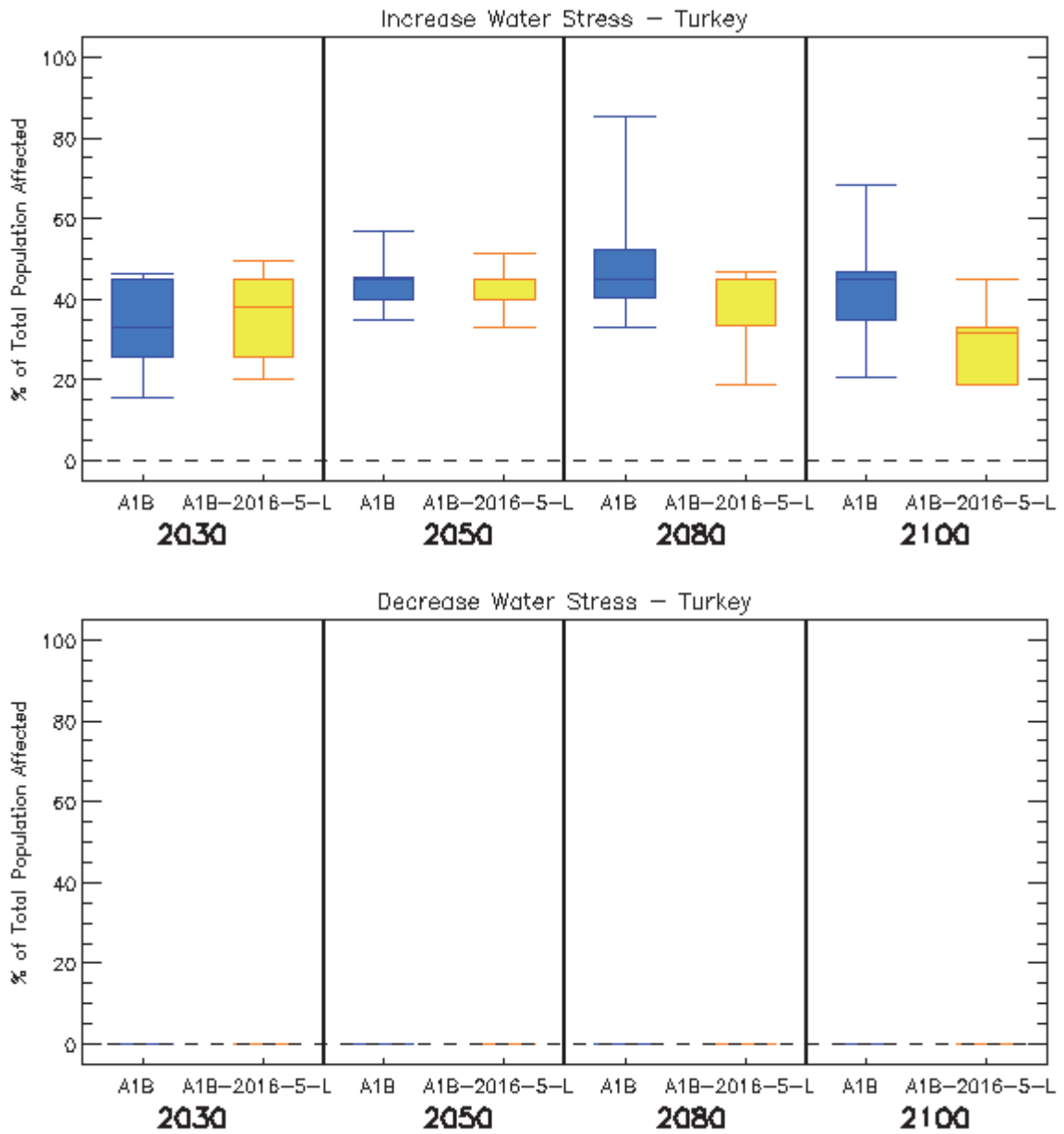


**Figure 15.** Box and whisker plots for the impact of climate change on increased water stress (top panel) and decreased water stress (bottom panel) in Turkey, from 21 GCMs under two emissions scenarios (A1B and A1B-2016-5-L), for four time horizons. The plots show the 25th, 50th, and 75th percentiles (represented by the boxes), and the maximum and minimum values (shown by the extent of the whiskers).

# Pluvial flooding and rainfall

## Headline

The IPCC AR4 (2007a) stated that annual precipitation is very likely to decrease across most of the Mediterranean area, including Turkey, and a number of recent studies confirm this.

## Supporting literature

Pluvial flooding can be defined as flooding derived directly from heavy rainfall, which results in overland flow if it is either not able to soak into the ground or exceeds the capacity of artificial drainage systems. This is in contrast to fluvial flooding, which involves flow in rivers either exceeding the capacity of the river channel or breaking through the river banks, and so inundating the floodplain. Pluvial flooding can occur far from river channels, and is usually caused by high intensity, short-duration rainfall events, although it can be caused by lower intensity, longer-duration events, or sometimes by snowmelt. Changes in mean annual or seasonal rainfall are unlikely to be good indicators of change in pluvial flooding; changes in extreme rainfall are of much greater significance. However, even increases in daily rainfall extremes will not necessarily result in increases in pluvial flooding, as this is likely to be dependent on the sub-daily distribution of the rainfall as well as local factors such as soil type, antecedent soil moisture, land cover (especially urbanisation), capacity and maintenance of artificial drainage systems etc. It should be noted that both pluvial and fluvial flooding can potentially result from the same rainfall event.

## Assessments that include a global or regional perspective

### Climate change studies

Onol and Semazzi (2009) explored the impact of climate change for the Eastern Mediterranean, under the SRES A2 emissions scenario. They noted a large projected decrease in precipitation over south-eastern Turkey, in the recharge regions of the Euphrates and Tigris River basins. For Turkey there was a statistically significant decrease in precipitation of 12.5% by 2071-2100 during winter, and a significant increase of 18% in autumn. Spring and summer both indicated non-significant decreases in precipitation.

Similar results were reported by Evans (2009). The author applied 18 GCMs under the SRES A2 scenario, and found that the general pattern of change during the 21<sup>st</sup> century is for a decrease in precipitation over the Eastern Mediterranean, including Turkey, as result of a decrease in storm track activity over the region. Particularly large decreases of 25% of current precipitation (125mm) were simulated over south-western Turkey.

Further supporting evidence for a decrease in precipitation with climate change for Turkey is provided by a study presented by Bozkurt et al. (2008). The authors showed that under the A2 emissions scenario, winter precipitation could decrease substantially along the eastern Mediterranean coasts, Greece, and southern Turkey. However precipitation increases in northern parts of Turkey and the east coast of the Black Sea were simulated in both winter and spring.

## **National-scale or sub-national scale assessments**

### **Recent past**

Zhang et al. (2005) compiled an analysis of recent observed changes in precipitation and precipitation extremes over the Middle East and found that it was characterized by strong interannual variability with few stations showing significant trends in the indices analysed. However, a more recent observational study by Tayanc et al. (2009), which was conducted at the national-scale for Turkey, found that the variability of urban precipitation series is generally larger than rural series, implying an increased risk of floods and droughts. The authors reported significant decreases in precipitation for western parts of Turkey, such as the Aegean and Trachea regions. However, some northern Turkish stations showed increases in precipitation.

# Fluvial flooding

## Headline

Few studies have explored the impact of climate change on fluvial flooding for Turkey. However, the consensus across the few published studies available suggests that extreme flood events could become smaller in magnitude and occur less frequently than present under climate change. Simulations from the AVOID programme, based on climate projections from 21 GCMs, largely support this, showing high agreement across the 21 projections that flood risk in Turkey could decrease with climate change throughout the 21<sup>st</sup> century.

## Supporting literature

### Introduction

This section summarises findings from a number of post IPCC AR4 assessments on river flooding in Turkey to inform and contextualise the analysis performed by the AVOID programme for this project. The results from the AVOID work are discussed in the next section.

Fluvial flooding involves flow in rivers either exceeding the capacity of the river channel or breaking through the river banks, and so inundating the floodplain. A complex set of processes is involved in the translation of precipitation into runoff and subsequently river flow (routing of runoff along river channels). Some of the factors involved are; the partitioning of precipitation into rainfall and snowfall, soil type, antecedent soil moisture, infiltration, land cover, evaporation and plant transpiration, topography, groundwater storage. Determining whether a given river flow exceeds the channel capacity, and where any excess flow will go, is also not straightforward, and is complicated by the presence of artificial river embankments and other man-made structures for example. Hydrological models attempt to simplify and conceptualise these factors and processes, to allow the simulation of runoff and/or river flow under different conditions. However, the results from global-scale hydrological modelling need to be interpreted with caution, especially for smaller regions, due to the necessarily coarse resolution of such modelling and the assumptions and

simplifications this entails (e.g. a 0.5° grid corresponds to landscape features spatially averaged to around 50-55km for mid- to low-latitudes). Such results provide a consistent, high-level picture, but will not show any finer resolution detail or variability. Smaller-scale or catchment-scale hydrological modelling can allow for more local factors affecting the hydrology, but will also involve further sources of uncertainty, such as in the downscaling of global climate model data to the necessary scale for the hydrological models. Furthermore, the application of different hydrological models and analysis techniques often makes it difficult to compare results for different catchments.

Flooding is, after earthquakes, the second most important natural hazard in Turkey. Between 1955 and 1995 more than 1,000 people in Turkey lost their lives as a consequence of floods and the economic damage was more than \$650 million during this period (Ceylan et al., 2007). A flood inventory covering the years 1955 to 2009 counted 2089 events, or 39 events causing 25 deaths per year on average (Gürer and Uçar, 2009).

## **Assessments that include a global or regional perspective**

### **Climate change studies**

A global modelling study that applied a single GCM under the A1B emissions scenario (Hirabayashi et al., 2008) found mostly little change in flood hazard across Turkey in the coming decades (2001-2030). By the end of the century (2071-2100), the return period of what was a 100-year flood event in the 20<sup>th</sup> century was generally projected to remain unchanged or increase to 120 years or more. However, Hirabayashi et al. (2008) also found a widespread shift in the peak flow occurrence from early spring (March-April) to 3-4 months later in summer, suggesting a completely different flood regime under climate change. There is therefore a need for a comprehensive and detailed analysis of changes in flood hazard in Turkish river basins, taking into account the uncertainties in the climate change projections. It should be noted, however, that results from studies that have applied only a single climate model or climate change scenario should be interpreted with caution. This is because they do not consider other possible climate change scenarios which could result in a different impact outcome, in terms of magnitude and in some cases sign of change.

## **National-scale or sub-national scale assessments**

### **Climate change studies**

Few national or local-scale studies have assessed the impact of climate change on flood hazard in Turkey. River basins that are dominated by snowfall and snowmelt could be highly sensitive to a rise in temperature with climate change. For example, in the Seyhan Basin in



Southern Turkey, Fujihara et al. (2008b) simulated a strong reduction in spring river discharge due to less snow accumulation, and a shift in the timing of the peak runoff due to earlier snowmelt under climate change. The authors also found a considerable decrease in the 95<sup>th</sup> percentile flow level (i.e. the flow level that is exceeded only 5% of the time), meaning that flood events could occur less frequently in the future.

Using an inverse modelling approach, Fujihara et al. (2008a) estimated that flood events in the Seyhan Basin with a 100-year return period under present conditions could have a 102-year return period with climate change; the return period of 200-year events could increase to 293 years; and events with a 300-year return period could have a return period of 1370 years under future climate conditions. This means that extreme flood events could occur much less frequently under climate change (Fujihara et al., 2008a).

## **AVOID programme results**

To quantify the impact of climate change on fluvial flooding and the inherent uncertainties, the AVOID programme calculated an indicator of flood risk for all countries reviewed in this literature assessment based upon the patterns of climate change from 21 GCMs (Warren et al., 2010). This ensures a consistent methodological approach across all countries and takes consideration of climate modelling uncertainties.

### **Methodology**

The effect of climate change on fluvial flooding is shown here using an indicator representing the percentage change in average annual flood risk within a country, calculated by assuming a standardised relationship between flood magnitude and loss. The indicator is based on the estimated present-day (1961-1990) and future flood frequency curve, derived from the time series of runoff simulated at a spatial resolution of 0.5°x0.5° using a global hydrological model, MacPDM (Gosling and Arnell, 2011). The flood frequency curve was combined with a generic flood magnitude–damage curve to estimate the average annual flood damage in each grid cell. This was then multiplied by grid cell population and summed across a region, producing in effect a population-weighted average annual damage. Flood damage is thus assumed to be proportional to population in each grid cell, not the value of exposed assets, and the proportion of people exposed to flood is assumed to be constant across each grid cell (Warren et al., 2010).

The national values are calculated across major floodplains, based on the UN PREVIEW Global Risk Data Platform (preview.grid.unep.ch). This database contains gridded estimates, at a spatial resolution of 30 arc-seconds ( $0.00833^{\circ} \times 0.00833^{\circ}$ ), of the estimated frequency of flooding. From this database the proportion of each  $0.5^{\circ} \times 0.5^{\circ}$  grid cell defined as floodplain was determined, along with the numbers of people living in each  $0.5^{\circ} \times 0.5^{\circ}$  grid cell in flood-prone areas. The floodplain data set does not include “small” floodplains, so underestimates actual exposure to flooding. The pattern of climate change from 21 GCMs was applied to MacPDM, under two emissions scenarios; 1) SRES A1B and 2) an aggressive mitigation scenario where emissions follow A1B up to 2016 but then decline at a rate of 5% per year thereafter to a low emissions floor (denoted A1B-2016-5-L). Both scenarios assume that population changes through the 21<sup>st</sup> century following the SRES A1 scenario as implemented in IMAGE 2.3 (van Vuuren et al., 2007). The application of 21 GCMs is an attempt to quantify the uncertainty due to climate modelling, although it is acknowledged that only one impacts model is applied (MacPDM). Simulations were performed for the years 2030, 2050, 2080 and 2100. The result represents the change in flood risk due to climate change, not the change in flood risk relative to present day (Warren et al., 2010).

## Results

The results for Turkey are presented in Figure 16. By the 2030s, the models project a range of changes in mean fluvial flooding risk over Turkey in both scenarios, with a few models projecting increases, but the majority projecting decreases. The largest decrease projected for the 2030s is -60%, and the largest increase is +5%. The mean projected change is a decrease in average annual flood risk of -33%.

By 2100 the difference in projections from the different models becomes greater, and this is more pronounced for the A1B scenario than the mitigation scenario. Under the mitigation scenario, most models still project a decrease in flood risk (down to -70%), but a small number project an increase. The mean of all projections is a decrease of -40%, and the upper projection is approximately a 15% increase. Under the A1B scenario, nearly all models project a decreased flood (down to a minimum of -90%). A small number of models project an increase, with the largest increase being approximately +60%, but the mean of all projections is a decrease in the average annual flood risk of -55%.

So for Turkey, the models show a much greater tendency towards decreasing flood risk throughout the 21<sup>st</sup> century under both emissions scenarios, but the differences between the model projections are greater later in the century and particularly for A1B.

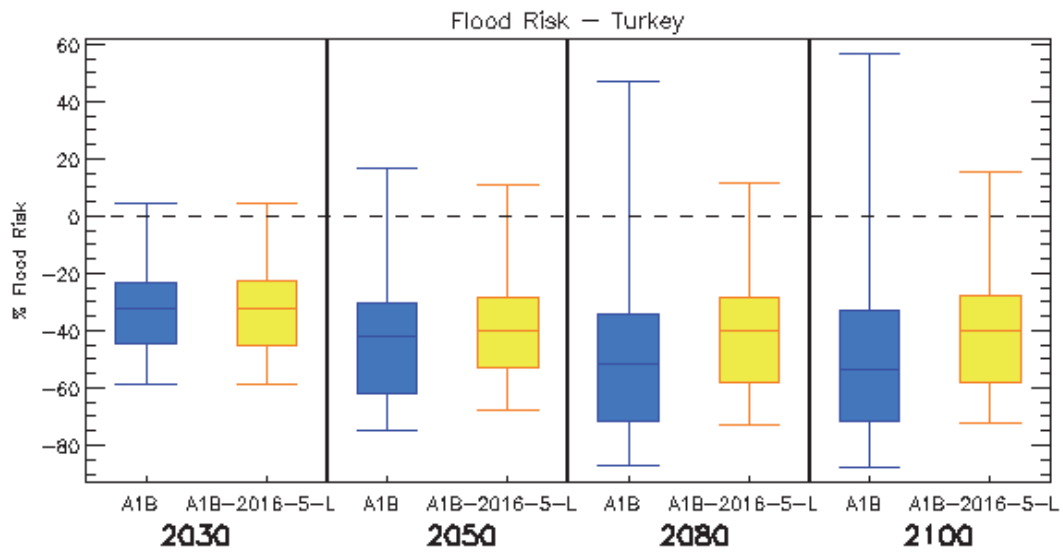


**Figure 16.** Box and whisker plots for the percentage change in average annual flood risk within Turkey, from 21 GCMs under two emissions scenarios (A1B and A1B-2016-5-L), for four time horizons. The plots show the 25th, 50th, and 75th percentiles (represented by the boxes), and the maximum and minimum values (shown by the extent of the whiskers).

## **Tropical cyclones**

This country is not impacted by tropical cyclones.

# Coastal regions

## Headline

There are no global-scale assessments of the impacts of sea level rise (SLR) on coastal regions that provide national-scale estimates for Turkey. However, a number of national-scale studies suggest that Turkey could experience appreciable coastal impacts from SLR (Demirkesen et al., 2008, Kuleli, 2010, Kuleli et al., 2009). One study estimates that the population in Turkey exposed to SLR is around 428,000 along the Mediterranean coast, 208,000 along the Aegean coast, 842,000 in the Marmara region and 201,000 along the Black Sea coast.

## Supporting literature

### Assessments that include a global or regional perspective

#### Climate change studies

The IPCC AR4 concluded that at the time, understanding was too limited to provide a best estimate or an upper bound for global SLR in the twenty-first century (IPCC, 2007b). However, a range of SLR, excluding accelerated ice loss effects was published, ranging from 0.19m to 0.59m by the 2090s (relative to 1980-2000), for a range of scenarios (SRES A1FI to B1). The IPCC AR4 also provided an illustrative estimate of an additional SLR term of up to 17cm from acceleration of ice sheet outlet glaciers and ice streams, but did not suggest this is the upper value that could occur. Although there are published projections of SLR in excess of IPCC AR4 values (Nicholls et al., 2011), many of these typically use semi-empirical methods that suffer from limited physical validity and further research is required to produce a more robust estimate. Linking sea level rise projections to temperature must also be done with caution because of the different response times of these two climate variables to a given radiative forcing change.

Nicholls and Lowe (2004) previously showed that mitigation alone would not avoid all of the impacts due to rising sea levels, adaptation would likely be needed too. Recent work by van Vuuren et al. (2011) estimated that, for a world where global mean near surface temperatures reach around 2°C by 2100, global mean SLR could be 0.49m above present

levels by the end of the century. Their sea level rise estimate for a world with global mean temperatures reaching 4°C by 2100 was 0.71m, suggesting around 40% of the future increase in sea level to the end of the 21<sup>st</sup> century could be avoided by mitigation. A qualitatively similar conclusion was reached in a study by Pardaens et al. (2011), which examined climate change projections from two GCMs. They found that around a third of global-mean SLR over the 21st century could potentially be avoided by a mitigation scenario under which global-mean surface air temperature is near-stabilised at around 2°C relative to pre-industrial times. Under their baseline business-as-usual scenario the projected increase in temperature over the 21st century is around 4°C, and the sea level rise range is 0.29-0.51m (by 2090-2099 relative to 1980-1999; 5% to 95% uncertainties arising from treatment of land-based ice melt and following the methodology used by the IPCC AR4). Under the mitigation scenario, global mean SLR in this study is projected to be 0.17-0.34m.

The IPCC 4th assessment (IPCCa) followed Nicholls and Lowe (2004) for estimates of the numbers of people affected by coastal flooding due to sea level rise. Nicholls and Lowe (2004) projected for the north Mediterranean region that an additional 200 thousand people per year could be flooded due to sea level rise by the 2080s relative to the 1990s for the SRES A2 Scenario (note this region also includes other countries, such as Greece and Italy). However, it is important to note that this calculation assumed that protection standards increased as GDP increased, although there is no additional adaptation for sea level rise. More recently, Nicholls et al. (2011) also examined the potential impacts of sea level rise in a scenario that gave around 4°C of warming by 2100. Readings from Figure 3 from Nicholls et al. (2011) for the north Mediterranean region suggest that less than an approximate 1 million additional people per year could be flooded for a 0.5 m SLR (assuming no additional protection). Nicholls et al. (2011) also looked at the consequence of a 2m SLR by 2100, however as we consider this rate of SLR to have a low probability we don't report these figures here.

To further quantify the impact of SLR and some of the inherent uncertainties, the DIVA model was used to calculate the number of people flooded per year for global mean sea level increases (Brown et al., 2011). The DIVA model (DINAS-COAST, 2006) is an integrated model of coastal systems that combines scenarios of water level changes with socio-economic information, such as increases in population. The study uses two climate scenarios; 1) the SRES A1B scenario and 2) a mitigation scenario, RCP2.6. In both cases an SRES A1B population scenario was used. The results are shown in Table 10. While globally there is evidence that the impacts results are not significantly affected by driving

DIVA with global mean sea level rise, there are regions where may make a difference. Once such region is the Mediterranean.

	A1B		RCP	
	Low	High	Low	High
Additional people flooded (1000s)	18.15	182.14	9.24	129.65
Loss of wetlands area (% of country's total wetland)	53.46%	73.80%	54.80%	70.57%

**Table 10.** Number of additional people flooded (1000s), and percentage of total wetlands lost by the 2080s under the high and low SRES A1B and mitigation (RCP 2.6) scenarios (Brown et al., 2011).

## National-scale or sub-national scale assessments

### Climate change studies

Kuleli et al. (2009) notes that SLR along the Turkish coast is not likely to be as significant as in some other areas of the globe but there could be local vulnerability due to topography and subsidence. Kuleli et al. (2009) explored the population, settlements, land use, contribution to national agricultural production and taxes within 0–10m elevation of national level, as an indicator of risk to SLR. The study found that approximately 7,319km<sup>2</sup> of land area lies below 10m elevation in Turkey, and is hence highly vulnerable to SLR. 28 coastal cities, 191 districts and 181 villages or towns are located below 10m elevation. Kuleli et al. (2009) estimated that the population in Turkey at risk to SLR was around 428,000 along the Mediterranean coast, 208,000 along the Aegean coast, 842,000 in the Marmara region and 201,000 along the Black Sea coast. The analyses were extended and presented in a later study (Kuleli, 2010), which showed that although the Marmara Region is the most vulnerable area in terms of population at risk, the Mediterranean coast is the area most vulnerable to land loss. Demirkesen (2008) explored the vulnerability of low-lying coastal areas in Turkey to inundation from prescribed SLR scenarios of 1, 2, and 3m by 2205. The analysis revealed inundated coastal areas of 545 km<sup>2</sup>, 1,286 km<sup>2</sup>, and 2,125 km<sup>2</sup> by 2205. This is equivalent to minimum and maximum land losses by 2205 of 0.1–0.3% of the total area and of 1.3–5.2% of the coastal areas with elevations of less than 100 m in the country, respectively. Assuming SLR rates of 5mm, 10mm and 15mm per year respectively from present, Demirkesen (2008) estimated the area inundated in 2025 to be 52 km<sup>2</sup>, 123 km<sup>2</sup> and 203

km<sup>2</sup> respectively – by 2085 these values increased to 216 km<sup>2</sup>, 510 km<sup>2</sup> and 844 km<sup>2</sup> respectively.



## References

- AINSWORTH, E. A. & MCGRATH, J. M. 2010. Direct Effects of Rising Atmospheric Carbon Dioxide and Ozone on Crop Yields. *In: LOBELL, D. & BURKE, M. (eds.) Climate Change and Food Security*. Springer Netherlands.
- ALLISON, E. H., PERRY, A. L., BADJECK, M.-C., NEIL ADGER, W., BROWN, K., CONWAY, D., HALLS, A. S., PILLING, G. M., REYNOLDS, J. D., ANDREW, N. L. & DULVY, N. K. 2009. Vulnerability of national economies to the impacts of climate change on fisheries. *Fish and Fisheries*, 10, 173-196.
- ARNELL, N. W. 2004. Climate change and global water resources: SRES emissions and socio-economic scenarios. *Global Environmental Change*, 14, 31-52.
- AVNERY, S., MAUZERALL, D. L., LIU, J. F. & HOROWITZ, L. W. 2011. Global crop yield reductions due to surface ozone exposure: 2. Year 2030 potential crop production losses and economic damage under two scenarios of O<sub>3</sub> pollution. *Atmospheric Environment*, 45, 2297-2309.
- BENESTAD, R. 2008. Heating degree days, Cooling degree days, and precipitation in Europe: Analysis for the CELECT-project.
- BONAZZA, A., MESSINA, P., SABBIONI, C., GROSSI, C. M. & BRIMBLECOMBE, P. 2009a. Mapping the impact of climate change on surface recession of carbonate buildings in Europe. *Science of The Total Environment*, 407, 2039-2050.
- BONAZZA, A., SABBIONI, C., MESSINA, P., GUARALDI, C. & DE NUNTIIS, P. 2009b. Climate change impact: Mapping thermal stress on Carrara marble in Europe. *Science of The Total Environment*, 407, 4506-4512.
- BOZKURT, D., SEN, O. L., TURUNCOGLU, U. U., KARACA, M. & DALFES, H. N. 2008. Regional climate change projections for Eastern Mediterranean: Preliminary results. *Geophysical Research Abstracts, Vol. 10, EGU General Assembly, Vienna, Austria*.
- BROWN, S., NICHOLLS, R., LOWE, J.A. and PARDAENS, A. (2011), Sea level rise impacts in 24 countries. Faculty of Engineering and the Environment and Tyndall Centre for Climate Change Research, University of Southampton.

CEYLAN, A., ALAN, I. & UĞURLU, A. 2007. Causes and effects of flood hazards in Turkey. *International Congress on River Basin Management*. Antalya, Turkey.

CHAKRABORTY, S. & NEWTON, A. C. 2011. Climate change, plant diseases and food security: an overview. *Plant Pathology*, 60, 2-14.

CHEUNG, W. W. L., LAM, V. W. Y., SARMIENTO, J. L., KEARNEY, K., WATSON, R. E. G., ZELLER, D. & PAULY, D. 2010. Large-scale redistribution of maximum fisheries catch potential in the global ocean under climate change. *Global Change Biology*, 16, 24-35.

CIA 2011. World Factbook. US Central Intelligence Agency.

CTF 2011. CTF Investment Plan for Turkey - Climate Investment Funds. Clean Technology Funds.

DEMIRKESEN, A., EVRENDILEK, F. & BERBEROGLU, S. 2008. Quantifying coastal inundation vulnerability of Turkey to sea-level rise. *Environmental Monitoring and Assessment*, 138, 101-106.

DINAS-COAST Consortium. 2006 DIVA 1.5.5. Potsdam, Germany: Potsdam Institute for Climate Impact Research (on CD-ROM).

DOLL, P. 2009. Vulnerability to the impact of climate change on renewable groundwater resources: a global-scale assessment. *Environmental Research Letters*, 4.

DOLL, P. & SIEBERT, S. 2002. Global modeling of irrigation water requirements. *Water Resources Research*. Vol: 38 Issue: 4. Doi: 10.1029/2001WR000355.

ESKELAND, G. A. & MIDEKSA, T. K. 2009. Climate Change and Residential Electricity Demand in Europe. *Center for International Climate and Environmental Research (CICERO)*.

EVANS, J. P. 2009. 21st century climate change in the Middle East. *Climatic Change*, 92, 417-432.

FALKENMARK, M., ROCKSTRÖM, J. & KARLBERG, L. 2009. Present and future water requirements for feeding humanity. *Food Security*, 1, 59-69.

FAO. 2008. *Food and Agricultural commodities production* [Online]. Available: <http://faostat.fao.org/site/339/default.aspx> [Accessed 1 June 2011].

FAO. 2010. *Food Security country profiles* [Online]. Available: <http://www.fao.org/economic/ess/ess-fs/ess-fs-country/en/> [Accessed 1 Sept 2011].

FISCHER, G. 2009. World Food and Agriculture to 2030/50: How do climate change and bioenergy alter the long-term outlook for food, agriculture and resource availability? *Expert Meeting on How to Feed the World in 2050*. Food and Agriculture Organization of the United Nations, Economic and Social Development Department.

FUJIHARA, Y., SIMONOVIC, S. P., TOPALOGLU, F., TANAKA, K. & WATANABE, T. 2008a. An inverse-modelling approach to assess the impacts of climate change in the Seyhan River basin, Turkey. *Hydrological Sciences Journal-Journal Des Sciences Hydrologiques*, 53, 1121-1136.

FUJIHARA, Y., TANAKA, K., WATANABE, T., NAGANO, T. & KOJIRI, T. 2008b. Assessing the impacts of climate change on the water resources of the Seyhan River Basin in Turkey: Use of dynamically downscaled data for hydrologic simulations. *Journal of Hydrology*, 353, 33-48.

GAO, X. J. & GIORGI, F. 2008. Increased aridity in the Mediterranean region under greenhouse gas forcing estimated from high resolution simulations with a regional climate model. *Global and Planetary Change*, 62, 195-209.

GERTEN D., SCHAPHOFF S., HABERLANDT U., LUCHT W., SITCH S. 2004 . Terrestrial vegetation and water balance: hydrological evaluation of a dynamic global vegetation model *International Journal Water Resource Development* 286:249–270.

GIANNAKOPOULOS, C., BINDI, M., MORIONDO, M., LESAGER, P. & TIN, T. 2005. Climate change impacts in the Mediterranean resulting from a 2C global temperature rise. *WWF Report*. Gland, Switzerland: WWF.

GIANNAKOPOULOS, C., LE SAGER, P., BINDI, M., MORIONDO, M., KOSTOPOULOU, E. & GOODESS, C. M. 2009. Climatic changes and associated impacts in the Mediterranean resulting from a 2 °C global warming. *Global and Planetary Change*, 68, 209-224.

GORNALL, J., BETTS, R., BURKE, E., CLARK, R., CAMP, J., WILLETT, K., WILTSHIRE, A. 2010. Implications of climate change for agricultural productivity in the early twenty-first century. *Phil. Trans. R. Soc. B*, DOI: 10.1098/rstb.2010.0158.

- GOSLING, S., TAYLOR, R., ARNELL, N. & TODD, M. 2011. A comparative analysis of projected impacts of climate change on river runoff from global and catchment-scale hydrological models. *Hydrology and Earth System Sciences*, 15, 279–294.
- GOSLING, S. N. & ARNELL, N. W. 2011. Simulating current global river runoff with a global hydrological model: model revisions, validation, and sensitivity analysis. *Hydrological Processes*, 25, 1129-1145.
- GOSLING, S. N., BRETHERTON, D., HAINES, K. & ARNELL, N. W. 2010. Global hydrology modelling and uncertainty: running multiple ensembles with a campus grid. *Philosophical Transactions of the Royal Society A: Mathematical, Physical and Engineering Sciences*, 368, 4005-4021.
- GÜRER, I. & UÇAR, I. 2009. Flood Disasters' Inventory in Turkey in 2009. *International Symposium on Water Management and Hydraulic Engineering*. Ohrid, Macedonia.
- HARDING, R., BEST, M., BLYTH, E., HAGEMANN, D., KABAT, P., TALLAKSEN, L.M., WARNAARS, T., WIBERG, D., WEEDON, G.P., van LANEN, H., LUDWIG, F., HADDELAND, I. 2011. Preface to the “Water and Global Change (WATCH)” special collection: Current knowledge of the terrestrial global water cycle. *Journal of Hydrometeorology*, DOI: 10.1175/JHM-D-11-024.1.
- HIRABAYASHI, Y., KANAE, S., EMORI, S., OKI, T. & KIMOTO, M. 2008. Global projections of changing risks of floods and droughts in a changing climate. *Hydrological Sciences Journal-Journal Des Sciences Hydrologiques*, 53, 754-772.
- IFPRI. 2010. *International Food Policy Research Institute (IFPRI) Food Security CASE maps. Generated by IFPRI in collaboration with StatPlanet*. [Online]. Available: [www.ifpri.org/climate-change/casemaps.html](http://www.ifpri.org/climate-change/casemaps.html) [Accessed 21 June 2010].
- IGLESIAS, A., GARROTE, L., QUIROGA, S. & MONEO, M. 2009. Impacts of climate change in agriculture in Europe. PESETA-Agriculture study. *JRC Scientific and Technical Reports*.
- IGLESIAS, A. & ROSENZWEIG, C. 2009. Effects of Climate Change on Global Food Production under Special Report on Emissions Scenarios (SRES) Emissions and Socioeconomic Scenarios: Data from a Crop Modeling Study. . Palisades, NY: Socioeconomic Data and Applications Center (SEDAC), Columbia University.

IPCC 2007a. Climate Change 2007: The Physical Science Basis. Contribution of Working Group I to the Fourth Assessment Report of the Intergovernmental Panel on Climate Change *In*: SOLOMON, S., QIN, D., MANNING, M., CHEN, Z., MARQUIS, M., AVERYT, K. B., TIGNOR, M. & MILLER, H. L. (eds.). Cambridge, United Kingdom and New York, NY, USA.

IPCC 2007b. Summary for Policymakers. *In*: PARRY, M. L., CANZIANI, O. F., PALUTIKOF, J. P., VAN DER LINDEN, P. J. & HANSON, C. E. (eds.) *Climate Change 2007: Impacts, Adaptation and Vulnerability. Contribution of Working Group II to the Fourth Assessment Report of the Intergovernmental Panel on Climate Change*. Cambridge: Cambridge University Press.

KULELI, T. 2010. City-Based Risk Assessment of Sea Level Rise Using Topographic and Census Data for the Turkish Coastal Zone. *Estuaries and Coasts*, 33, 640-651.

KULELI, T., ŞENKAL, O. & ERDEM, M. 2009. National assessment of sea level rise using topographic and census data for Turkish coastal zone. *Environmental Monitoring and Assessment*, 156, 425-434.

LEHNER, B., CZISCH, G. & VASSOLO, S. 2005. The impact of global change on the hydropower potential of Europe: a model-based analysis. *Energy Policy*, 33, 839-855.

LEHNER, B., DOLL, P., ALCAMO, J., HENRICH, T. & KASPAR, F. 2006. Estimating the impact of global change on flood and drought risks in Europe: A continental, integrated analysis. *Climatic Change*, 75, 273-299.

LOBELL, D. B., BANZIGER, M., MAGOROKOSHO, C. & VIVEK, B. 2011. Nonlinear heat effects on African maize as evidenced by historical yield trials. *Nature Clim. Change*, 1, 42-45.

LOBELL, D. B., BURKE, M. B., TEBALDI, C., MASTRANDREA, M. D., FALCON, W. P. & NAYLOR, R. L. 2008. Prioritizing climate change adaptation needs for food security in 2030. *Science*, 319, 607-610.

LUCK, J., SPACKMAN, M., FREEMAN, A., TREBICKI, P., GRIFFITHS, W., FINLAY, K. & CHAKRABORTY, S. 2011. Climate change and diseases of food crops. *Plant Pathology*, 60, 113-121.

NELSON, G. C., ROSEGRANT, M. W., PALAZZO, A., GRAY, I., INGERSOLL, C., ROBERTSON, R., TOKGOZ, S., ZHU, T., SULSER, T. & RINGLER, C. 2010. Food Security, Farming and Climate Change to 2050. *Research Monograph, International Food Policy Research Institute*. Washington, DC.

NICHOLLS, R. J. and LOWE, J. A. (2004). "Benefits of mitigation of climate change for coastal areas." *Global Environmental Change* **14**(3): 229-244.

NICHOLLS, R. J., MARINOVA, N., LOWE, J. A., BROWN, S., VELLINGA, P., DE GUSMÃO, G., HINKEL, J. and TOL, R. S. J. (2011). "Sea-level rise and its possible impacts given a 'beyond 4°C world' in the twenty-first century." *Philosophical Transactions of the Royal Society A* **369**: 1-21.

ONOL, B. & SEMAZZI, F. H. M. 2009. Regionalization of Climate Change Simulations over the Eastern Mediterranean. *Journal of Climate*, **22**, 1944-1961.

ÖZDOĞAN, M. 2011. Modeling the impacts of climate change on wheat yields in Northwestern Turkey. *Agriculture, Ecosystems & Environment*, **141**, 1-12.

OZKUL, S. 2009. Assessment of climate change effects in Aegean river basins: the case of Gediz and Buyuk Menderes Basins. *Climatic Change*, **97**, 253-283.

PARDAENS, A. K., LOWE, J., S, B., NICHOLLS, R. & DE GUSMÃO, D. 2011. Sea-level rise and impacts projections under a future scenario with large greenhouse gas emission reductions. *Geophysical Research Letters*, **38**, L12604.

PARRY, M. L., ROSENZWEIG, C., IGLESIAS, A., LIVERMORE, M. & FISCHER, G. 2004. Effects of climate change on global food production under SRES emissions and socio-economic scenarios. *Global Environmental Change-Human and Policy Dimensions*, **14**, 53-67.

RAMANKUTTY, N., EVAN, A. T., MONFREDA, C. & FOLEY, J. A. 2008. Farming the planet: 1. Geographic distribution of global agricultural lands in the year 2000. *Global Biogeochemical Cycles*, **22**, GB1003.

RAMANKUTTY, N., FOLEY, J. A., NORMAN, J. & MCSWEENEY, K. 2002. The global distribution of cultivable lands: current patterns and sensitivity to possible climate change. *Global Ecology and Biogeography*, **11**, 377-392.

ROCKSTROM, J., FALKENMARK, M., KARLBERG, L., HOFF, H., ROST, S. & GERTEN, D. 2009. Future water availability for global food production: The potential of green water for increasing resilience to global change. *Water Resources Research*, 45.

SMAKHTIN, V., REVENGA, C. & DOLL, P. 2004. A pilot global assessment of environmental water requirements and scarcity. *Water International*, 29, 307-317.

STOCKLE, C.O., DONATELLI, M., NELSON, R., 2003 CropSyst, a cropping systems simulation model. *European Journal of Agronomy* 18, 289-307.

TATSUMI, K., YAMASHIKI, Y., VALMIR DA SILVA, R., TAKARA, K., MATSUOKA, Y., TAKAHASHI, K., MARUYAMA, K. & KAWAHARA, N. 2011. Estimation of potential changes in cereals production under climate change scenarios. *Hydrological Processes*, Published online.

TAYANC, M., IM, U., DOGRUEL, M. & KARACA, M. 2009. Climate change in Turkey for the last half century. *Climatic Change*, 94, 483-502.

TELLI, C., VOYVODA, E. & YELDAN, E. 2008. Economics of environmental policy in Turkey: A general equilibrium investigation of the economic evaluation of sectoral emission reduction policies for climate change. *Journal of Policy Modeling*, 30, 321-340.

VAN VUUREN, D., DEN ELZEN, M., LUCAS, P., EICKHOUT, B., STRENGERS, B., VAN RUIJVEN, B., WONINK, S. & VAN HOUT, R. 2007. Stabilizing greenhouse gas concentrations at low levels: an assessment of reduction strategies and costs. *Climatic Change*, 81, 119-159.

VAN VUUREN, D. P., ISAAC, M., KUNDZEWICZ, Z. W., ARNELL, N., BARKER, T., CRIQUI, P., BERKHOUT, F., HILDERINK, H., HINKEL, J., HOF, A., KITOUS, A., KRAM, T., MECHLER, R. & SCRIECIU, S. 2011. The use of scenarios as the basis for combined assessment of climate change mitigation and adaptation. *Global Environmental Change*, 21, 575-591.

VOROSMARTY, C. J., MCINTYRE, P. B., GESSNER, M. O., DUDGEON, D., PRUSEVICH, A., GREEN, P., GLIDDEN, S., BUNN, S. E., SULLIVAN, C. A., LIERMANN, C. R. & DAVIES, P. M. 2010. Global threats to human water security and river biodiversity. *Nature*, 467, 555-561.

WARREN, R., ARNELL, N., BERRY, P., BROWN, S., DICKS, L., GOSLING, S., HANKIN, R., HOPE, C., LOWE, J., MATSUMOTO, K., MASUI, T., NICHOLLS, R., O'HANLEY, J., OSBORN, T., SCRIECRU, S. (2010) The Economics and Climate Change Impacts of Various Greenhouse Gas Emissions Pathways: A comparison between baseline and policy emissions scenarios, AVOID Report, AV/WS1/D3/R01.

[http://www.metoffice.gov.uk/avoid/files/resources-researchers/AVOID\\_WS1\\_D3\\_01\\_20100122.pdf](http://www.metoffice.gov.uk/avoid/files/resources-researchers/AVOID_WS1_D3_01_20100122.pdf).

WOOD, E.F., ROUNDY, J.K., TROY, T.J., van BEEK, L.P.H., BIERKENS, M.F.P., BLYTH, E., de ROO, A., DOLL, P., EK, M., FAMIGLIETTI, J., GOCHIS, D., van de GIESEN, N., HOUSER, P., JAFFE, P.R., KOLLET, S., LEHNER, B., LETTENMAIER, D.P., PETERS-LIDARD, C., SIVAPALAN, M., SHEFFIELD, J., WADE, A. & WHITEHEAD, P. 2011. Hyperresolution global land surface modelling: Meeting a grand challenge for monitoring Earth's terrestrial water. *Water Resources Research*, 47, W05301.

WOS. 2011. *Web of Science* [Online]. Available:

[http://thomsonreuters.com/products\\_services/science/science\\_products/a-z/web\\_of\\_science](http://thomsonreuters.com/products_services/science/science_products/a-z/web_of_science) [Accessed August 2011].

WU, W., TANG, H., YANG, P., YOU, L., ZHOU, Q., CHEN, Z. & SHIBASAKI, R. 2011. Scenario-based assessment of future food security. *Journal of Geographical Sciences*, 21, 3-17.

YANO, T., AYDIN, M. & HARAGUCHI, T. 2007. Impact of climate change on irrigation demand and crop growth in a Mediterranean environment of Turkey. *Sensors*, 7, 2297-2315.

ZHANG, X. B., AGUILAR, E., SENSOY, S., MELKONYAN, H., TAGIYEVA, U., AHMED, N., KUTALADZE, N., RAHIMZADEH, F., TAGHIPOUR, A., HANTOSH, T. H., ALBERT, P., SEMAWI, M., ALI, M. K., AL-SHABIBI, M. H. S., AL-OULAN, Z., ZATARI, T., KHELET, I. A., HAMOUD, S., SAGIR, R., DEMIRCAN, M., EKEN, M., ADIGUZEL, M., ALEXANDER, L., PETERSON, T. C. & WALLIS, T. 2005. Trends in Middle East climate extreme indices from 1950 to 2003. *Journal of Geophysical Research-Atmospheres*, 110.



## **Acknowledgements**

Funding for this work was provided by the UK Government Department of Energy and Climate Change, along with information on the policy relevance of the results.

The research was led by the UK Met Office in collaboration with experts from the University of Nottingham, Walker Institute at the University of Reading, Centre for Ecology and Hydrology, University of Leeds, Tyndall Centre – University of East Anglia, and Tyndall Centre – University of Southampton.

Some of the results described in this report are from work done in the AVOID programme by the UK Met Office, Walker Institute at the University of Reading, Tyndall Centre – University of East Anglia, and Tyndall Centre – University of Southampton.

The AVOID results are built on a wider body of research conducted by experts in climate and impact models at these institutions, and in supporting techniques such as statistical downscaling and pattern scaling.

The help provided by experts in each country is gratefully acknowledged – for the climate information they suggested and the reviews they provided, which enhanced the content and scientific integrity of the reports.

The work of the independent expert reviewers at the Centre for Ecology and Hydrology, University of Oxford, and Fiona's Red Kite Climate Consultancy is gratefully acknowledged.

Finally, thanks go to the designers, copy editors and project managers who worked on the reports.

Met Office  
FitzRoy Road, Exeter  
Devon, EX1 3PB  
United Kingdom

Tel: 0870 900 0100  
Fax: 0870 900 5050  
[enquiries@metoffice.gov.uk](mailto:enquiries@metoffice.gov.uk)  
[www.metoffice.gov.uk](http://www.metoffice.gov.uk)

Produced by the Met Office.  
© Crown copyright 2011 11/0209u  
Met Office and the Met Office logo  
are registered trademarks